UNIVERSITÀ DEGLI STUDI DI PADOVA

SEDE AMMINISTRATIVA: UNIVERSITÀ DEGLI STUDI DI PADOVA
Dipartimento di Scienze del Farmaco
Dipartimento di Biologia - Istituto di Tecnologie Biomediche-CNR

SCUOLA DI DOTTORATO DI RICERCA IN:
BIOLOGIA E MEDICINA DELLA RIGENERAZIONE
INDIRIZZO: BIOLOGIA DELL'INTEGRAZIONE INTERCELLULARE
CICLO: XXV

Role of metal ions dyshomeostasis in neurodegeneration

DIRETTORE DELLA SCUOLA: CH.MA PROF.SSA Maria Teresa Conconi
SUPERVISORE: CH.MO PROF. Paolo Zatta

DOTTORANDO: Alberto Granzotto

La natura, Signor mio, si burla delle costituzioni e decreti

de i principi, degl'imperatori e dei monarchi, a richiesta dei quali ella non

muterebbe un iota delle leggi e statuti suoi.

Galileo Galilei
Lettera a Francesco Ingoli
1624

CONTENTS

Sommario 7

Summary 9

Abbreviations 11

1. Metal ions dyshomeostasis in Alzheimer's disease 13

1.1 Conformational disease 13

1.2 Alzheimer's disease 13

1.2.1 From Aβ to senile plaques 14

1.2.2 Role of metal ions in Aβ folding 15

1.2.3 From tau protein to neurofibrillary tangles 20

1.2.4 Aβ toxicity mechanisms 20

1.3 Materials and methods 21

1.3.1 Chemicals 21

1.3.2 Aβ and aβ-metal conjugates preparation 22

1.3.3 Congo Red spectroscopic assay 22

1.3.4 ANS fluorescence measurements 22

1.3.5 Turbidity assay 23

1.3.6 Transmission Electron Microscopy (TEM) 23

1.3.7 X-Ray diffraction studies of phospholipid multilayers 23

1.3.8 Neuroblastoma cell cultures 23

1.3.9 Cell viability assay 24

1.3.10 SOD assay 24

1.3.11 Microarray analysis of neuroblastoma exposed to Aβ-metal conjugates 24

1.3.12 Microarray analysis of young and aged 3xTg-AD hippocampi 26

1.3.13 Statistical analysis 27

1.4 Results 28

1.4.1 Resveratrol in Aβ and Aβ-metal conjugates aggregation and toxicity 28

1.4.2 Physiological cholesterol concentration is neuroprotective against Aβ and Aβ-metal conjugates toxicity 34

1.4.3 Microarray analysis of gene expression profiles in human neuroblastoma cells exposed to Aβ-Zn and Aβ-Cu conjugates 40

1.4.4 Early and sustained altered expression of aging-related genes in young 3xTg-AD mice 52

1.5 Discussions 63

1.5.1 Resveratrol in Aβ and Aβ-metal conjugates aggregation and toxicity 63

1.5.2 Physiological cholesterol concentration is neuroprotective against Aβ and Aβ-metal conjugates toxicity 64
1.5.3 Microarray analysis of gene expression profiles in human neuroblastoma cells exposed to Aβ-Zn and Aβ-Cu conjugates 67
1.5.4 Early and sustained altered expression of aging-related genes in young 3xTg-AD mice 69
2. Calcium dyshomeostasis in neurodegeneration 77
2.1 Intracellular calcium homeostasis 77
2.2 Calcium dyshomeostasis in aging and disease: a lay summary 78
2.3 Materials and methods 78
2.3.1 Chemicals 78
2.3.2 Neuronal striatal cultures 79
2.3.3 Imaging studies 79
2.4 Results 81
2.4.1 nNOS(+) striatal neurons possess functional NMDA receptors but fail to generate mitochondrial ROS in response to an excitotoxic challenge 81
2.5 Discussion 86
3. Conclusions 89
References 91
Publications 115

SOMMARIO

Il presente lavoro di tesi si è suddiviso in due filoni principali che hanno come filo conduttore la disomeostasi di ioni metallici nei processi neurodegenerativi.

La prima parte riporta lo studio sul ruolo di alcuni ioni metallici (alluminio, ferro, rame e zinco) nel processo di *folding* della proteina β-amiloide (Aβ), ritenuta uno dei fattori eziopatogenici del morbo di Alzheimer. I dati ottenuti dimostrano come i complessi Aβ-metallo-ione acquistino una peculiare conformazione dipendente dal metallo legato, conferendo così all'Aβ particolari proprietà citotossiche. Tale citotossicità risulta particolarmente evidente per il complesso Aβ-Al che è in grado di aumentare, in maniera significativa, la tossicità data dalla sola Aβ o dalla stessa Aβ coniugata con metalli diversi dall'Al.

All'interno di questo quadro sperimentale si è poi cercato di indagare più nel dettaglio i meccanismi con i quali Aβ, e i suoi complessi metallici, esercitassero la loro citotossicità. A questo scopo sono stati impiegati due composti quali il resveratrolo e il colesterolo, che vanno ad agire su due meccanismi che stanno alla base della tossicità dell'Aβ, come lo stress ossidativo e l'alterata fluidità delle membrane cellulari.

Nel primo caso, i dati in vitro hanno permesso di dimostrare come, agendo in maniera selettiva sulla produzione di specie reattive dell'ossigeno (ROS) Aβ-mediata, sia possibile ridurre la tossicità di Aβ e dei suoi complessi con metalli redox (rame e ferro) mediante un meccanismo di scavenging dei ROS ad opera del resveratrolo, dalle spiccate proprietà anti-ossidanti e neuro-protettive.

A questo punto **s**i è indagata la capacità dei vari complessi Aβ-metalloioni di alterare la struttura di membrane lipidiche attraverso l'uso di modelli di membrane cellulari. In precedenza si era dimostrato come il complesso Aβ-Al fosse l'unico complesso in grado di alterare significativamente la fluidità di layer lipidici. I dati ottenuti ci permettono di affermare che tale capacità è dovuta principalmente alla elevata idrofobicità superficiale del complesso Aβ-Al. Inoltre, agendo sulle membrane cellulari con concentrazioni fisiologiche di colesterolo è stato possibile ridurre l'"irrigidimento" delle membrane (lipidico) conseguente alla presenza di Aβ-Al, e ridurne la citotossicità.

Si é quindi approfondito il ruolo geno-tossico dei succitati complessi Aβ-metalloioni andando ad indagare come questi siano in grado di modulare in maniera significativa (e metallo-dipendente) l'espressione genica di numerosi trascritti coinvolti nella patologia di Alzheimer. In particolare, il nostro interesse si è focalizzato sui complessi Aβ-Cu e Aβ-Zn, che si sono rivelati in grado di modulare selettivamente l'espressione di geni coinvolti in processi infiammatori, nello stress ossidativo e nella morte cellulare (apoptosi).

Dopo questa serie di studi *in vitro* si è passati ad indagare l'espressione genica dell'intero genoma umano in un modello in vivo di patologia di Alzheimer. Lo scopo era quello di identificare il network o il pathway d'espressione coinvolti della disomeostasi cationica. I profili d'espressione del modello murino 3xTg-AD sono stati pertanto confrontati con quelli del controllo wild type. In questo contesto, si è scoperta una significativa sovrapposizione dei geni sovra- e sotto-espressi tra topi *wild type* anziani e topi 3xTg-AD

giovani. Questo dato supporta l'idea che il substrato patologico dell'AD possa favorire un processo di invecchiamento precoce. All'interno del gruppo di geni trovati differenzialmente espressi, molti erano coinvolti nell'omeostasi del calcio, ione chiave per la fisiopatologia cellulare.

Il secondo filone di ricerca ha riguardato lo studio del ruolo dello ione calcio nell'eccitotossicità dei neuroni dello striato. Tale fenomeno è particolarmente importante in alcune patologie neurodegenerative che hanno come segno caratteristico una progressiva e irreversibile perdita del controllo motorio, come ad esempio il morbo di Huntington. L'interesse si è focalizzato nel determinare il perchè una subpopolazione di neuroni striatali, caratterizzata dalla sovraespressione di nitrico-ossidosintasi, non vada incontro ad apoptosi in seguito a stress eccitotossico. I dati raccolti ci hanno permesso di stabilire che la resistenza di tale sottopopolazione al sovraccarico di calcio è dovuta principalmente ad una potenziata capacità di questi neuroni di detossificarsi rapidamente dalle specie ROS, di origine mitocondriale, specie che si generano durante fenomeni eccitotossici.

Conclusione. Nel complesso i dati ottenuti sottolineano una volta di più un ruolo centrale degli ioni metallici nello sviluppo e/o nella progressione di alcune patologie a carattere neurodegenerativo. In particolare è importante notare come, a fianco di alcuni ioni metallici endogeni - che hanno un rilevante ruolo fisiologico (ferro, rame, zinco, calcio) -, anche altri ioni privi (apparentemente) di un ruolo biologico, ma coi quali ci interfacciamo quotidianamente, come ad esempio l'alluminio, sembrino svolgere un ruolo chiave in processi eziopatogenetici legati a fenomeni neurodegenerativi.

SUMMARY

In the present study metal ions role in neurodegenerative processes has been investigated. Two major pathways have been developed: 1) metal ions role in β-amyloid (Aβ folding and deposition from *in vitro* to *in vivo*; 2) calcium dyshomeostasis in an *in vitro* model of neurodegeneration.

Firstly, metal ions role (aluminum, copper, iron, zinc) in Aβ folding and deposition was assessed. Aβ misfolding is, in fact, believed to play a critical role in Alzheimer's disease pathogenesis. Our data confirm that Aβ folding is closely related to the conjugated metal ion, thereby following peculiar metal ion-dependent conformational changes. Strikingly, we report that aluminum, a non physiological metal ion, is the most efficient in "freezing" Aβ in its oligomeric and most toxic state.

Within this framework we investigated the mechanisms underlying Aβ and Aβ-metal conjugates toxicity. To that aim we employed two natural compounds (resveratrol and cholesterol) acting on two different Aβ mechanisms of toxicity: oxidative stress and membrane damage, respectively.

In both cases, *in vitro* analysis revealed that resveratrol and cholesterol do not influence Aβ and Aβ-metal conjugates folding processes, but are still effective in protecting a neuronal-like cell line against Aβ toxicity. We reported that resveratrol was able to significantly reduce the Aβ-triggered generation of reactive oxygen species, meanwhile physiological concentrations of cholesterol were effective in protecting cellular membrane structure against Aβ (especially Aβ-Al) lipid disrupting activity.

To further assess that differently shaped Aβ-metal conjugates result in different biological responses, we investigated Aβ-Cu and Aβ-Zn role in influencing/altering gene expression profile in a neuronal-like cell line. We found that these two conjugates are effective in modulating expression of transcripts involved in inflammatory processes, oxidative stress, and in apoptotic cell death.

Following these *in vitro* studies we decided to investigate whether expression of transcripts involved in metal ions homeostasis resulted affected in an *in vivo* model of the disease, represented by the 3xTg-AD mice. Our data highlight a significant overlapping between the expression profiles of young 3xTg-AD mice compared with aged wild type mice; this finding support the notion that Alzheimer's disease can be interpreted as a boosted variant of otherwise naturally occurring age-driven changes. In our dataset we found several differentially expressed transcripts involved in calcium homeostasis, a key metal ion for the physiology of the cell.

Secondly, calcium dyshomeostasis in striatal neurons following excitotoxic challenge was assessed. Striatal neurons degeneration is involved in several pathologies showing motor and behavioral sequelae, such as Huntington's disease (HD). We tried to determine why a subpopulation of striatal neurons results spared in HD striata, showing a peculiar resistance towards excitotoxic challenges. Our data demonstrate that the striking resistance of these cells may be due to boosted scavenging capabilities embedded in such neuronal subpopulation, resulting in lack of ROS generation upon excitotoxic insults.

Collectively, these findings highlight the pivotal role played by metal ions in the development of neurodegenerative disorders. Noteworthy, not only endogenous and biologically relevant metal ions (iron, copper, zinc and calcium) seem involved in the pathogenesis of neurodegenerative disorders, but also exogenous metals (i.e.: aluminum) could have a key and subtle, although less investigated, role in neuronal degeneration.

ABBREVIATIONS

Aβ	β-amyloid
AD	Alzheimer's disease
ANS	8-Anilino-1-naphthalenesulfonic acid
APP	Amyloid Precursor Protein
BBB	Blood Brain Barrier
CR	Congo Red
HFIP	Hexafluorisopropanol
HD	Huntington's disease
MAP	Microtubule Associated Protein
NFT	Neurofibrillary Tangles
nNOS	neuronal Nitric Oxide Synthase
ROS	Reactive Oxygen Species
SEM	Scanning Electron Microscopy
SP	Senile Plaque
TEM	Transmission Electron Microscopy

1. METAL IONS DYSHOMEOSTASIS IN ALZHEIMER'S DISEASE

1.1 CONFORMATIONAL DISEASE

Biological systems rely on a huge number of protein interactions as they undergo the wide diversity of physiological functions. This is the case, for instance, regarding ionotropic glutamatergic receptor, where its full function relies on the correct subunit arrangement in the formation of highly ion-specific tetrameric structures.

Although cell quality-control systems provide for the correct folding of proteins during cell life, misfolded proteins can still interact each other, leading to a series of pathologies known as "*conformational diseases*". This definition belongs to a peculiar feature of these pathologies: the aberrant conformation of non-native proteins leading to their detrimental aggregation. Conformational diseases include: Alzheimer's disease (AD), Parkinson's disease (PD), Huntington's disease (HD), prion encephalopathies, and many others. All these pathologies arise when specific proteins undergo conformational changes, become prone to aggregation, and deposit within tissue or intracellular compartments (Kopito and Ron, 2000).

Protein misfolding and aggregation have been identified as potential pathological events in the neurodegenerative cascade. In the last two decades several findings helped to unravel the biochemical, biophysical, and molecular determinants lying behind protein misfolding, although downstream mechanisms of protein deposition are still largely unknown (Dobson, 2003; 2006).

1.2 ALZHEIMER'S DISEASE

AD is one of the most common forms of dementia in the elderly and accounts for an estimated 60 to 80 percent of cases (Querfurth and LaFerla, 2010). With the life expectancy increase in the developing countries AD is becoming a pathology with relevant health, social, and economic outcomes.

AD neurological symptoms have been described for the first time more than 100 years ago and are now well coded, they include: memory loss, challenges in planning or solving problems, confusion with time or place, problems with words in speaking or writing, and changes in mood and personality. AD patients shift from early stages of AD to fully blown pathology at different rates, with a progressive and unrestrainable loss of cognitive and functional abilities.

Meanwhile AD behavioral outcomes are well known, molecular determinants of the pathology are still under investigations. To date three main histological hallmarks characterize the disease at the molecular level: intra and extra-cellular deposition of β-amyloid (Aβ), formation of neurofibrillary tangles (NFTs; aggregates made from the hyperphosphorylated tau protein), and severe brain atrophy (Bibl et al., 2012).

Compelling evidence support a critical role played by Aβ in the disease pathogenesis. Deregulation of Aβ metabolism and its consequent aggregation set in motion a pathogenic cascade of

events that ultimately result in the development of AD-related pathology, cognitive decline, and behavioral deficits (Selkoe, 1991;Mucke and Selkoe, 2012).

1.2.1 From Ab to senile plaques

Aβ is a 39-43 amino-acid peptide and it is the main constituent of senile plaques (SPs). In AD patients, the most common forms of Aβ have 40 or 42 amino-acid residues, with the latter as the most amyloidogenic, prone to aggregation, and toxic form (Yin et al., 2007). Aβ derives from the cleavage of β-APP, which is itself a 695 to 770 amino-acid-residue transmembrane protein whose physiological role remains still largely unknown, although it has been recently proposed its involvement in metal homeostasis as well as in cell trafficking and signalling (Zhang et al., 2011).

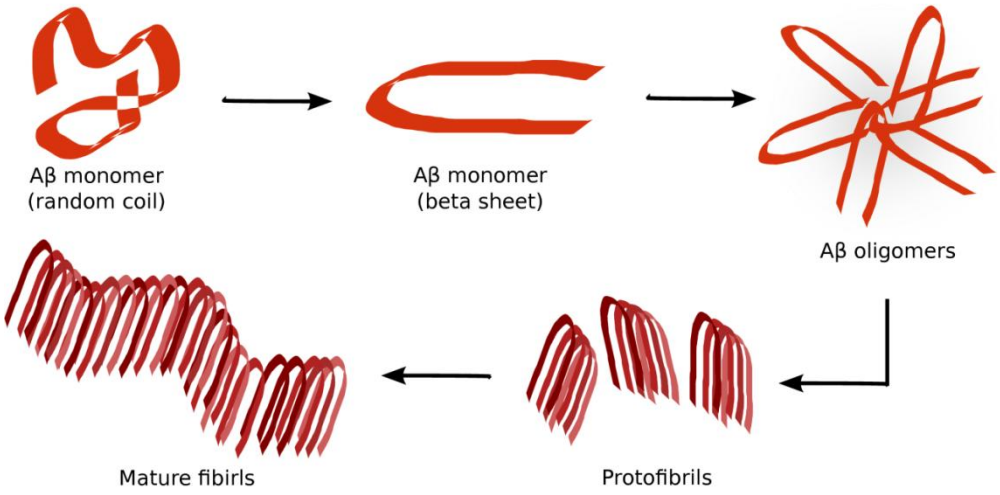

Figure 1 The Ab aggregation process follows a well-defined pathway. First, the Ab monomers with a random-coil structure acquire a b-sheet conformation. Then, these monomers aggregate into oligomeric structures that contain a variable number of Ab peptides (i.e. 2 to 50). These oligomers turn into higher-ordered structures known as protofibrils, and then these protofibrils lead to the formation of mature fibrils that deposit as senile plaques.

β-APP metabolism involves three enzymes: the α-, β- and γ-secretases. Only when β-APP is cleaved by the last two Aβ is formed. This β- and γ-secretases-mediated processing has been termed the "*amyloidogenic pathway*" (Hardy and Higgins, 1992). On the contrary, when the physiological non-amyloidogenic pathway occurs, β-APP is metabolised by α-secretase and γ-secretase, which releases neither toxic nor pro-aggregation byproducts (Wilquet and De Strooper, 2004). Once it has been released, Aβ follows a process of aggregation that has been largely characterized (Fig. 1).

The *in-vitro* aggregation kinetics of the 42-residue Aβ peptide can be summarised as follows (see Fig. 1): (i) Random coiled Aβ monomers turn quickly into (ii) β-sheet Aβ monomers. This shift leads to the

formation of (iii) soluble, low-molecular-weight oligomers, which become (iv) paranuclei (higher ordered structures), and then (v) protofibrils, and eventually (vi) larger fibrils, which represent the main constituent of SPs (Chiti and Dobson, 2006;Miller et al., 2010a).

However, SPs are the downstream event of a more complex process. Over these last two decades, research interest has shifted upstream, with the report that pre-fibrillar Aβ species, and especially Aβ oligomers, are significantly more toxic than mature Aβ fibrils (Sakono and Zako, 2010;Benilova et al., 2012;Marcello et al., 2012). These findings are in agreement with clinical observations in which has been reported that patients lacking SPs show AD-like cognitive impairment (Terry et al., 1991;Dickson et al., 1995;Walsh et al., 2002).

Meanwhile *in vitro* Aβ aggregation is performed in a tightly and highly controlled environment, Aβ behaviour *in vivo* can be influenced by a large number of variables. Within these, metal ions aroused great interest for three main reasons: 1) patients with AD show pronounced metal dyshomeostasis in the brain; 2) high metal concentrations have been found within SPs (Tab. 1); and 3) it is well established that metals can influence and/or alter the Aβ aggregation pathway (Bush, 2003;Zatta et al., 2009;Granzotto and Zatta, 2012;Roberts et al., 2012).

In the following sections, the roles of some of metal ions (Al, Fe, Cu and Zn) that can influence the folding behaviour of Aβ will be considered and critically discussed, along with the AD "metal hypothesis" (Bush, 2012).

Metal ion	Concentration (μg/g senile plaque)
Al^{3+}	40*
Cu^{2+}	30[#§]
Fe^{3+}	53[#§]
Zn^{2+}	87[#§]

*Yumoto et al. 2009; [#]Lovell et al. 1998; [§]Frederickson et al. 2005

TABLE 1. METAL ION CONCENTRATIONS DETECTED IN THE CORES OF SENILE PLAQUES FROM PATIENTS WITH AD.

1.2.2 ROLE OF METAL IONS IN AB FOLDING

ALUMINUM

Aluminum (Al^{3+}) is the most abundant element in the Earth crust, although it is not involved in any specific vital biological processes. For this reason, the discovery of relative high Al^{3+} concentrations in senile plaques of post-mortem brains from patients with AD aroused great interest, suggesting a possible role for Al^{3+} in the pathology of AD (Perl and Brody, 1980;Yumoto et al., 2009;Bolognin and Zatta, 2011).

Along with all of the other electrically charged elements and molecules, Al^{3+} cannot be passively transported through the blood–brain barrier (BBB). Once it has been absorbed through the digestive system, Al^{3+} enters the bloodstream; here, it appears to be linked mainly to citrate and transferrin.

However, when it reaches the brain vessels, Al^{3+} can indeed pass across the BBB via a transferrin-receptor-mediated endocytosis mechanism (Yokel, 2002). Once reached the cerebrospinal fluid, Al^{3+} can influence Aβ folding process, although its role in the pathology of AD is still debated and controversial (Tomljenovic, 2011). Furthermore, it has been demonstrated that Al^{3+} can pass through the BBB when conjugated with Aβ. In this case, the Aβ-Al(III) conjugate has a prompter access to brain cells than Aβ alone (Banks et al., 2006).

In contrast to Cu^{2+} and Zn^{2+} (discussed below), the Aβ-Al conjugates have been studied to a lesser extent. Nevertheless, data reported from our and other laboratories indicated that Al^{3+} can maintain Aβ in its oligomeric or prefibrillar state, and can promote Aβ exposure of hydrophobic clusters (Bolognin et al., 2011;Chen et al., 2011). On the contrary, other studies have supported a role for Al^{3+} in the coordination of higher Aβ structures, such as fibrils, and in the promotion of their deposition.

Focusing on the chemical level, the presence of binding sites for Al^{3+} on Aβ has not been well established. Two different binding mechanism for Al^{3+} with Aβ were proposed several years ago by Fasman et al. (1996), and more recently by our group (Ricchelli et al., 2005). In the former study, it was proposed Al^{3+} ability to coordinate with four Aβ amino acids: Asp, Ser, Tyr and Glu, probably because their high –OH-group content. In our study, we broadened the possible interaction sites to the 1-16 and 20-35 amino-acid sequences (Ricchelli et al., 2005).

As more recently reported (Kawahara and Kato-Negishi, 2011), the ability of Al^{3+} to coordinate Aβ and to modify its folding properties is due to two Al^{3+} properties: 1) Al^{3+} has a strong positive charge that is coupled to 2) a small ionic radius (50 pm), as compared to the other metal ions discussed here. These features mean that Al^{3+} can be considered as an excellent protein cross-linker. Thus, a role for Al^{3+} in τ folding needs to be investigated, because of its great number of phosphorylated sites; indeed, these R-OPO_3^{2-} sites result targets of choice for Al^{3+}-like metals.

Recently reported ESI-MS (Electrospray ionisation mass spectrometry) data (Bolognin et al., 2011) showed that a bare Al^{3+} ion can bind to a single Aβ peptide, although other groups (Chen et al., 2011) have hypothesised that two Al^{3+} ions can coordinate each Aβ peptide. In the latter study, the authors correctly reported a lack of data concerning Al^{3+} concentration in their stoichiometric experiments, questioning the obtained results. This issue arose because Al^{3+} can form hydroxide complexes at neural pH (Martin, 1992); however, the use of aluminum lactate can help to avoid, or at least delay, Al^{3+} hydroxide precipitation (Ricchelli et al., 2005).

Collectively, although several biophysical and immunological techniques have been used to demonstrate that Al^{3+} can 'freeze' Aβ in oligomeric and highly hydrophobic structures (Bolognin et al., 2011), two key data appear to be missing: 1) the structure of the exact Aβ-Al oligomeric conjugate; and 2) the association constant (K_a) of this complex. In agreement, Bolognin et al. (2011) hypothesised that Al^{3+} can form Aβ oligomers tout court, while Chen et al. (2011) proposed the formation of Aβ-Al annular protofibril structures.

The present lack of studies does not allow us to provide data concerning the issue of a K_a for Aβ-Al interaction; however, at the same time, it is possible to state with confidence that Aβ-Al K_a is greater than deferoxamine mesylate K_a ($K_a = 10^{-22}$ M), indeed, this iron/ aluminum chelating agent can reverse Al^{3+} influence on Aβ oligomerization process (House et al., 2004;Ricchelli et al., 2005).

COPPER

Copper (Cu^{2+}) is an essential metal ion involved in several biological processes and analytically found in senile plaques at lower levels (400 μM) compared with other metal ions, such as Zn^{2+} (1 mM) and Fe^{3+} (1 mM). A potential role for Cu^{2+} in AD aroused interest for two main reasons: Cu^{2+} influence on Aβ conformational changes, and the reduction of Cu^{2+} to Cu^{+}. The latter is particularly relevant for Aβ-derived reactive oxygen species (ROS) production [Hureau and Faller 2009], in fact the Aβ-Cu conjugate seems to exert its toxicity via ROS production [see Hung et al. 2010]. The electron necessary to reduce Cu^{2+} to Cu^{+} can be donated by either Aβ internal amino-acids or external reductant molecules [Smith et al., 2007].

On the structural level, Cu^{2+} role in Aβ aggregation has been widely studied, and a large body of evidence supports the hypothesis that Cu^{2+} might be involved in the acceleration of Aβ deposition into amorphous aggregates [Tougu et al., 2009; Bolognin et al., 2011]. State-of-the-art coordination chemistry of Aβ/Cu^{2+} has shown that there are four putative residues proposed as Cu^{2+} binding sites on Aβ: His6, His13, His14, Tyr10 [Faller, 2009; Hong et al., 2010; Eury et al., 2011]. Nevertheless, Cu^{2+} can bind other residues in the Aβ N-terminus (e.g. Asp1, Glu11) [Miller et al. 2010]. In agreement [Miller et al., 2010], this variability might be due to the different conditions under which the aggregation processes have been performed.

Conformational changes due to the Cu^{2+}/Aβ interaction appear to result in reduced exposure of the Aβ-Cu hydrophobic clusters, as compared with Aβ alone or with its complexes with other metal ions, such as Zn^{2+} and Al^{3+} (see above) [Granzotto et al., 2011]. This event might lead to decreased interactions between the Aβ-Cu conjugate and the hydrophobic cellular phospholipids [Suwalsky et al., 2009], although it has been proposed that in the presence of Cu^{2+}, Aβ forms channel-like structures in cell membranes [Curtain et al., 2001].

Recent findings supported by ESI-MS have reported that Aβ is metallated by a bare Cu^{2+} ion [Bolognin et al., 2011; Chen et al., 2011]. This interaction appears to increase Aβ random coil content, which leads to the formation of non-fibrillar amorphous aggregates. Indeed, it has been shown that an elevated β-sheet content is required for fibril formation [Lin et al., 2010], while the random coil content leads to disordered aggregate deposition.

Different Aβ-Cu affinities have been proposed for the $Aβ_{1-40}$ peptide, which depend on the Aβ secondary structure: 0.14 $μM^{-1}$ for $Aβ_{1-40}$ in a random-coil structure, and 0.05 $μM^{-1}$ for $Aβ_{1-40}$ in the beta-sheet stimulated conformation [Yang et al., 2010]. This scenario is further complicated by the variable molar ratios of Aβ and Cu^{2+} in the extracellular space. It has been reported that a sub-equimolar Aβ/Cu^{2+} ratio leads to amorphous and stable aggregates; vice versa, supra-equimolar ratios can lead to the

formation of more toxic oligomeric structures [Smith et al., 2007]. This hypothesis was recently confirmed by Pedersen et al. (2011), in which the discovery of distinct Cu^{2+}-concentration-dependent Aβ-aggregation pathways supports a key role for metal homeostasis in the folding of Aβ and, consequently, in its toxicity. Together with our recent findings [Granzotto et al., 2011; Bolognin et al. 2011], these data support the idea that Aβ-Cu conjugate exerts its toxicity mainly via ROS production.

IRON

As for Al^{3+}, iron (Fe^{3+}) has also been studied to a lesser extent than other metals, despite its key role in several biological functions (e.g. as a cofactor or an O_2 carrier, among other functions) and its redox properties. Here, we focus our attention on Fe^{3+}, instead of the reduced Fe^{2+} form.

Data in the literature support the idea that Fe^{3+} can lead to the formation of a heterogeneous population of amorphous aggregates, thus shifting from oligomers to larger, high-molecular-weight structures. ESI-MS analyses have shown that Aβ can bind two Fe^{3+} ions (Bolognin et al., 2011;Chen et al., 2011). These Fe^{3+} ions appear to be coordinated via His13, His14 and Tyr10 (Ali-Torres et al., 2011). The same study also supported the idea that Aβ forms more stable complexes when it binds to Fe^{3+} rather than to Fe^{2+}. It has been recently reported that Fe^{3+} increases Aβ random coil content (Liu et al., 2011a), which promotes the deposition of amorphous aggregates, as described for Cu^{2+}. This conformational change is associated with decreased exposure of hydrophobic clusters (Bolognin et al., 2011;Chen et al., 2011), reducing possible interactions between the Aβ-Fe conjugates and lipid bilayers of the cell (Suwalsky et al., 2009). Similarly to Cu^{2+}, Fe^{3+} interactions with Aβ can catalyse the generation of hydrogen peroxide (H_2O_2); consequently, a lack of detoxifying enzymes or an accumulation of Aβ-Fe species (both Fe^{2+} or Fe^{3+}) can trigger ROS formation via Fenton reaction (Zatta et al., 2009).

Very little is known about Aβ affinity for Fe^{3+}, as the lack of studies does not provide data related to this conjugate. Despite this, as for Aβ-Al, it is possible to assume that Aβ affinity for Fe^{3+} is lower than that of Fe^{3+}-chelating agents (e.g. deferoxamine mesylate); indeed, these compounds can revert the Aβ-Fe aggregation process (House et al., 2004).

Overall, data herein reported support the hypothesis that Aβ-Fe exerts its toxicity through two independent mechanisms. One mechanism involves ROS production, the other involves changes in Aβ conformation. The latter appears to be less convincing for two reasons: 1) Fe^{3+} only delays Aβ deposition in large amorphous aggregates, as Aβ-Fe oligomers are limited in time and tend to deposit into SPs; 2) data that support this hypothesis appear poor (Liu et al., 2011a) because do not discriminate between toxicity due to ROS production or to conformational changes in Aβ; moreover, Aβ concentration used was largely higher than that of other studies reported in literature (10 μM vs. 0.5 μM).

ZINC

The role of zinc (Zn^{2+}) in the pathophysiology of the central nervous system has been widely debated, and its involvement in neurodegenerative disorders appears to be well established. Its deregulation has an important role in AD (Sensi et al., 2009). At the same time, Zn^{2+} has key roles in synaptic functions, neurotransmission, and cell signalling. Intracellular Zn^{2+} is usually maintained at low basal concentrations through three mechanisms: 1) Zn^{2+} transporters; 2) Zn-importing proteins; and 3) the buffering action of metallothioneins. In addition to metallothioneins, Zn^{2+} is stored at high concentrations (≈1 mM) in presynaptic vesicles and co-released with glutamate during neurotransmission (Corona et al., 2011). Once in the synaptic cleft, Zn^{2+} can bind to Aβ, promoting its conformational modifications.

Due to the importance of Zn^{2+} in cell physiology, its ability to modify Aβ structure and Aβ aggregation pathway has been largely characterised. As for the other metal ions, Aβ-Zn stoichiometry was assessed through ESI-MS. Data reported in literature support the idea that a single Zn^{2+} ion binds to Aβ (Bolognin et al., 2011; Chen et al., 2011). In agreement with many nuclear magnetic resonance studies (Syme and Viles, 2006;Faller, 2009;Nair et al., 2010), the bare Zn^{2+} ion binds the N-terminal region of Aβ, probably involving the same Cu^{2+}-binding residues, His6, His13 and His14, although four other potential binding sites have been proposed: Asp1, Glu3, Asp7 and Glu11 (Miller et al., 2010b).

Morphology of Aβ-Zn aggregates has been investigated by different groups, with the use of several biophysical and immunological techniques. The results reported appear comparable and are largely accepted. Atomic force microscopy and transmission electron microscopy, together with dot-blotting, have shown that Zn^{2+} promotes Aβ deposition into amorphous aggregates that can coexist with heterogeneous oligomers (Bolognin et al., 2011; Chen et al., 2011; Miller et al., 2010).

Despite the similarities between Aβ-Cu and Aβ-Zn (which can be attributed to their comparable ionic radii: 74 pm for Zn^{2+}, and 73 pm for Cu^{2+}), Zn^{2+} is more effective in promoting Aβ exposure of hydrophobic clusters (Bolognin et al., 2011;Chen et al., 2011;Granzotto et al., 2011). This supports the idea that Zn^{2+} binding sites are different from Cu^{2+} ones (see above).

The apparent dissociation constants of Zn^{2+} from Aβ were reviewed by Faller and Hureau (2009), they hypothesised that Aβ-Zn K_d lies in the range of 1 μM to 20 μM. This variability is mainly due to the different conditions that are used to assess K_d values (e.g. buffer, metal-ion concentration, protein concentration, metal/protein stoichiometry).

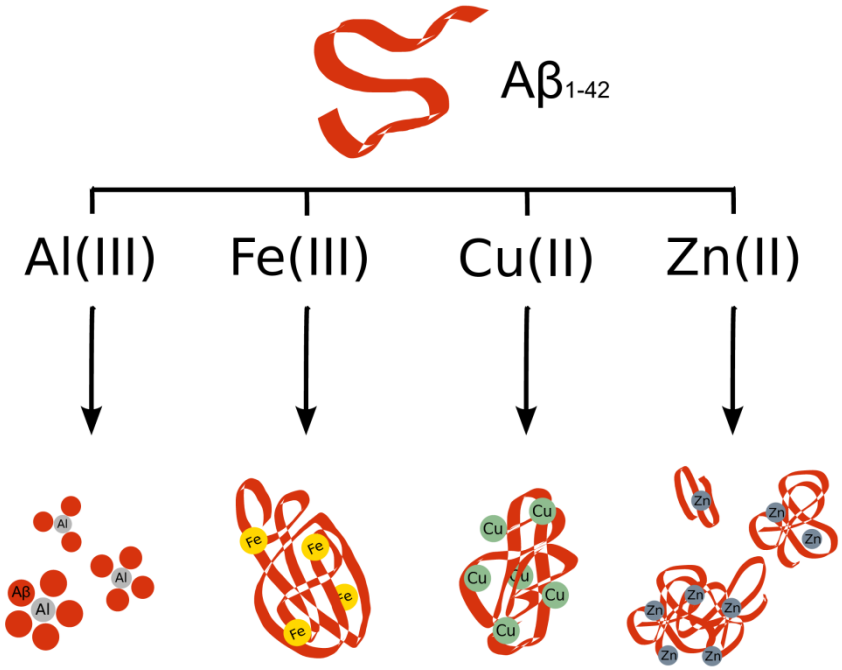

FIGURE 2 ALUMINUM, IRON, COPPER AND ZINC DIFFERENTIALLY ALTER AB AGGREGATION. AL(III) PROMOTES THE FORMATION OF HIGHLY HYDROPHOBIC AB OLIGOMERS (I.E. FROM TRIMERS TO HEXA-HEPTAMERS); FE(III) PROMOTES AB DEPOSITION INTO AMORPHOUS STRUCTURES; CU(II) LEADS TO THE FORMATION OF DISORDERED/ AMORPHOUS STRUCTURES; AND ZN(II) TRIGGERS THE FORMATION OF AMORPHOUS AGGREGATES.

1.2.3 FROM TAU PROTEIN TO NEUROFIBRILLARY TANGLES

Aberrant tau (τ) protein phosphorilation and aggregation lead to the formation of neurofibrillary tangles (NFTs). Natively, tau protein (a microtubule-associated protein, MAP) binds to microtubule in order to stabilize their structure during polymerization - depolymerization processes. Tau protein is enriched in positive charged amino acidic residues allowing its interaction with microtubule negative charged residues. In AD patients or those with frontotemporal dementia (FTD), tau becomes increasingly phosphorylated (hyperphosphorylated) at both physiological and "pathological" phosphorylation sites, which causes it to detach from microtubules (Ittner and Gotz, 2011). Thus, microtubules lack their stabilizing agent resulting in morphological impairment and compromise of axonal transport, possibly contributing to disease development (Gotz et al., 2006;Iqbal et al., 2009).

Similarly to Aβ fate, compelling evidence highlight that soluble hyperphosphorylated tau contributes to neuronal dysfunction before its deposition; a molecular mechanism that better correlates with the AD related cognitive decline (Santacruz et al., 2005).

1.2.4 AB TOXICITY MECHANISMS

Several Aβ toxicity mechanisms have been reported over the last decade, although only a fraction of these have addressed AD metal dyshomeostasis or the roles of metal ions in Aβ miss-folding. The most studied mechanism through which Aβ-metal conjugates exert their toxicity is ROS production. Aβ produces

H_2O_2 in the presence of biological reducing agents (Behl et al., 1994). Aβ ROS generation is promoted by the presence of transition metals, such as Cu^{2+} and Fe^{3+}, which can lead to the formation of free radical species through Fenton reaction (for a detailed review, see Hureau and Faller, 2009). The metal ions that are not involved in redox reactions (*i.e.* the aforementioned Al^{3+} and Zn^{2+}) appear to be involved indirectly in ROS production. As recently demonstrated (Duce et al., 2010), Aβ-Zn can inhibit iron-export ferroxidase activity; this results in Fe^{2+} accumulation, leading to detrimental oxidative stress in cortical neurons. Also, Al^{3+} has a pro-oxidative role, as it promotes Fe^{2+}-induced lipid peroxidation (Zatta et al., 2002). Unfortunately, data concerning the role of Aβ-Al^{3+} in lipid peroxidation is missing; therefore, the shedding of light on this issue would be of great interest.

As well as ROS production, we have recently demonstrated a second mechanism through which Aβ-metal conjugate exert their toxic effects. In comparing Aβ-metal aggregation data with the effects of Aβ-metal conjugates on membrane models and in toxicity essays, we found a close correlation between Aβ-metal exposure of hydrophobic clusters and membrane damage. This effect, together with other data in the literature herein reported, might explain why the Aβ-Al conjugate is the most effective in reducing cell viability in our cellular model. Indeed, Aβ-Al owns three characteristics that justify its toxicity under our experimental conditions: 1) it is the most effective Aβ-metal conjugate in retaining its oligomeric structure; 2) it is the most effective Aβ-metal conjugate in the exposure of hydrophobic clusters; and 3) it can induce lipid peroxidation. The other Aβ-metal conjugates express no more than two of these features. In addition to these two main mechanisms, others have been reported, and in particular, Aβ interaction with synaptic receptors, such as metabotropic glutamate receptors and NMDA receptors. In these cases, direct binding of Aβ to the receptor might not occur. More likely Aβ can indirectly modulate synaptic receptors through its membrane association (Ittner and Gotz, 2011); this hypotheses confirms the need for highly hydrophobic Aβ oligomers able to penetrate into lipid bilayers.

This scenario is further complicated by the difficulty of isolating well characterised and homogeneous Aβ or Aβ-metal aggregates. Furthermore, data reported in literature show large differences in data obtained with synthetic or with naturally occurring Aβ oligomers. Indeed, the latter require much lower concentrations to exert comparable toxic effects on cellular models (Li et al., 2011), highlighting possible structural, as well as biochemical (*e.g.* glycosylation), differences between these *in-vitro* and *in-vivo* Aβ aggregates.

1.3 Materials and methods

1.3.1 Chemicals

Human β-amyloid 1–42 was purchased from Invitrogen. L-lactic acid aluminum salt, $FeCl_3$, $CuCl_2$, $ZnCl_2$, hexafluorisopropanol (HFIP), 3-(4,5-dimethylthiazol-2-yl)-2,5-diphenyltetrazolium bromide (MTT), 8-anilinophtalene-sulfonic acid (ANS), resveratrol, and cholesterol were purchased from Sigma-Aldrich. Synthetic dimyristoylphosphatidylcholine (DMPC) and dimyristoyl-phosphatidylethanolamine (DMPE) were

purchased from Avanti Polar Lipids. Congo Red was purchased from Merck. All *in vitro* experiments were carried out in 0.1 M Tris/HCl pH 7.4 buffer plus 0.15 M NaCl (standard medium).

1.3.2 Aβ and Aβ-metal conjugates preparation

Human synthetic Aβ was solved in HFIP for 40 min at room temperature and then separated into aliquots. HFIP was removed under vacuum in a Speed Vac (Sc110 Savant Instruments). This treatment was repeated three times [modified protocol from Dahlgren et al. (2002)]. Aβ metal conjugates were prepared by 24-h dialysis against metal solutions 10 mM ($[CH_3CH(OH)COO]_3Al$, $FeCl_3$, $CuCl_2$, $ZnCl_2$) at T=4° C using Spectra/Por® Float-A-Lyser® tubes (Spectrum Labs) with 100 Molecular Weight Cut Offs (MWCO). Then, Aβ metal complexes were dialyzed against double distilled water (three water changes, pH=7) for 24 h in order to remove metal excess. The same treatment was also performed with Aβ alone. Aliquotes of Aβ, Aβ metal conjugates were stored at -20° C until used.

1.3.3 Congo Red spectroscopic assay

Congo Red (CR) spectroscopic assay was performed in agreement with Nilsson's protocol (2004) using a 300 µL 96-well plate with U-bottom. Kinetics were followed for 24h by monitoring changes in absorbance at 487nm using a Microplate SPECTRAmax® reader. Absorbance increase at this wavelength is indicative of amyloid fibrils formation.

During resveratrol experiments final protein concentration in each well was 1,5 µM, while resveratrol concentration was 45µM (concentration ratio protein-resveratrol was 1:30). Resveratrol was dissolved in absolute ethanol.

During cholesterol experiments final protein concentration in each well was 5 µM, while cholesterol concentration was set at 50 µM (concentration ratio protein-cholesterol was 1:10). Cholesterol was dissolved in absolute ethanol.

The final ethanol concentration in wells was 2% (v/v). This concentration of ethanol in solution did not change Aβ and Aβ-metal conjugates aggregation kinetics (data not shown). The signal due to the buffer alone was subtracted.

1.3.4 ANS fluorescence measurements

Fluorescence measurements were performed using a Perkin Elmer LS 50 spectrofluorimeter equipped with a thermostatic cell holder and a magnetic stirrer. The experiments were carried out at 25 °C. Fluorescence tests with ANS (25 µM) were developed in solutions containing 5 µM human Aβ, alone or conjugated with Al^{3+}, Fe^{3+}, Cu^{2+} or Zn^{2+}, in the presence/absence of 50 µM cholesterol previously dissolved in absolute ethanol (2% v/v concentration in the final solution). Aβ and Aβ-metal conjugates spectra were recorded after 24 h of incubation with cholesterol at room temperature.

1.3.5 Turbidity assay

Turbidity assay was performed using a 300µL 96-well plate with flat bottom. Absorbance at 405nm was read using a Microplate SPECTRAmax® reader. The concentrations in the wells were the following: resveratrol 200µM, metals (Al, Fe, Cu, Zn) 400µM, ethanol 2%. The absorbance due to metallic solutions only was subtracted.

1.3.6 Transmission Electron Microscopy (TEM)

All samples at 10 µM protein concentration, after an incubation period of 24 h, were absorbed onto glow-discharged carbon-coated butwar films on 400-mesh copper grids. Grids were negatively stained with 1% uranyl acetate and observed at 40,000x by transmission electron microscopy (TEM) (Tecnai G2, FEI). The samples observed contained Aβ and its metal conjugates in the presence/absence of resveratrol (300µM in 2% v/v of absolute ethanol) or cholesterol (100 µM, 1:10 molar ratio, in 2% v/v of absolute ethanol).

1.3.7 X-Ray diffraction studies of phospholipid multilayers

We determined by X-ray diffraction the capacity of cholesterol, Aβ, the four Aβ-metal conjugates alone and in the presence of cholesterol to modify the bilayer structures of DMPC and DMPE. About 2 mg of each phospholipid was mixed in Eppendorf tubes with 160 µL of double distilled water, and aqueous solutions of Aβ, Aβ-Al, Aβ-Fe, Aβ-Cu and Aβ-Zn in the absence and presence of cholesterol (previously dissolved in absolute ethanol). The effect of cholesterol alone on DMPC and DMPE multilayers was tested in a range of concentrations (5 to 50 µM). The final concentrations used consisted in 5 µM for the Aβ-metal conjugates, 50 µM for cholesterol (1:10 molar ratio) and 0.2% v/v for the ethanol as cosolvent. Each sample was incubated for 15 min at 30 °C and 60 °C with DMPC and DMPE, respectively. After that, samples were centrifuged for 10 min at 2200 rpm, specimens were then transferred into 1.6 mm dia special glass capillaries (Glas Technik and Konstruktion, Berlin, Germany) and X-ray diffracted with Ni-filtered CuKα from a Bruker Kristalloflex 760 (Karlsruhe, Germany). Sample distances from the detector were 8 and 14 cm. The relative reflections intensities were obtained in a MBraun PSD-50M linear position-sensitive detector system (Garching, Germany); all the experiments were performed at 17 ± 2°C, which is below the main phase transition temperature of both DMPC and DMPE. Each experiment was repeated twice, and further measurements were performed if there was uncertainty in the data.

1.3.8 Neuroblastoma cell cultures

SH-SY5Y human neuroblastoma cells were from ECACC (European Collection of Cell Culture). The medium in which they were cultured contained DMEM/F12 (Gibco, Carlsbad, CA, USA) with 15% (v/v) fetal bovine serum (FBS, Sigma-Aldrich), 100 units/ml penicillin and 100 µg/ml streptomycin (Gibco) and 1% (v/v) MEM (Minimum Essential Media) non essential amino acid (NEAA) (Sigma-Aldrich). Cells were stored

at 37° C with 5% CO_2 in a humidified atmosphere (90% humidity). Cells were plated onto 24-wells plate for MTT viability assay, or onto 25/75 cm^2 flaks. SH-SY5Y were used until passage 25. The culture medium was replaced every two days with complete fresh medium.

1.3.9 Cell viability assay

Cell viability was determined through MTT reduction assay. SH-SY5Y cells were seeded into 24-wells plates at a density of 15 x 10^4 cells per well in 1 ml culture medium. 15% FBS-culture medium containing: Aβ, Aβ-metal conjugates (0.5µM) with/without resveratrol (15 µM) or cholesterol (5 µM) was added to the cells for 24 hours. Resveratrol and cholesterol were dissolved in absolute ethanol, the final ethanol concentration in the medium was 0,2% (v/v). This ethanol concentration resulted largely non-toxic. 24 h after the treatment 100 µL of 5 mg/ml MTT were added to each well and incubated in the dark at 37° C for 3 hours. Then, medium was removed and cells were lysed with 1 ml of acidic isopropanol (0.04 M HCl in absolute isopropanol) (Hawtin et al., 1995). MTT color intensity was measured with a 96-well ELISA plate reader at 550 nm (Microplate SPECTRAmax®). Toxicity due to metals alone (5 µM) in the presence and in the absence of resveratrol (15 µM) or cholesterol (5 µM) was also tested. All MTT essays were performed at least three times, in triplicate. Viability was defined as the relative absorbance of treated *vs.* untreated, expressed as a percentage.

1.3.10 SOD assay

Total cellular superoxide dismutase (SOD) activity was determined with a SOD assay kit (Sigma-Aldrich) by following manufacturer's protocol. 1.0 x 10^6 neuroblastoma cells were seeded into 25cm^2 flasks. Cells were grown at 80% confluency, and then treated with Aβ, Aβ-metal complexes (0.5µM in the medium) and metals alone (5 µM), in the presence or in the absence of resveratrol (15µM in the medium). After 24h cells were scraped, washed three times in cold PBS buffer and then disrupted using Cell Extraction Buffer (Invitrogen) containing 1mM PMSF and 1x protease inhibitor cocktail (Sigma-Aldrich). Whole cell lysates of SH-SY5Y was centrifuged at 10,000 rpm (4° C, 10 minutes). Supernatant was transferred into 0.5 mL Eppendorf tube. Obtained solutions were used to determine protein concentration and SOD activity.

1.3.11 Microarray analysis of neuroblastoma exposed to Ab-metal conjugates

Cell treatment

Cells were plated onto 6-well plates; the day after, standard medium was replaced with 2% FBS medium containning Aβ-Cu and Aβ-Zn at 0.5µM concentration. Cells were incubated for 24 h. As control, cells were treated with medium containing metals alone at a concentration 10-fold higher than that of the peptide (5µM).

RNA ISOLATION, QUALITY CONTROL AND LABELING

Total RNA isolation from neuroblastoma cells was performed using Qiagen RNA/DNA Mini Kit (Qiagen) following manufacturer's instructions. RNA quality was determined through RNA 6000 Nano LabChip and the Agilent Bioanalyzer 2100 (Agilent Technologies). Afterwards 1 µg of total RNA was amplified following the Superscript™ Indirect RNA Amplification System Kit (Invitrogen™). First, single-stranded complementary DNA (cDNA) was generated and then synthesis of the second-strand cDNA was obtained. The double stranded cDNA was used as template for the *in vitro* transcription reaction performed using T7-RNA polymerase to generate antisense RNA (aRNA), complementary to the cell exctracted mRNA. To allow RNA fluorescent detection 10 µg of aRNA were conjugated with Alexa Fluor 555 or Alexa Fluor 647 dyes (Invitrogen) following manufacturer's instructions.

MICROARRAY

Labeled aRNA was dissolved in 90 µl of hybridization buffer, denaturated at 90° C for 3 min and applied directly to human OpArrays DNA microarray slides containing 35130 spotted oligonucleotide sequences representing 29166 different human genes (Operon Biotechnologies). Each slide was hybridizated with treated (Aβ, Aβ-Cu, Aβ-Zn, Cu or Zn) and untreated (sham) samples. Microarray hybridization was carried out in an ArrayBooster Hybridization Station (Advalytix). The reaction was carried out overnight at 42° C. Posthybridization washing was performed according to the microarray slides manufacturer's instructions. Two replicates of each experiment were performed using different microarray slides, in which sample and control RNA, labeled either with Alexa Fluor 555 or Alexa Fluor 647 fluorochromes, were crossed in both combinations (dye-swapping procedure). Each experiment used material from the same cell culture and therefore represents a technical replicate. The microarrays slides were scanned using a GenePix 4000B laser scanner (Molecular Devices Corp., Sunnyvale, CA, USA) and images were processed using Genepix 6.0 software. Microarray data are deposited in the GEO public database (accession number: GSE23000). All data are MIAME compliant.

STATISTICAL ANALYSIS OF MICROARRAY DATA

Statistical analysis of the microarray data was performed using Acuity 4.0 software (Molecular Devices). Initial results were normalized using Lowess algorithm and filtered to exclude extreme outliers and flags. We also excluded any spot that had no detectable response on all slides. The log-ratios of expression were calculated as the base 2 logarithm of the ratios of background-corrected intensity medians of red dye over green dye intensities. In order to obtain a single expression value for each gene, the internal replicates (1 to 14) were plotted versus the technical replicates (6 for Aβ treatment and 2 for Al and Aβ-Al complex treatment). The X-Y scatter plot confirmed that the data were generally reproducible but we observed the presence of extreme outlier values. Then we excluded the outliers and the values of

spots replicates within arrays were averaged using a trimmed mean. We excluded any spot that had no detectable response in all three treatments. Consequently, the final dataset was composed of 28676 genes. In order to identify important genes with great statistical confidence, statistical testing and fold change criteria were employed simultaneously. A gene was considered to be differentially expressed if it had an absolute value of a log-ratio higher or equal to 0.5, representing a fold-change of 1.4 in transcript quantity. Student's t-test was applied and statistical significance set at $p<0.05$.

1.3.12 Microarray analysis of young and aged 3xTg-AD hippocampi

Animal models

All the procedures involving animals were approved by the institutional Ethics Committee (Ce.S.I. protocol #: AD-301) and performed accordingly to institutional guidelines, and in compliance with national (D.L. n. 116, G.U., suppl. 40, 18 February 1992) and international laws and policies. 3xTg-AD female mice (n=4) and their age-matched control wild-type mice (129SV x C57BL/6; n=4) were kept in a temperature-controlled room at 25° C under a 12-h light/dark cycle and fed *ad libitum* with tap water and commercial feed. Once mice reached 3 or 12 months of age, they were anesthetized and killed by decapitation. Hippocampi were excised, transferred into RNA-later solution, and stored at -80° C for RNA processing.

Microarray analysis

Obtained hippocampi were homogenized using a hand glass potter, and total RNA was extracted using the SVtotal RNA Isolation System kit following manufacturer's instructions (Promega). RNA purity and quantity were assessed using an Agilent 8453 spectrophotometer (Agilent). RNA quality was determined by both evaluation of rRNA bands integrity using agarose electrophoresis, and absorption readings at 260 and 280 nm. Extracted RNA was linearly amplified and fluorescently labeled using the Amino Allyl MessageAmp™ II aRNA Amplification Kit accordingly to manufacturer's instructions (Ambion). Five to ten µg of amplified aRNA were fluorescently labeled with Cy3-Cy5 cyanins and then hybridized on high-density array (Mouse OneArray Whole Genome DNA microarray - Biosense) containing 31,802 well-characterized mouse transcripts.

In order to increase experimental homogeneity we performed three replicates with a dye swap and each experiment contained RNA from hippocampi of young (3 m.o.a.) and old (12 m.o.a.) 3xTg-AD mice versus age-matched WT mice hippocampal RNA as control. After hybridization, Cy3-Cy5 fluorescent signals were detected with a Confocal Laser Scanner "ScanArray Express" (Packard BioScience) and analyzed using "ScanArray Express - MicroArray Analysis System" software version 3.0 (Perkin Elmer). Experimental raw data were stored in the GEO public database (accession number: GSE35210). Values of the median signal intensity from each spot were subtracted from the local median background intensity. For each slide, after local background subtraction, LOWESS algorithm was used to normalize row data, a procedure used to evaluate signal to noise ratio and generate log ratios of sample *vs.* reference signal. A

gene was considered to be differentially expressed when showing an absolute log-ratio value higher or equal to 0.5, an index that translates into a 1.4 fold-change in transcript quantity. Analysis of data obtained by microarray experiments was performed by means of hierarchical gene clustering using Cluster 3.0 and TreeView software (Stanford University Labs) (Saldanha, 2004). To include in clustering analysis only well measured transcripts we selected spots with a present call (that means identified transcripts with measurable expression) in at least 80% of experiments and being > 1.7 fold up or downregulated. Identified clusters were then analyzed by Ingenuity Pathways Analysis (IPA) software (Ingenuity Systems), based on known molecule-molecule functional interactions, in order to classify genes accordingly to their biological functions and to disclose putative functional networks connecting specific genes. IPA infers and ranks networks by a score, expressed as a numerical value, which is a probabilistic fit between: (1) the amount of focused genes potentially eligible for network composition and present on a given gene list, (2) network size, as well as (3) all molecules present in the Ingenuity Knowledge Base that can be part of such network.

REAL TIME-PCR

Microarray results were validated performing qRT-PCR analysis on RNA extracted from hippocampi obtained from the same samples used for microarray analysis. Gene expression of three upregulated genes (BECN1, CST3, GABRA5) evidenced by microarray data was evaluated. GAPDH housekeeping gene was used as internal control to normalize the relative expression of target genes. qRT-PCR was performed in a total volume of 50 μl containing: 1x TaqMan Universal PCR Master Mix, no AmpErase UNG and 2 μl of cDNA using TaqMan assay on an Abi 7900HT Sequencing Detection System (Applied Biosytems). Real time amplifications included 10 minutes at 95°C, followed by 48 cycles of 15 seconds at 95°C and 1 minute at 60° C. Relative expression levels were calculated for each sample after normalization against the housekeeping gene GAPDH using the ΔΔCt method for comparing relative fold expression differences (Livak and Schmittgen, 2001).

1.3.13 STATISTICAL ANALYSIS

Congo Red spectroscopy, ANS fluorescence, MTT , turbidity, and SOD essays were statistically analyzed by Student's *t* test and one-way analysis of variance. Results were reported as highly statistically significant if $P<0.01$ and statistically significant if $P<0.05$. Results are presented as mean ± standard deviation (SD) or standard error (SEM).

1.4 RESULTS

In order to increase thesis readability, Results section will be broken down into different subsection, each one addressing a single topic developed to unravel Aβ-metal conjugates role in neurodegeneration. For each subsection a brief insight into the topic and the obtained results will be provided.

The four major subsections involve:

- Role of resveratrol in Aβ and Aβ-metal folding;
- Role of cholesterol in Aβ, Aβ-metal folding, and Aβ-metal conjugates interaction with cellular membrane;
- Gene expression profile of neurablastoma cells exposed to Aβ-Cu and Aβ-Zn conjugates;
- Gene expression profile of young and aged 3xTg-AD hippocampi compared with wild-type mice.

1.4.1 RESVERATROL IN AB AND AB-METAL CONJUGATES AGGREGATION AND TOXICITY

BACKGROUND

A mechanism used by Aβ, in the presence of metal ions, to exert its toxicity is the production of free radicals. In order to reduce oxidative stress in AD patients several natural compounds have been studied (Darvesh et al., 2010;Lee et al., 2010;Manczak et al., 2010). Among these drugs, resveratrol aroused great interest. This compound is a natural polyphenol present in the skin of red grapes and consequently in wine, its antioxidant properties have been well demonstrated (Fremont, 2000), it has a wide range of biological effects (Karuppagounder et al., 2009), it seems to have no adverse effects (Boocock et al., 2007) and several papers underline its Aβ anti-aggregative properties (Ono et al., 2003;Vingtdeux et al., 2008). Despite this wide range of positive effects, a major constraint holding back resveratrol use is its poor bioavailability when taken as dietary supplement (Kapetanovic et al., 2011); for that reason resveratrol has been proposed as adjunctive or supportive care for AD and not as stand-alone treatment.

RESULTS

Congo Red assay: CR is largely used in histochemical analysis for the detection of Aβ fibrils deposits. Accordingly to Nilsson et al. (2004) CR can be also used to follow amyloid fibrillization *in vitro*. As shown in fig. 3 we did not observe variations in the fibrillization process promoted by the presence of resveratrol in solution, except for Aβ-Cu metal complex. The presence of resveratrol seemed to enhance Aβ-Cu complex ability to form fibrils. Well this is interesting to note that Aβ-Al and Aβ-Fe showed no or little propensity to aggregate if compared with Aβ alone and its complexes with Cu^{2+} and Zn^{2+}. These results are not surprising, it has been previously demonstrated by this laboratory that Al^{3+} is able to "freeze" Aβ in its oligomeric state, stabilizing this assembly (Drago et al., 2008b).

In order to exclude cross-interactions, the absorbance of a solution containing resveratrol, metal ions (Al, Fe, Cu and Zn) and CR dye was measured at two wavelengths: 405nm and 487nm. The first wavelength to exclude precipitates formation, the second to exclude the capability of resveratrol and metal ions to coordinate CR. Concentrations in each well were: as for CR and resveratrol the same used in Aβ fibrils detection (70µg/ml and 15µM respectively), while for metal ions 3µM. Results obtained allow us to state that resveratrol and metal ions did not seem to bias CR spectroscopic activity (data not shown).

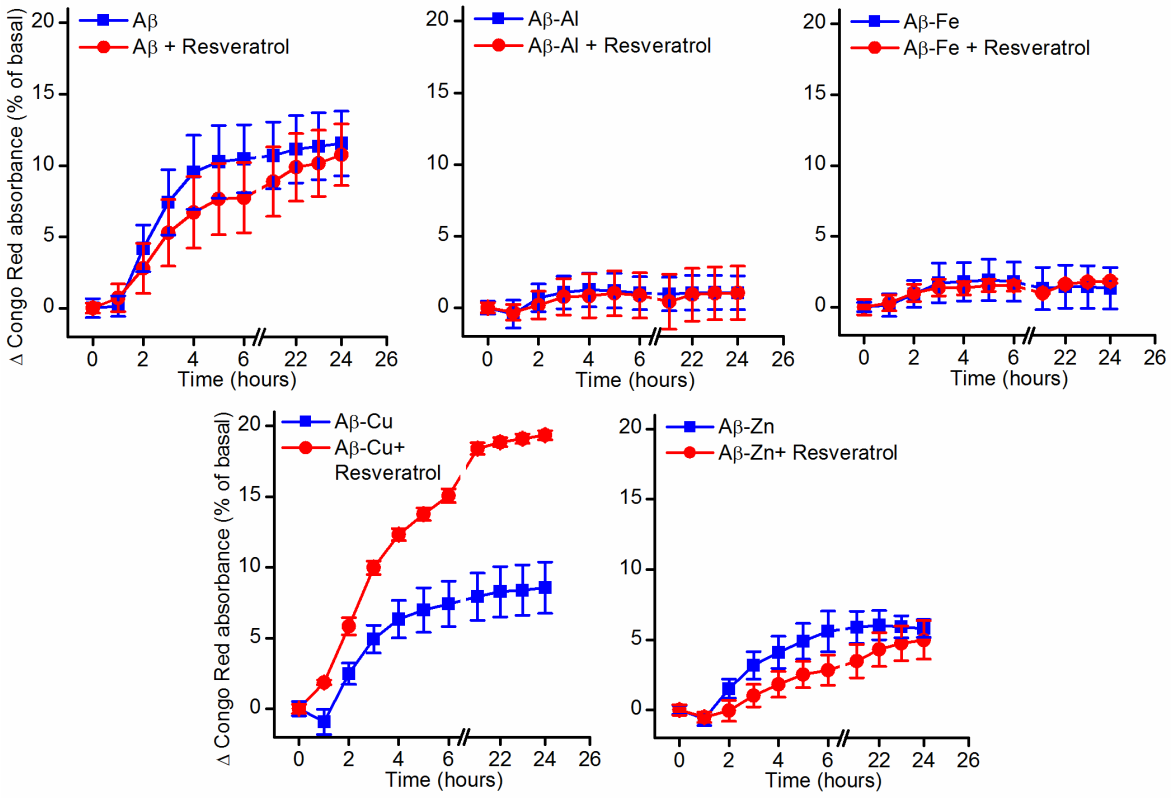

FIGURE 3 TIME-DEPENDENCE OF CONGO RED (CR) ABSORPTION WHEN CR IS BOUND TO AB AND TO AB-METAL COMPLEXES, IN THE PRESENCE AND IN THE ABSENCE OF RESVERATROL. THE REACTION MIXTURES CONTAINING 1,5 µM AB OR AB-METAL COMPLEXES, 0.1 M TRIS/HCL, 0.15 M NACL, PH 7,4 AND 0 (BLUE LINE) OR 45 µM (RED LINE) RESVERATROL, WERE INCUBATED AT ROOM TEMPERATURE FOR THE INDICATED TIMES. THE ABSORBANCE DUE TO CR WAS SUBTRACTED. EACH POINT REPRESENTS MEANS ± SEM OF THREE INDIVIDUAL EXPERIMENTS.

Turbidity measurements: in order to define a possible role of resveratrol as metal ions chelating compound, turbidity measurements of resveratrol in the presence of metal ions (Al, Fe, Cu and Zn) were performed. An increase in absorbance value at 405nm is indicative of the ability of resveratrol to chelate metal ions. Absorbance values over time are shown in Fig. 4. As reported in literature resveratrol showed a strong propensity to form complexes with Cu *in vitro* (Fremont, 2000); in agreement, solutions containing resveratrol and Cu showed a significant increase in absorbance. Data herein reported seemed to show also the ability of resveratrol to form complexes with Fe and to a lesser extent with Al and Zn. Resveratrol only

kinetics is reported to exclude possible hydrophobic interaction between the molecules in solution causing precipitation; resveratrol is sparingly soluble in water (solubility 0.03 g/L). Data reported are not biased by spectroscopic interferences due to resveratrol, its UV spectrum shows a maximum at 308nm, while all turbidity measurements were carried out at 405nm.

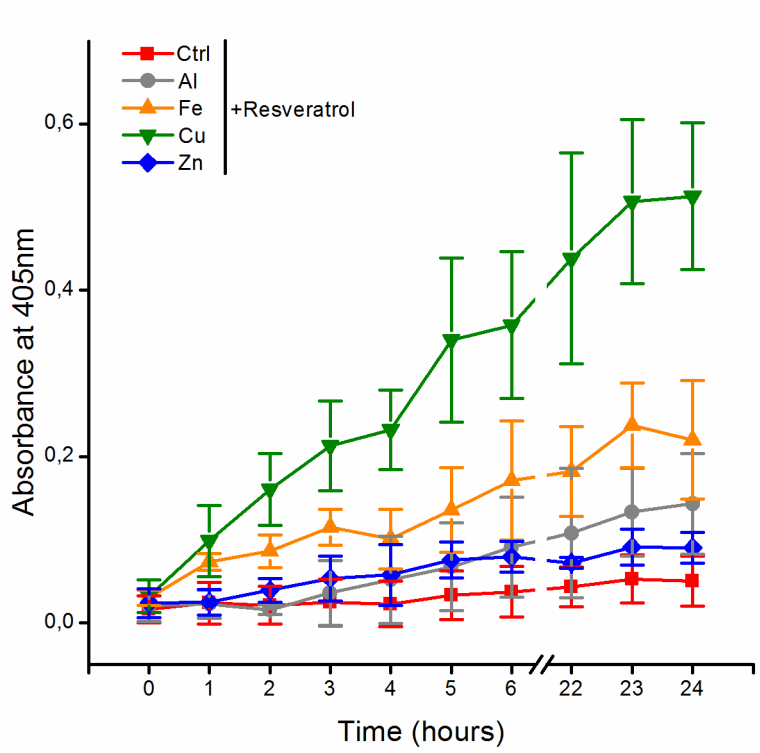

FIGURE 4 TURBIDITY ASSAY OF RESVERATROL IN THE PRESENCE OF AL, FE, CU AND ZN. EACH WELL CONTAINED 200 µM RESVERATROL AND 400 µM METAL IONS. THE EXPERIMENT WAS CARRIED OUT IN TRIS/HCL BUFFER, AS DESCRIBED IN MATERIALS AND METHODS. THE ABSORBANCE DUE TO METALLIC SOLUTIONS WAS SUBTRACTED. DATA REPRESENTED ARE MEAN ± SD OF THREE INDEPENDENT EXPERIMENTS.

Cell viability assay: before testing the effect of resveratrol on neuroblastoma cells in the presence of Aβ and its metal complexes, a toxicity profile of this compound solved in ethanol was performed. The toxicity on SH-SY5Y was evaluated by a standard MTT assay. As shown in fig. 5 the concentration needed to inhibit 50% (IC_{50}) of cell viability was 100µM. Resveratrol concentration of 15µM proved to be largely non toxic and has been chosen to perform the viability essays in the presence of metal ions and Aβ complexes.

To exclude a possible toxicity due to the interaction between resveratrol and metal ions (as confirmed by turbidity assay), cell viability assay of resveratrol in the presence of Al, Fe, Cu and Zn was performed. As shown in fig. 6 all treatments were not toxic at the concentrations used (15µM for resveratrol and 5µM for metal ions).

As previously and largely demonstrated by this laboratory (Drago et al., 2008a) Aβ-Al resulted more effective in reducing cell viability on neuroblastoma cells if compared with Aβ alone and the other Aβ metal complexes. In the presence of resveratrol there was a significant decline in cells mortality, especially

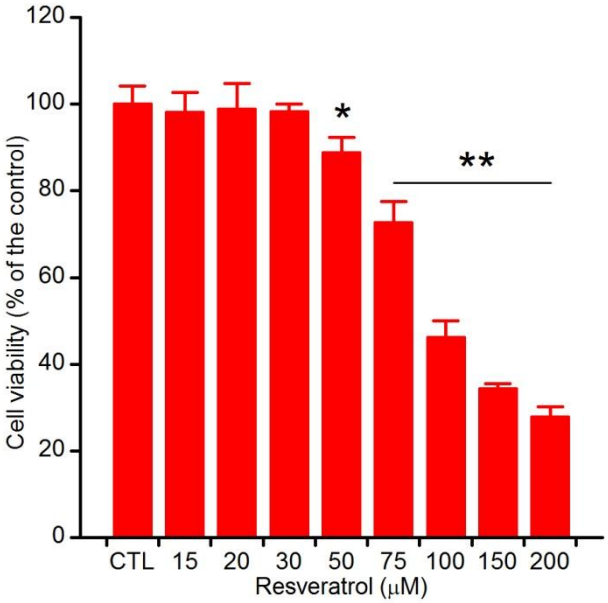

FIGURE 5 CYTOTOXICITY ASSAY IN NEUROBLASTOMA CELLS. THE DEPENDENCE OF NEUROTOXICITY (% CELL DEATH COMPARED WITH THE CONTROL) ON THE CONCENTRATION OF RESVERATROL.

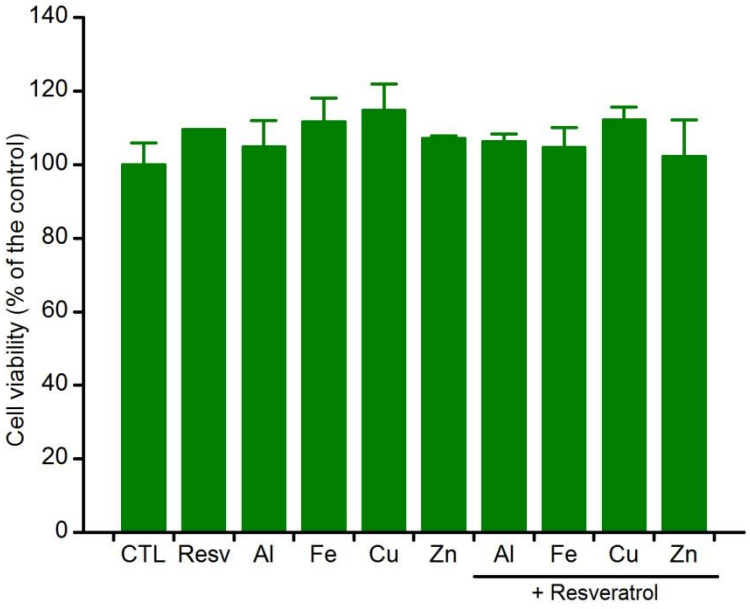

FIGURE 6 TO EXCLUDE NEUROTOXICITY DUE TO THE INTERACTION BETWEEN RESVERATROL AND METAL IONS, SH-SY5Y CELLS WERE INCUBATED FOR 24 HOURS WITH AL, FE, CU AND ZN (5 MM) IN THE PRESENCE AND IN THE ABSENCE OF RESVERATROL (15 MM); IN THIS CASE NO SIGNIFICANT TOXICITY WAS OBSERVED (B).

for Aβ, Aβ-Fe and Aβ-Zn. If we compare Aβ and its metal conjugates treatments with Aβ and Aβ-metals in the presence of resveratrol all results are significant, but in different ways. Resveratrol drastically reduced toxicity due to Aβ-Fe and Aβ-Zn ($p<0.01$), meanwhile it seemed less effective on Aβ, Aβ-Al and Aβ-Cu ($p<0.05$).

Similarly the significance of Aβ toxicity and its metal conjugates compared with the control (resveratrol only) was calculated. Only Aβ-Al and Aβ-Cu resulted significantly toxic despite the presence of

resveratrol, this result is probably due to different mechanisms by which complexes exert their toxicity (Fig. 7).

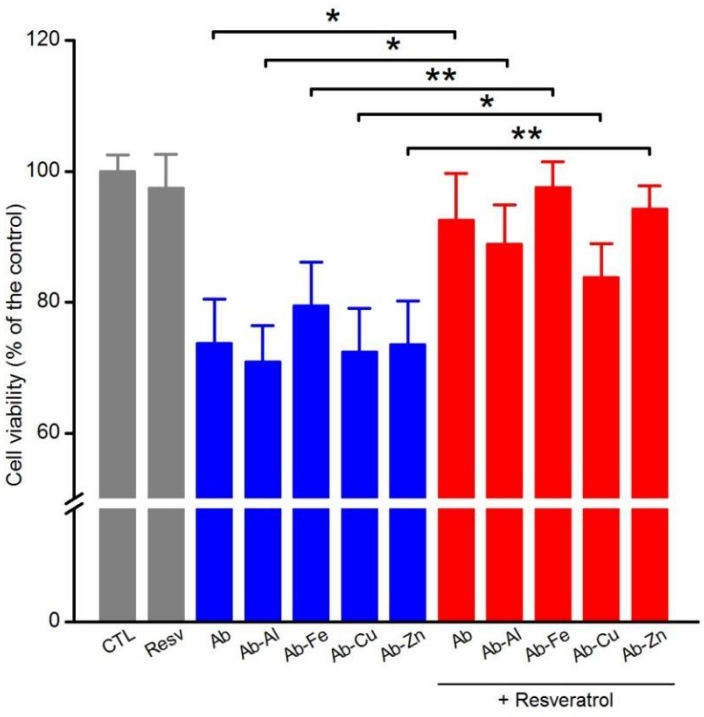

FIGURE 5 CELL VIABILITY AFTER TREATMENT WITH AB AND AB-METAL COMPLEXES (0,5 MM) WITH OR WITHOUT RESVERATROL (15 MM). RESULTS WERE OBTAINED IN FOUR INDIVIDUAL EXPERIMENTS. ERROR BAR INDICATE THE MEAN ± SD. * P<0,05; ** P<0,01.

TEM: the obtained micrographs allow us to assess and to compare the morphology of the Aβ and Aβ metal ions aggregates in the presence or in the absence of resveratrol after 24 hours of incubation. The results are consistent with CR assay. Aβ retains the ability to form fibrils in the presence of resveratrol (fig. 8A), likewise Aβ-Al retains its oligomeric structure. It is worth noting that CR assay confirms once more what has been already demonstrated by this laboratory with other biophysical techniques (ThT fluorescence and TEM) (Drago et al., 2008a). Aβ-Cu and Aβ-Zn formed unstructured aggregates both in the presence and absence of resveratrol (Fig. 8C-D). Unlike the results obtained during CR assay Aβ-Fe showed the proclivity to form unstructured fibrils similar to those of Aβ-Cu and Aβ-Zn (Fig. 8E).

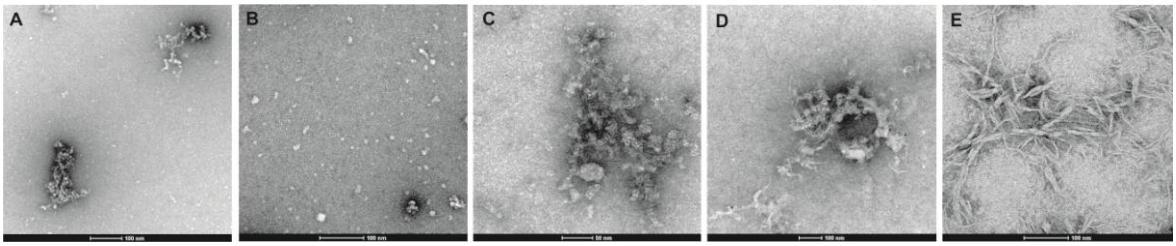

FIGURE 6 TEM MICROGRAPHS OF AB AND AB-METAL COMPLEXES IN THE PRESENCE OF RESVERATROL AFTER 24 HOURS OF INCUBATION AT ROOM TEMPERATURE. THE FINAL PROTEIN CONCENTRATION WAS 10 MM, WHILE RESVERATROL CONCENTRATION WAS 300 MM (MOLAR RATIO 1:30). A) AB + RESVERATROL; B) AB-AL + RESVERATROL; C) AB-FE + RESVERATROL; D) AB-CU + RESVERATROL; E) AB-ZN + RESVERATROL.

SOD assay: we tested the effect of Aβ and Aβ-metal complexes on SOD activity, in the presence

SOD assay: finally, we tested the effect of Aβ and Aβ-metal complexes on SOD activity in the presence or absence of resveratrol. As for Aβ and Aβ-metal complexes alone the results were heterogeneous after 24 hours of incubation. The treatments with Aβ-Fe, Aβ-Cu and Aβ-Zn caused a significative increase in SOD activity ($p<0.05$), while Aβ and Aβ-Al showed negligible effects, even though Aβ-Al complex seemed to reduce SOD activity. After the treatment with resveratrol we observed a decrease in SOD activity especially with Aβ-Fe, followed by Aβ-Cu and Aβ-Zn. These results seemed to confirm the anti-oxidant properties of resveratrol. As for Aβ and Aβ-Al we did not observed significative changes in SOD expression in the presence of resveratrol (Fig. 9). SOD activity was also tested after treating neuroblastoma cells with metal ions alone (with or without resveratrol), to rule out that SOD increase was merely due to the presence of metals. In this case a large excess of Al, Fe, Cu and Zn ions was used.

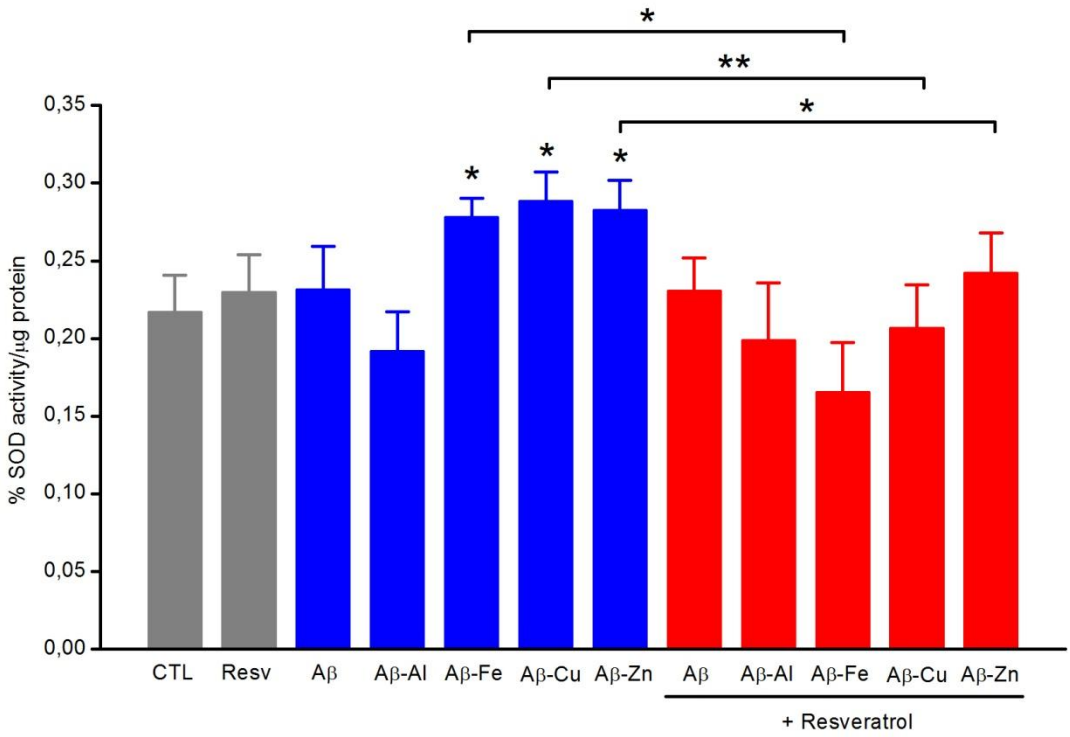

FIGURE 7 SOD ACTIVITY ASSAY. SOD ACTIVITY WAS MEASURED ON CELLS TREATED WITH AB AND AB-METAL IONS, WITH OR WITHOUT RESVERATROL. CONCENTRATIONS WERE THE SAME USED FOR MTT ASSAY. RESULTS WERE OBTAINED IN FOUR INDIVIDUAL EXPERIMENTS. ERROR BAR INDICATE THE MEAN ± SD. * P<0,05; ** P<0,01.

1.4.2 PHYSIOLOGICAL CHOLESTEROL CONCENTRATION IS NEUROPROTECTIVE AGAINST AB AND AB-METAL CONJUGATES TOXICITY

BACKGROUND

Growing evidence support the relevance of cholesterol in AD development (Wolozin, 2001;Schonknecht et al., 2002;Panza et al., 2006); however, its role in Aβ and Aβ-metal conjugates aggregation has not been well researched and data in literature seem contradictory and inconsistent (Simons et al., 2001;Harris, 2002;Ji et al., 2002). This work aimed at shedding some light on the role played by cholesterol, used at physiological concentrations (Schonknecht et al., 2002;Evans et al., 2009), in influencing Aβ and Aβ-metal conjugates aggregation and toxicity on neuroblastoma cells cultures. In order to better understand the interaction of Aβ and Aβ-metal conjugates with cell membranes, we used molecular models consisting of bilayers of dimyristoylphosphatidylcholine (DMPC) and dimyristoylphosphatidylethanolamine (DMPE), representative of phospholipid classes located in the outer and inner monolayers of many cell membranes, respectively (Devaux and Zachowsky, 1994;Boon and Smith, 2000). The capacity of Aβ and of its complexes with Al, Zn, Cu and Fe in the absence and presence of cholesterol to perturb the multibilayer structures of DMPC and DMPE was evaluated by X-ray diffraction.

RESULTS

To understand Aβ conjugates aggregation pathway in the presence of cholesterol, three biophysical techniques were used: Congo Red spectroscopic assay to detect fibril formation, ANS fluorescence assay to detect exposure of hydrophobic clusters and TEM micrographs to visualize the morphology of the aggregates. While, to determine Aβ complexes interaction with cellular membrane, X-ray diffraction of DMPC and DMPE was used.

Congo Red assay: data herein reported are expressed as percentage increase of absorbance compared to the controls. As shown in fig. 10 cholesterol seemed to have a modest anti-aggregative role. In fact every Aβ complex showed a reduction of fibrillogenesis after 24 hours of incubation with cholesterol (50μM) at room temperature. The most notable decrease was observed for Aβ-Al, Aβ-Cu and Aβ-Zn. But only the last one was statistically significant. It is notable that cholesterol did not stop the aggregation process but only slowed it, except for Aβ-Zn complex, in this case was not observed an increase in CR absorbance. It is worth noting that Al did not promote amyloid fibrillization; on the contrary aluminum seemed to “freeze” Aβ in an oligomeric state, as previously demonstrated by Drago et al. (2008a), while the presence of cholesterol in solution promoted the not aggregative role played by aluminum. Thioflavine T (ThT) fluorescence assay was not performed to show Aβ-metal complexes aggregation because preliminary analysis suggested that cholesterol could bias the results through non spectroscopic interferences (data not shown).

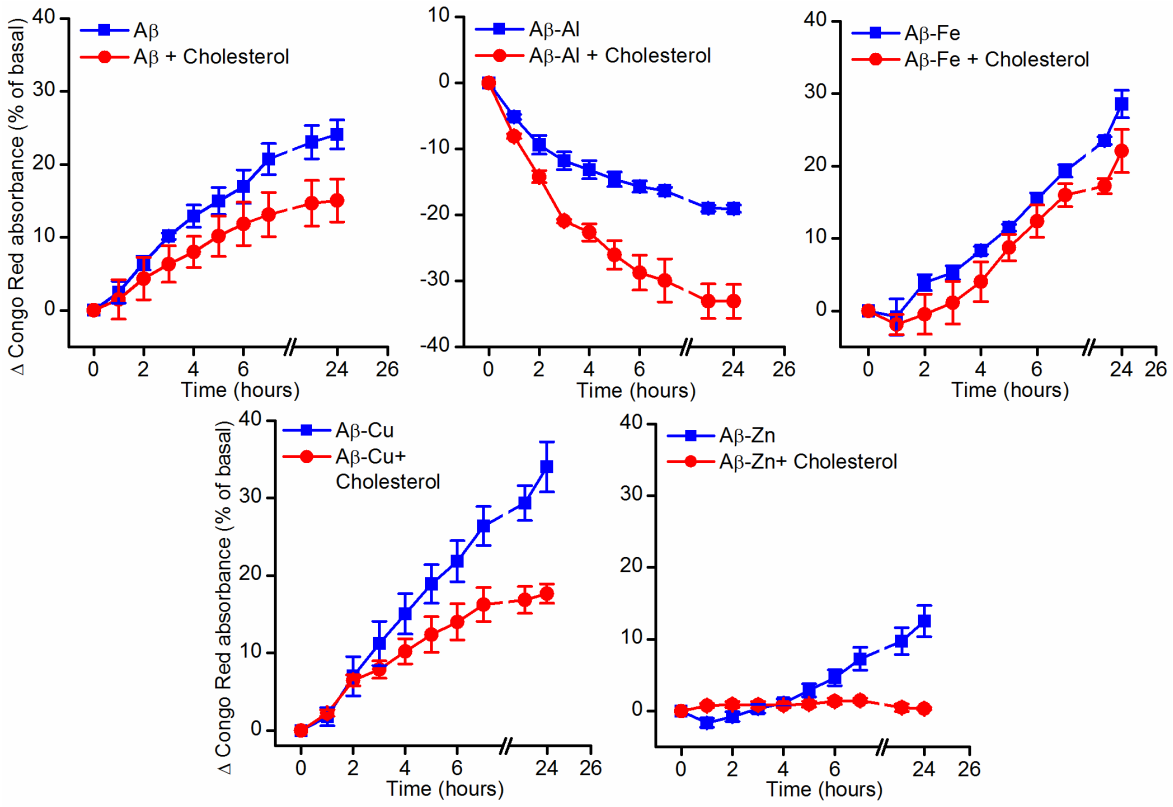

FIGURE 10 CONGO RED PERCENTAGE INCREASE OF ABSORBANCE VERSUS TIME IS INDICATIVE OF AMYLOID FIBRIL FORMATION. PROTEIN CONCENTRATION IN EACH WELL WAS 5MM, WHILE CHOLESTEROL CONCENTRATION WAS 50µM (MOLAR RATIO 1:10). ETHANOL CONCENTRATION IN THE MEDIUM WAS 2% V/V. SOLUTIONS CONTAINING CR AND METAL IONS (AL, FE, CU AND ZN) WAS ALSO TESTED TO AVOID INTERACTIONS BETWEEN THE DYE AND METALS; NO SIGNIFICANT DIFFERENCES WERE OBSERVED (DATA NOT

ANS fluorescence: in agreement with Uversky et al. (1996), changes in ANS fluorescence are characteristic hallmarks of the interaction of this dye with the solvent-exposed hydrophobic clusters of partially folded peptides. Each Aβ-metal conjugate was tested for surface hydrophobicity after 24 hours of incubation with cholesterol (50µM). Aβ and Aβ-metal conjugates concentration was 5µM in each cuvette. Fig. 11 showed that aluminum is the metal that promoted the greatest increase in ANS fluorescence if compared with the other metals and Aβ alone. This implied that Aβ-Al is the complex that exposed most its hydrophobic clusters. The exposition was enhanced by the presence of cholesterol for both Aβ-Al and Aβ-Zn and Aβ alone. As for Aβ-Cu we observed a negligible effect of cholesterol in promoting exposition of hydrophobic clusters. Aβ-Fe metal complex showed the lowest capability of exposing lipophilic clusters; the presence in solution of cholesterol did not change ANS fluorescence intensity, but unlike the other complexes the signal due to Aβ-Fe + cholesterol was lower than the signal due to Aβ-Fe alone.

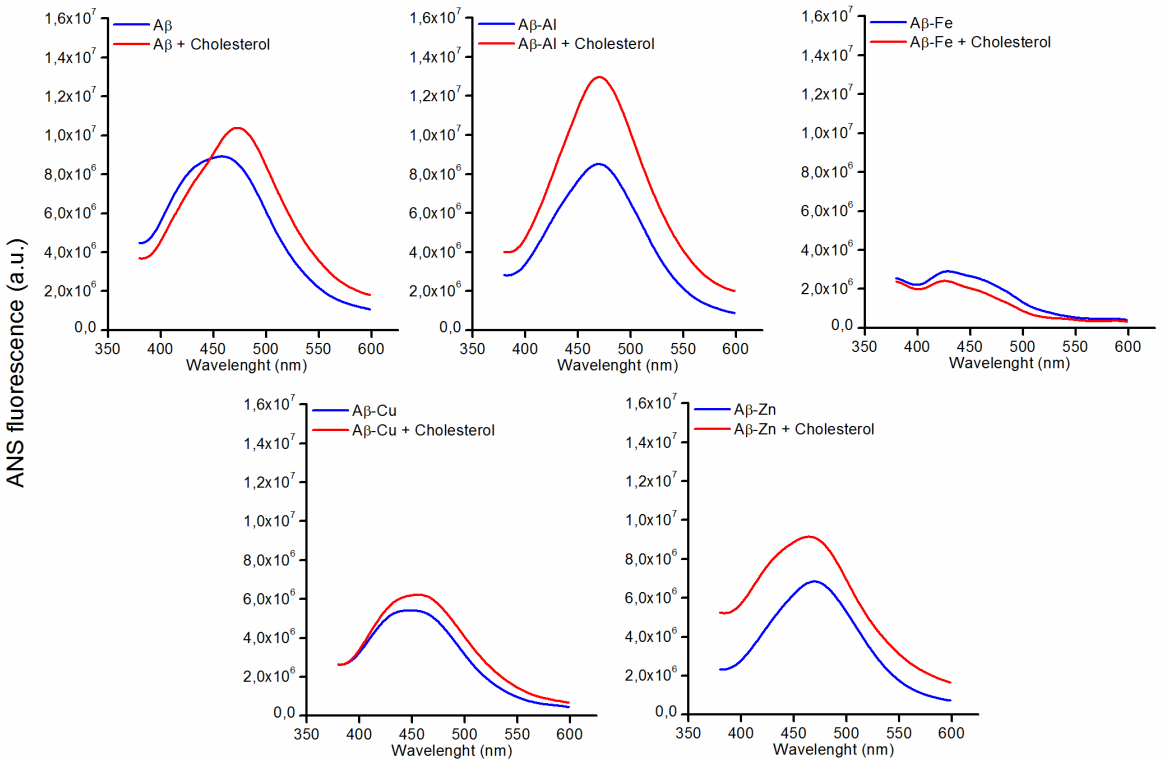

Toxicity on cell culture: to evaluate the viability of cell cultures the capability to convert 3-(4,5-dimethylthiazole-2-yl)-2,5-diphenyl-tetrazolium bromide (MTT) to formazan crystals by mitochondrial respiratory chain reactions was measured. Cells were treated with Aβ and Aβ-metal conjugates with or without cholesterol. The final Aβ-metal conjugates concentration in the medium was 0,5µM, while the final cholesterol concentration was 5µM. As shown in fig. 12, cholesterol seemed to reduce the toxicity of the two most toxic species of amyloid: Aβ and Aβ-Al. In fact it was previously demonstrated by this laboratory that Aβ-Al is more effective in decreasing cell viability if compared with the other Aβ-metal complexes (Drago et al., 2008a). Simultaneously cholesterol showed a modest and not significant capability to increase Aβ-Cu toxicity, meanwhile no effects were observed both for Aβ-Fe and Aβ-Zn in the presence of cholesterol.

→ **FIGURE 12** SH-SY5Y NEUROBLASTOMA CELLS WERE INCUBATED WITH AB AND AB-METAL COMPLEXES (0,5MM) FOR 24H IN THE PRESENCE OR IN THE ABSENCE OF CHOLESTEROL (5MM). DATA PRESENTED ARE EXPRESSED AS % CELL DEATH AS COMPARED WITH CONTROL. RESULTS ARE MEAN ± SD OF THREE INDIVIDUAL EXPERIMENTS, EACH DONE IN TRIPLICATE. (* P<0.05 , ** P< 0.01)

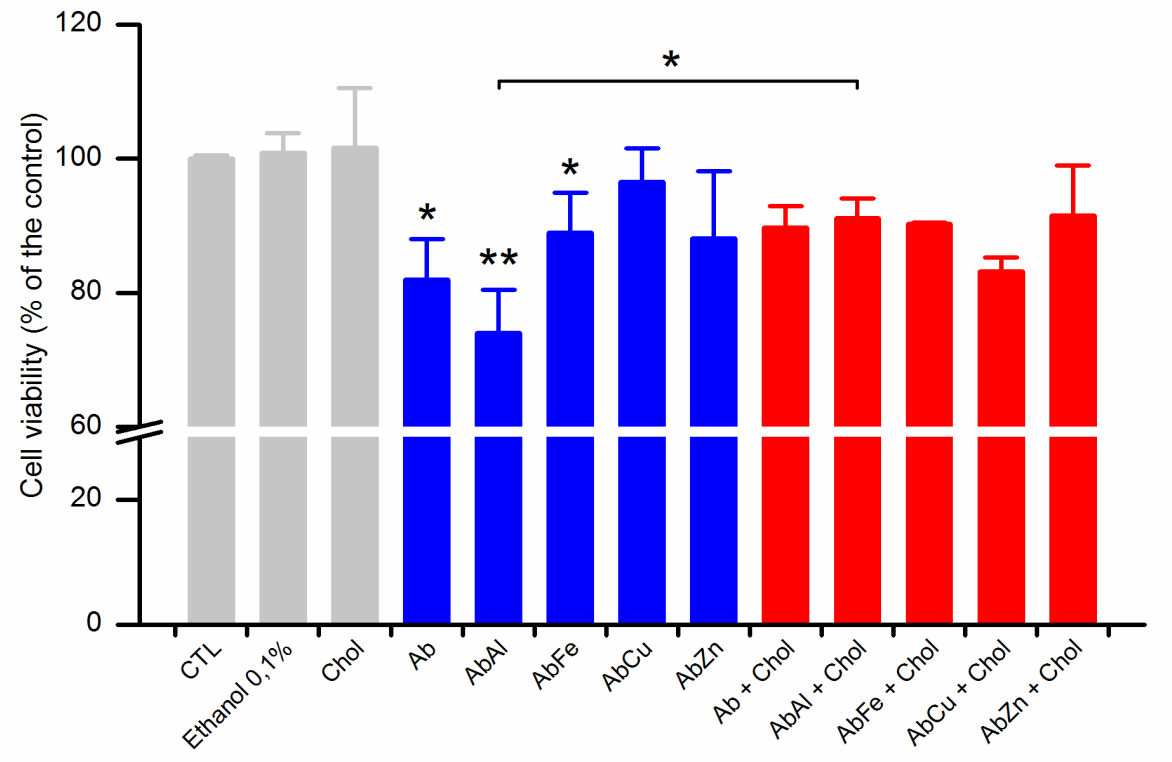

TEM: Electron micrographs were recorded to assess the morphology of aggregates in the presence of cholesterol. Aβ and Aβ-metal conjugates were incubated with cholesterol at the same concentrations used during Congo Red spectroscopic assay. Aliquots were removed at time zero and after 24 hours of incubation at room temperature. As shown in fig. 13 we observe in each micrographs the presence of cholesterol microcrystal. Aβ oligomers observed at time zero, reassembled in mature fibrils after 24 hours of incubation, while Aβ-Al retained its oligomeric state, accordingly to the capability of aluminum to hold fibrils formation (Zatta et al., 2009). Aβ-Cu in the presence of cholesterol appeared to form unstructured aggregates already at time zero, then, after 24 hours fibrils become the dominant specie intercalated within cholesterol micro crystals. The aliquot containing Aβ-Fe + cholesterol showed the typical aggregation pathway of Aβ-Fe complex. In fact the micrograph recorded at time zero shows the presence of small oligomers (≈15 nm of diameter); after 24 hours of incubation a large amount of amorphous aggregates was detected. Aβ-Zn, as confirmed by CR spectroscopic assay, forms at the beginning small and unstructured aggregates that after 24 hours do not increase in dimension and do not assume a well defined fibrillary structure, as already discussed by our laboratory (Zatta et al., 2009) and confirmed by other studies (Drago et al., 2008a). Furthermore Aβ-Zn micrographs, after 24 hours, confirmed the anti-aggregative role of cholesterol to the amyloid-zinc complex.

→ **Figure 13** TEM micrographs of Ab and Ab-metal complexes in the presence of cholesterol at time 0 and after 24h of incubation at room temperature.

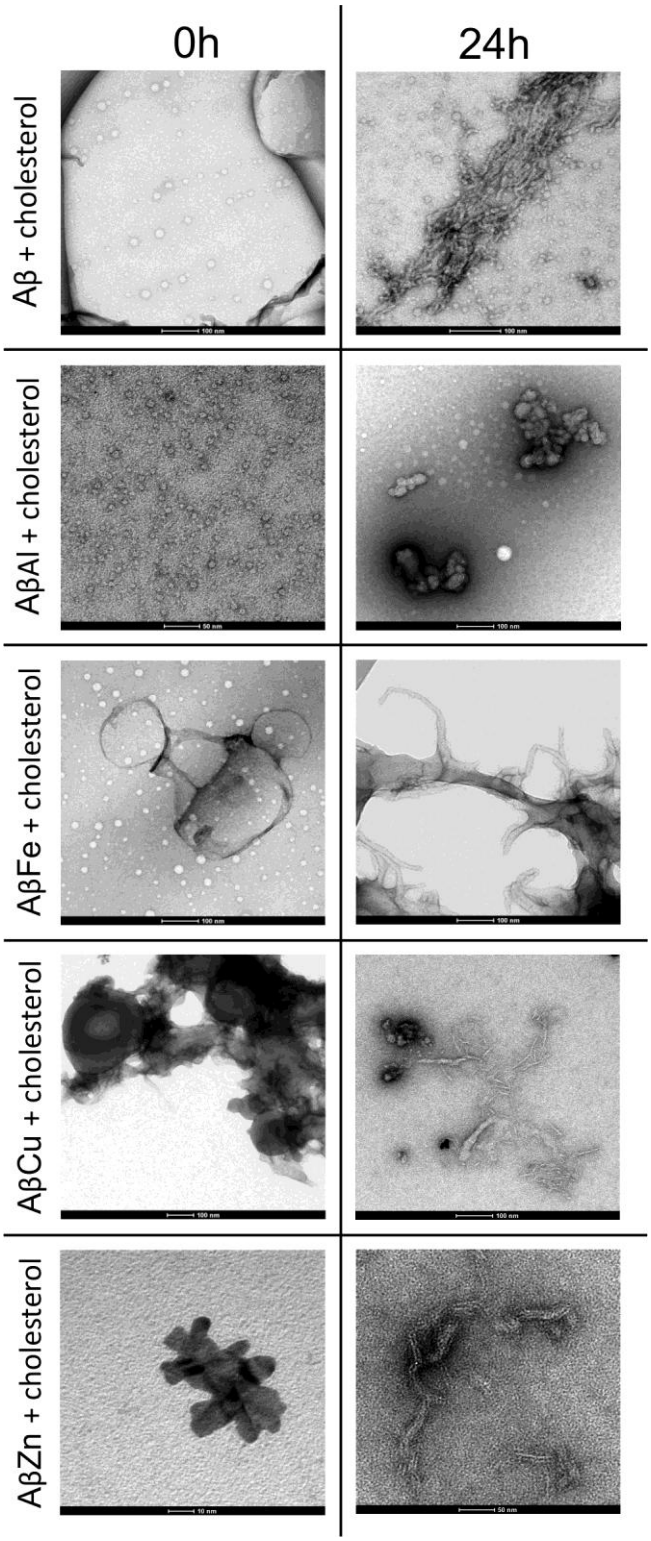

X-ray diffraction studies of phospholipids multilayers: fig. 14 exhibits the results obtained by incubating DMPC with water, metal-free Aβ, and Aβ-metal conjugates. As expected, water altered the DMPC structure: its bilayer repeat (bilayer width plus the width of the water layer between bilayers)

increased from about 55 Å in its dry crystalline form (Suwalsky et al., 1996) to 64.5 Å when immersed in water, and its low-angle reflections [indicated as (LA) in the figure], which correspond to DMPC polar terminal groups, were reduced to only the first two orders of the bilayer repeat. On the other hand, only one strong reflection of 4.2 Å [indicated as (WA) showed up in the wide-angle region], which corresponds to the average distance between fully extended acyl chains organized with rotational disorder in hexagonal packing. These results were indicative of the fluid state reached by DMPC bilayers, showing the typical characteristics of a Pβ' phase (Katsaras, 1998). Fig. 14A shows that after its exposure to metal-free Aβ and Aβ conjugates with Fe, Cu and Zn in the 5 μM concentration the DMPC diffraction pattern remained practically unchanged. However, 5 μM Aβ-Al induced a considerable weakening of the low- and wide-angle lipid reflection intensities, indicative of a strong interaction of the Al complex with DMPC bilayers. Fig. 14B shows that cholesterol in the 5-50 μM concentration range did not induced changes to DMPC bilayers. Results from incubating DMPC with 5 μM metal-free Aβ and Aβ-metal complexes including that of Al in the presence of 50 μM cholesterol showed no perturbation effects of any of these compounds on the lipid structure (Fig. 14C). Similar experiments were performed on DMPE bilayers. Fig. 14 shows that the DMPE bilayer repeat expanded from about 51 Å when dry (Suwalsky, 1996) to 56.4 Å when subjected to maximum hydration. On the other hand, only two reflections were observed, one more pronounced of 56.4 Å, corresponding to the first order of the bilayer repeat, and the other of 4.2 Å, indicating the fluid state reached by DMPE. Fig. 14 (A, B, C, below) also show that 5 μM metal-free Aβ and the four Aβ-metal complexes in the absence and presence of cholesterol did not induce changes to DMPE bilayers. From these results it can be concluded that neither metal-free Aβ, cholesterol nor the Aβ-metal complexes with Fe, Cu and Zn produced any significant structural perturbation to DMPC or to DMPE bilayers, and only that of Al significantly affected DMPC. On the other hand, the results presented in Fig. 14A demonstrate that the strong interaction of the Aβ-Al complex with DMPC bilayers was not due to the metal-free peptide, as a similar concentration of Aβ did not induce any structural perturbation to this lipid. Therefore, it can be concluded that only the association of Al with Aβ is able to interact and disturb the structure of DMPC, which is preferentially located in the outer monolayer of many cell membranes (Devaux and Zachowsky, 1994; Boon and Smith, 2000).

→ **FIGURE 14** ABOVE: MICRODENSITOGRAMS FROM X-RAY DIFFRACTION DIAGRAMS OF DMPC IN THE PRESENCE OF (A) AB AND AB-METAL COMPLEXES, (B) CHOLESTEROL, AND (C) CHOLESTEROL AND AB COMPLEXES; (LA) LOW-ANGLE AND (WA) WIDE-ANGLE REFLECTIONS.

BELOW: MICRODENSITOGRAMS FROM X-RAY DIFFRACTION DIAGRAMS OF DMPE IN THE PRESENCE OF (A) AB AND AB-METAL COMPLEXES, (B) CHOLESTEROL, AND (C) CHOLESTEROL AND AB COMPLEXES; (LA) LOW-ANGLE AND (WA) WIDE-ANGLE REFLECTIONS.

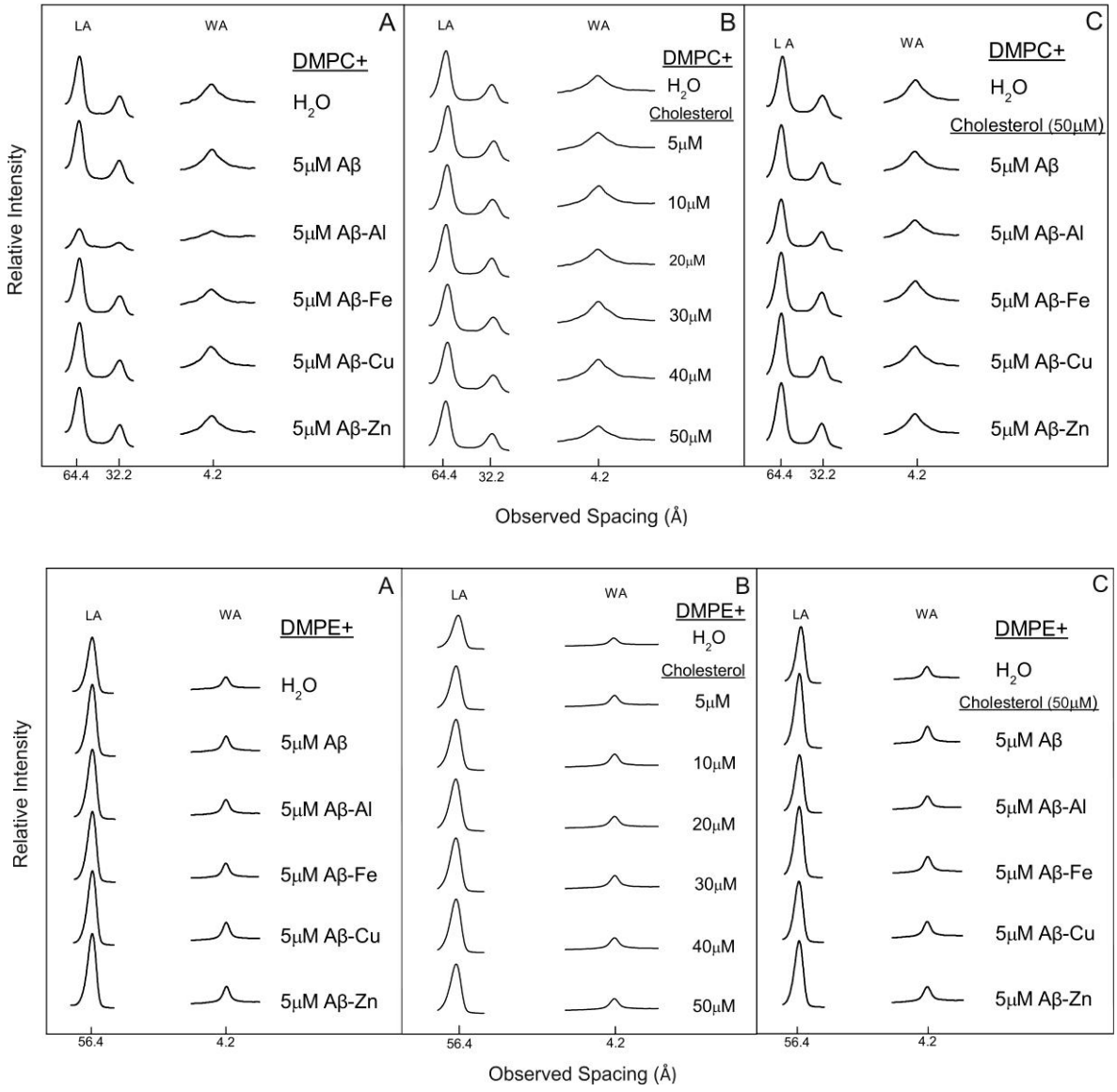

1.4.3 MICROARRAY ANALYSIS OF GENE EXPRESSION PROFILES IN HUMAN NEUROBLASTOMA CELLS EXPOSED TO AB-ZN AND AB-CU CONJUGATES

BACKGROUND

In the present study, we analyzed the gene expression profile changes due to exposure to Aβ-Zn or Aβ-Cu in a neuronal-like cell line (SH-SY5Y). SH-SY5Y were chosen because as cell line they offer the advantage of being a homogenous population that does not show the subtype heterogeneity present in primary neuronal cultures, a confounding factor that can make results more difficult to interpret. We employed the same experimental paradigm previously used in a study analyzing gene expression changes triggered by exposure to $A\beta_{1-42}$ conjugated with Al (Gatta et al., 2011). Cultures were exposed to Aβ, Aβ-Zn, Aβ-Cu, Zn or Cu alone and the transcriptomic profile investigated with microarray analysis. The main goal of the study was to offer a better understanding of biological downstream effects triggered by Aβ conjugated with metals, a condition that is the pathogenic scenario occurring in the AD brain. To that aim,

we took in account only the genes that, compared to the ones changed by exposures to Aβ, Cu or Zn alone, resulted selectively modified in cells treated with Aβ-Zn or Aβ-Cu conjugates. These selectively modified genes were investigated with Ingenuity Pathway Analysis (IPA) to assess their roles and functions.

RESULTS

SH-SY5Y cells were treated for 24h with Aβ conjugated with Zn or Cu. In parallel control experiments, SH-SY5Y were also treated with Aβ alone or metal ions at a concentration 10-fold higher than what used for Aβ exposure.

As we have previously reported in the case of Aβ-Al complexes, Aβ-Zn or Aβ-Cu treatments significantly affected gene expression profiles (Gatta et al., 2011). When analyzing these changes, we focused our attention on up- or down-regulated genes strongly related to AD pathology. Unfortunately, technical issues did not allow the validation of microarray data by RT-PCR (real-time polymerase chain reaction); however, to reduce the risk of false positive/negative results we employed a conservative statistical analysis that considered as "differentially expressed" only spots showing a detectable response across all slides and that, on average, had a log-ratio higher or equal to 0.5, a value that represents a strong fold-change (i.e.: 1.4 in transcript quantity).

To increase the clarity and readability of the study, we chose to divide the "Results" section in two sub-sections where we separately describe Aβ-Zn or Aβ-Cu data. Few gene changes were common to both Aβ-metal treatments and are shown as Venn diagram (Fig. 15).

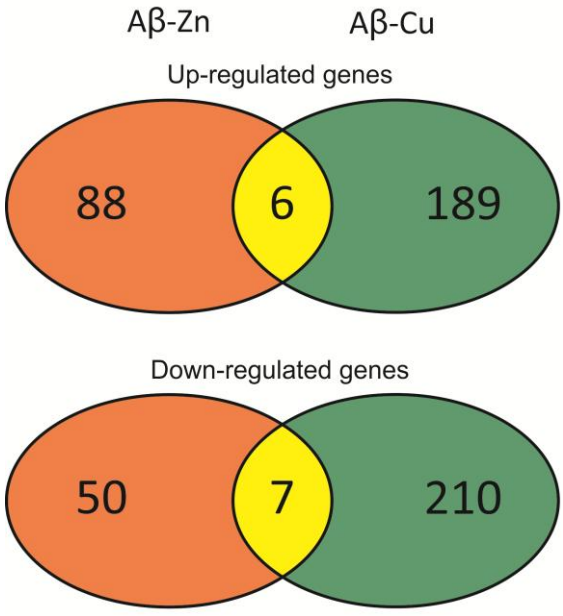

EFFECTS OF AB-ZN EXPOSURE

Aβ-Zn treatment resulted in selective up- and down-regulation of 88 and 50 transcripts, respectively. Ingenuity Pathway Analysis was then carried out to identify biological functions of the genes.

For up-regulated transcripts we found that main involved functions were: Protein Synthesis, Carbohydrate Metabolism, Cellular Assembly and Organization, Cellular Function and Maintenance, Lipid Metabolism, Nervous System Development and Function, Neurological Diseases, Cell Death and Energy Production (Fig. 16). As for down-regulated genes, functions belonged to: Cell Morphology, Cellular Development, Cell Death, Cellular Assembly and Organization, Nervous System Development and Function, Lipid Metabolism, and Free Radical Scavenging (Fig. 17).

A

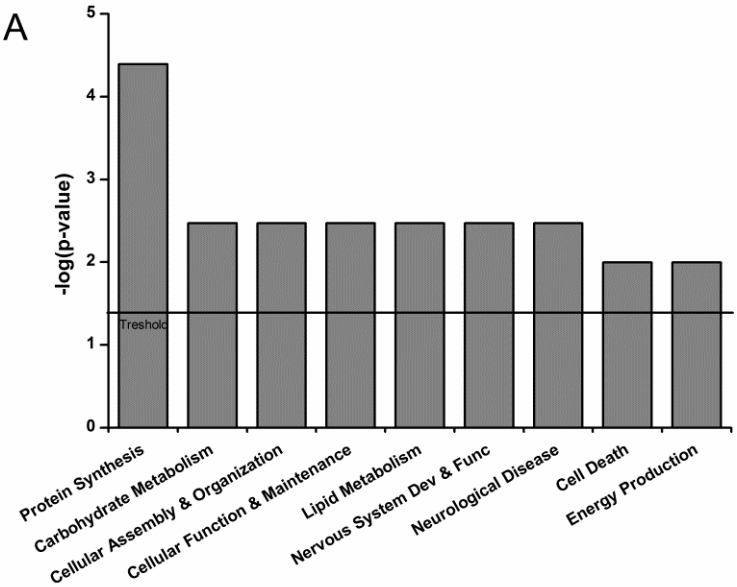

B

Category	p-value	Molecules
Protein Synthesis	4,06E-05-2,53E-02	IL1RN,BIN3,RPL17,USP11,RPL21,CUTA,RPL26,CAST,RPS3,EEF1G
Carbohydrate Metabolism	3,38E-03-4,31E-02	ARF1,SCARB1,CHGA,IL1RN,INPP5K
Cellular Assembly and Organization	3,38E-03-4,96E-02	ARF1,WNT3A,MYL6,SCARB1,MT2A,ACTB,KPTN,CAST,MSTO1
Cellular Function and Maintenance	3,38E-03-4,31E-02	FTL,ARF1,WNT3A,SCARB1,MT2A,IL1RN,IL21R,KPTN,PFDN5,CAST,MECOM
Lipid Metabolism	3,38E-03-4,63E-02	ARF1,SCARB1,IL1RN,SULT1A1,INPP5K
Nervous System Development and Function	3,38E-03-4,96E-02	ARF1,WNT3A,CHGA,MT2A,IL1RN,CAST
Neurological Disease	3,38E-03-4,63E-02	UPF2,FTL,CHGA,SLC15A1,IL1RN,PQBP1,ACTB,RPL17,RPL21,TUFT1,CAST,null
Cell Death	1,01E-02-3,98E-02	ACTB,NAA35,CBX5,PSIP1,MECOM,HSPA4,TADA3,WNT3A,SCARB1,ENO1,IL1RN,MT2A,PQBP1,EIF5A,CAST,RPS3
Energy Production	1,01E-02-1,01E-02	IL1RN

FIGURE 16 INGENUITY PATHWAY ANALYSIS FUNCTIONAL ANALYSIS OF UP-REGULATED GENES MODULATED BY EXPOSURE TO AB-ZN. (A) BAR CHART SHOWS KEY MODULATED FUNCTIONS. (B) TABLE SHOWS GENES UP-REGULATED BY AB-ZN TREATMENT AND RELATED TO FUNCTIONS SHOWN IN (A).

A

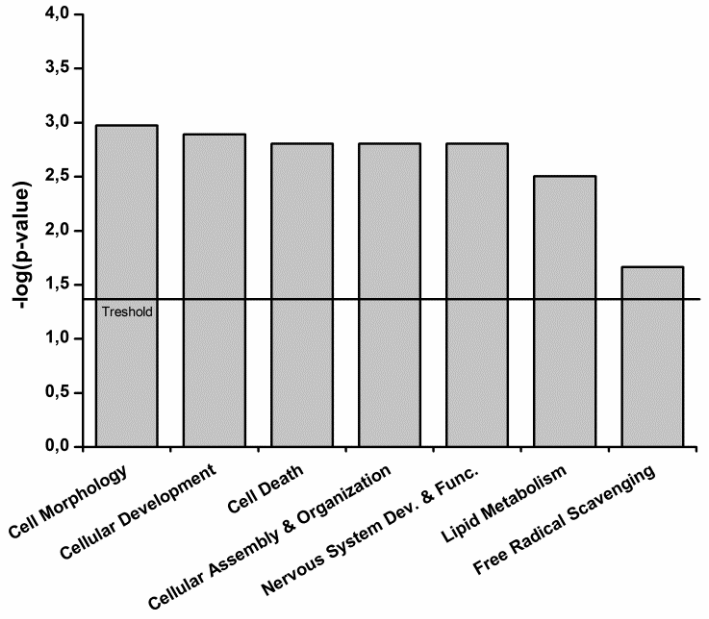

B

Category	p-value	Molecules
Cell Morphology	1,06E-03-4,87E-02	CCNG1,NR4A1,NEFH,C5,CLIC4,ACE,CITED2
Cellular Development	1,28E-03-3,69E-02	LAMA1,C5,CLIC4,CITED2,NFE2L1,ACE
Cell Death	1,57E-03-4,95E-02	CCNG1,ZNF148,ACIN1,NR4A1,NEFH,C5,CLIC4,CITED2,ACE,NFE2L1
Cellular Assembly and Organization	1,57E-03-4,6E-02	HAUS5,NEFH,C5,PIK3R4,C11orf73,ACE
Nervous System Development and Function	1,57E-03-2,78E-02	KCNJ1,NEFH,C5,CITED2,ACE
Lipid Metabolism	3,13E-03-4,15E-02	NR4A1,C5,PIK3R4,CITED2,ACE
Free Radical Scavenging	2,17E-02-3,95E-02	NR4A1,C5

FIGURE 17 INGENUITY PATHWAY ANALYSIS FUNCTIONAL ANALYSIS OF DOWN-REGULATED GENES MODULATED BY EXPOSURE TO THE AB-ZN. (A) BAR CHART SHOWS KEY MODULATED FUNCTIONS. (B) TABLE SHOWS GENES DOWN-REGULATED BY AB-ZN TREATMENT AND RELATED TO FUNCTIONS SHOWN IN (A).

AD-related up-regulated genes

CAST: this gene encodes for calpastatin, an endogenous calpain inhibitor. Calpains are calcium-activated intracellular cysteine proteases involved in physiological and neurotoxic processes. The role of calpains in AD is still elusive; however, important activities are described as far as involvement in BACE1 expression, APP processing, and Aβ deposition in a AD mouse model (Liang et al., 2010).

EIF5A: the protein encoded by this gene, called eukaryotic translation initiator factor 5A, modulates protein synthesis. Interestingly, EIF5A affects the activity of nerve growth factor (NGF) in the modulation of neurotrophism and neuroprotection (Huang et al., 2007).

ENO1: this gene encodes for enolase-α (also known as phosphopyruvate hydratase), a key enzyme for glycidic metabolism. A study has shown (Butterfield et al., 2006) that oxidative stress mediates ENO1

inactivation and that can have a role in AD development in subjects showing signs of mild cognitive impairment (MCI).

HSPA4 (as known as HSP70): this gene encodes for heat shock protein 4 (70 kDa isoform), a chaperone that is involved in protein assembly. As recently reported (Cui et al., 2011), HSPA4 up-regulation counteracts intracellular Aβ toxicity; however, some data also indicate that the protein can promote neuroprotection in AD (Turturici et al., 2011).

IL1RN: this gene encodes for the interleukin 1 receptor antagonist. Levels of the protein is increased in AD patients (Yasuhara et al., 1997). Furthermore, IL1RN over-expressions resulted in marked reduction of brain volume without upregulation of compensatory pro-inflammatory cytokines in a AD mouse model (Oprica et al., 2007).

MT2A: this gene encodes for metal ion binding metallothionein (MT) 2A. MT2A shows high affinity for heavy metals such as Zn^{2+} and Cu^{2+}. MT2A, as all MTs, is an antioxidant and cytoprotective (Mocchegiani et al., 2006).

PQBP1: the protein encoded by this gene is a nuclear polyglutamine-binding protein involved in transcription activation. Knock-out models for this gene show learning impairment (Tamura et al., 2010), PQBP1 dysfunction causes mitochondrial-induced cell death (Marubuchi et al., 2005) while mutations are involved in X-linked mental retardation (Kalscheuer et al., 2003).

PSIP1: this gene encodes for a transcription co-activator. Data from fetal and adult human brains indicate a possible role of the protein in the regulation of neurogenesis and neuroepithelial stem cell differentiation (Chylack et al., 2004).

RPS3: this gene encodes for the 40S ribosomal protein S3. RPS3 over-expression has been reported to occur in ischemia-damaged hippocampal CA1 neurons likely exerting neuroprotective effects (Hwang et al., 2008).

SCARB1: this gene encodes for the high density lipoproteins (HDLs) receptor. An involvement of the receptor has been reported in a AD mouse model, SCARB1 down-regulation has been shown to enhance amyloid pathology and exacerbate memory deficits (Thanopoulou et al., 2010).

WNT3A: this gene encodes for WNT3, a protein involved in transcription signaling and cell development. WNT3 expression appears to counteract Aβ-mediated blockade of neuronal differentiation as well as damage of neural progenitor cells (Shruster et al., 2011).

AD related under-expressed genes

ACE: this gene encodes for the angiotensin-converting enzyme (ACE), a protein involved in catalyzing conversion of angiotensin I to the physiologically active peptide angiotensin II. Interestingly, recent data suggest that the enzyme also participates to Aβ degradation (Akatsu et al., 2011).

ACIN1 (also known as Acinus): the protein encoded by this gene induces apoptotic chromatin condensation after cleavage induced by caspase-3 activity (Sahara et al., 1999).

C5: this gene encodes for the C5, a protein of the complement family. C5 plays a critical role in inflammation and induction of apoptosis. The role of C5 in AD is controversial. Some studies indicate increase in C5 expression in post mortem AD brains; however, in a transgenic AD model (APP23) no changes have been found (Reichwald et al., 2009).

CCNG1: this gene encodes for cyclin G1, a protein participating to the regulation of cell cycle and to negative regulation of apoptosis. CCNG1 has been shown to be over-expressed in a zebrafish AD model carrying human presenilin point mutations (Newman et al., 2009).

CITED2: the protein encoded by CITED2 gene plays several roles in proliferation, differentiation, migration, development, and apoptosis. Up-regulation of CITED2 promotes cellular death whereas its deficiency is cytoprotective (Gonzalez et al., 2008). A recent study also suggested that CITED2 can affect neuronal differentiation (Dijkmans et al., 2009).

CLIC4: this gene encodes for the chloride intracellular channel, CLIC4. The channel is ubiquitously distributed in cells. In neurons, CLIC4 is present in the plasma membrane, in intracellular compartments (Suginta et al., 2001), and its translocation to the nucleus involved in stress-induced apoptosis (Suh et al., 2004). Furthermore, the CLIC4 homologue, CLIC1 has been reported to promote Aβ-induced reactive oxygen species (ROS) generation in microglia (Milton et al., 2008).

NFE2L1: the role played by the protein encoded by this gene is still obscure, though some findings speculate involvement in modulation of redox responses. Supporting this idea, NFE2L1 has been shown to mediate cellular adaptation to redox stress in the endoplasmatic reticulum (Zhang et al., 2006) and to be critical to favor redox balance in liver cells during development (Chen et al., 2003).

NR4A1 (as known as TR3): this gene encodes for a protein of the so called “death receptor family”. A close correlation between NR4A1 expression and AD-affected brain regions has been shown in patients (Newman et al., 2000).

ZNF148: this gene encodes for a DNA binding protein. ZNF148 acts as a pro-apoptotic factor enhancing Bak expression and promotes cell death in hepatocellular cancer cells (To et al., 2011).

Effects of Ab-Cu exposure

Aβ-Cu exposure resulted in selective up-regulation and down-regulation of 189 and 210 genes, respectively. Ingenuity Pathway Analysis of the up-regulated gene dataset, showed transcripts involved in: Neurological Diseases, Cell Death, Carbohydrate Metabolism, Protein Synthesis, Lipid Metabolism, Molecular Transport and Nervous System Development and Function (Fig. 18). Functions related to down-regulated genes were: Cell Death, Neurological Disease, Lipid Metabolism, Cell Morphology, Cellular Growth and Proliferation, Inflammatory Response, Nervous System Development and Function, and Free Radical Scavenging (Fig. 19).

A

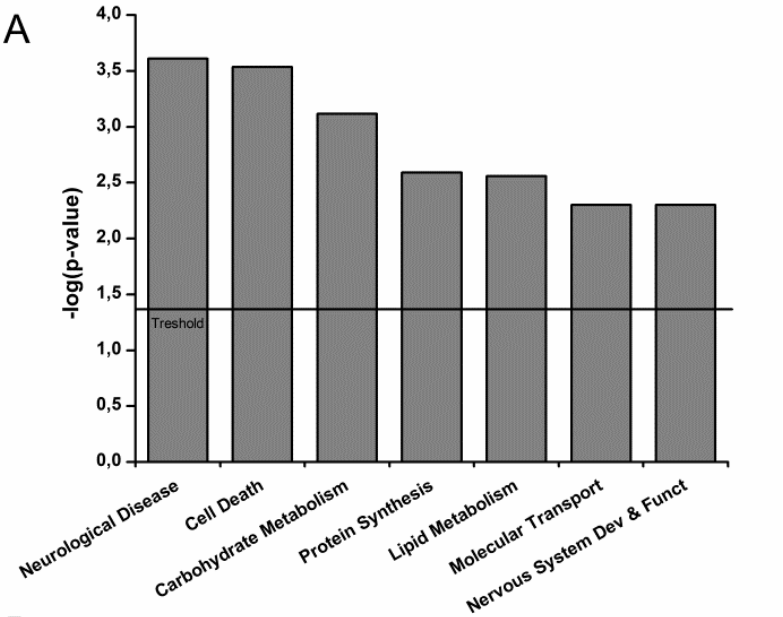

B

Category	p-value	Molecules
Neurological Disease	2,45E-04-3,48E-02	NFKBIA,SNAP23,CRP,DLG4,SFPQ,SLC12A9,SSR1,HMGCR,MED12,HMBS,LRRC23
Cell Death	2,91E-04-4,9E-02	PER1,MAGED1,NTN4,CALM1 (includes others),GNB2L1,IRAK1,EN1,SIVA1,PTRH2,NFKBIA,MT2A,FBLN1,WWOX,CD209,RHOBTB2,DLG4,C1QBP,NCR2,PHB,NDOR1,DLL1,TCF3,FAU,MTPN,ENO1,CRP,KIDINS220,ALDOA
Carbohydrate Metabolism	7,67E-04-3,94E-02	NDOR1,ARF1,NFKBIA,PGM3,ENO1,ACP6,ALDOA,ENPP2,B3GALNT2,C1QBP
Protein Synthesis	2,57E-03-1,55E-02	MTPN,RPS27,FAU,MVK,EIF4A1,RPL19,LRSAM1,FBXO3,EEF1G
Lipid Metabolism	2,77E-03-5E-02	ARF1,NFKBIA,ACP6,MVK,CRP,WWOX,ENPP2,HMGCR
Molecular Transport	5,01E-03-4,08E-02	ARL2,ARF1,MTPN,NFKBIA,EXOC3L1,SNAP23,ACP6,CRP,ALDOA,ENPP2,C1QBP,IRAK1
Nervous System Development and Function	5,01E-03-4,9E-02	EN1,PER1,ARF1,MAGED1,NFKBIA,NTN4,MT2A,WWOX,CSNK1D,DLG4

FIGURE 18 INGENUITY PATHWAY ANALYSIS FUNCTIONAL ANALYSIS OF UP-REGULATED GENES MODULATED BY EXPOSURE TO AB-CU. (A) BAR CHART SHOWS KEY MODULATED FUNCTIONS. (B) TABLE SHOWS GENES UP-REGULATED BY AB-CU TREATMENT AND RELATED TO FUNCTIONS SHOWN IN (A).

A

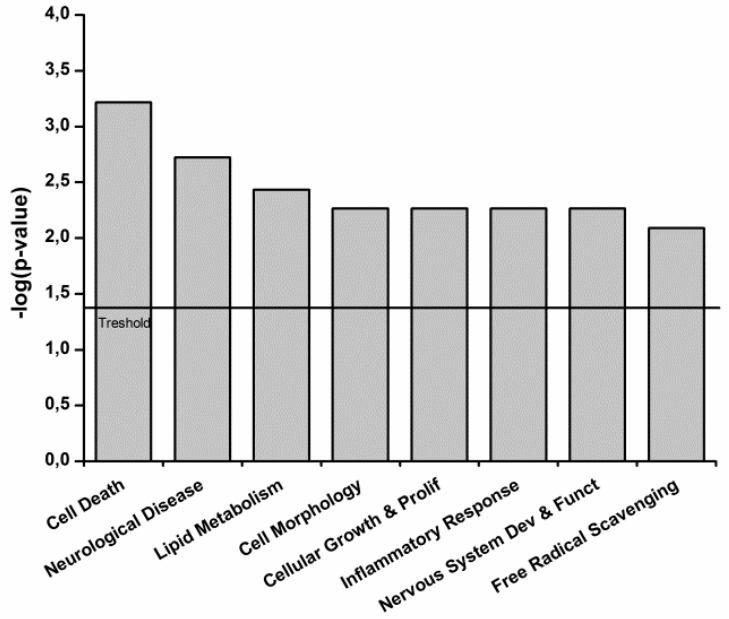

B

Category	p-value	Molecules
Cell Death	6,05E-04-4,8E-02	SAT1,GAPDH,USP2,ACIN1,PTK2 (includes EG:14083),TACR1,PRDM2,TXK,BMI1,LPAR2,PPP3CB,INPP5B,HSPBAP1,SORT1,HIPK2,PARVA,DUT,SRA1,IRF4,HIPK3,MAD2L1,CDC42BPA,YARS,MDK,BCL2A1,FOXC2,FANCA
Neurological Disease	1,9E-03-3,6E-02	APBA2,AGAP1,SAT1,GAPDH,BEST3,PDE1A,USP2,TOR3A,PTK2 (includes EG:14083), TACR1, HTR1B,BMI1,PRDM2,PPP3CB,HECW1,LAMA1,GSTM4,DARS,SORT1,NR2F6,HIPK2,CHRNA3,PARVA,IRF4,HIPK3,FXYD1,CXorf40A/CXorf40B,TTC23L,RXRG,CDC42BPA,PEX5,YARS,C21orf91
Lipid Metabolism	3,7E-03-4,8E-02	PTK2 (includes EG:14083), LTA4H,ABCD3, PEX5,HSPA1L,INPP5B,PCYT2,TSHR,SAT1,ECH1
Cell Morphology	5,45E-03-3,69E-02	PTK2 (includes EG:14083), MAD2L1,COL5A3,PARVA,HTR1B,SYNE2,LAMA1
Cellular Growth and Proliferation	5,45E-03-4,8E-02	,IRF4,RUVBL1,PTK2 (includes EG:14083), TACR1,MAD2L1,BMI1,TXK,LPAR2,LAMA1,TSHR, MDK,HIPK2,BCL2A1,,FANCA
Inflammatory Response	5,45E-03-4,59E-02	PTK2 (includes EG:14083), TACR1,IRF4, INPP5B, TSHR,MDK,BCL2A1
Nervous System Development and Function	5,45E-03-2,69E-02	PTK2 (includes EG:14083), APBA2,COL5A3, BMI1, HTR1B,PEX5,LAMA1,MDK, CHRNA3, FOXC2
Free Radical Scavenging	8,11E-03-8,11E-03	ME3

FIGURE 19 INGENUITY PATHWAY ANALYSIS FUNCTIONAL ANALYSIS OF DOWN-REGULATED GENES MODULATED BY EXPOSURE TO THE AB-CU. (A) BAR CHART SHOWS KEY MODULATED FUNCTIONS. (B) TABLE SHOWS GENES DOWN-REGULATED BY AB-CU TREATMENT AND RELATED TO FUNCTIONS SHOWN IN (A).

AD related up-regulated genes

ARF1: this gene encodes for the ADP-ribosylation factor (ARF1). The protein is localized in the Golgi apparatus and plays a crucial role in regulating the formation of coat protein complex I vesicle (ARFGAPs). Dysfunctional regulation of ARFGAPs has been implicated in several diseases including AD (Scheper et al., 2000).

C1QBP: this gene encodes for complement family proteins, C1r and C1s. These proteins co-localize with fibrillar amyloid plaques in the hippocampus and cerebral cortex of AD patients. Activated complement components are found in association with AD lesions and can contribute to local inflammation (Shen et al., 1997;Zhou et al., 2008).

CRP: this gene encodes for C-reactive protein. C-reactive protein plasma levels increase as result of tissue injury, infection or inflammatory stimuli, and have been reported in AD patients (Mulder et al., 2010).

DLG4: this gene encodes for post-synaptic scaffold protein PSD-95 that is involved in synaptic clustering and trafficking of ionotropic glutamate receptors. A correlation between AD and increased PSD-95 protein levels has been reported by some authors (Leuba et al., 2008); however, others have shown different results (Pham et al., 2010).

DLL1: this gene encodes for DLL1, a protein that is a downstream effector involved in Notch signaling, a key step in the cascade leading to Aβ production. Upregulation of DLL1 has been shown in Down syndrome and AD patients (Fischer et al., 2005).

ENO1: (described above in the Aβ-Zn section).

ENPP2: this gene encodes for a protein that has a role in active myelination and/or late stages of oligodendrocyte differentiation. Intriguingly, microarray analysis of rat brains revealed that mRNA levels of Enpp2 are increased by estrogens in the hippocampus, an interesting link as estrogens have a role in AD and promote neuronal survival against Aβ-mediated neurotoxicity (Aston et al., 2005;Takeo et al., 2009;Mateos et al., 2012).

GNB2L1 (as known as RACK-1): this gene encodes for the guanine nucleotide binding protein (G protein). GNB2L1 has been suggested to promote Aβ-driven cognitive impairment by favoring blockade of muscarinic receptor signaling (Zhong et al., 2003) and metabotropic glutamate receptor activation (Tyszkiewicz and Yan, 2005). Furthermore, GNB2L1 over-expression is effective in rescuing GABAergic neurotransmission in Aβ-treated cortical neurons (Liu et al., 2011b).

HMGCR: this gene encodes for HMG-CoA reductase that is the rate-limiting enzyme controlling cholesterol synthesis in the brain. Over-expression of HMGCR results in increased cholesterol plasma levels, induction of Aβ production, and increased AD risk (Rodriguez-Rodriguez et al., 2009).

IRAK-1: the protein encoded by this gene is the interleukin-1 receptor-associated kinase 1, a serine/threonine kinase associated with interleukin-1 receptor (IL1R) upon stimulation. The protein

modulates a plethora of biological processes, including activation of MAPK activity, activation of NF-κB-inducing kinase activity and Toll-like/IL-1 receptor signaling. Interestingly, unlike what we find here, the protein has been found decreased in human astroglial cells exposed to Aβ and in the hippocampus and neocortex of AD patients (Cui et al., 2010).

KIDINS220 (as known as ARMS): this gene encodes for a transmembrane scaffold protein that plays a critical role as BDNF-TrkB signaling (Wu et al., 2010). Down-regulation of this gene results in aberrant neuronal development (Higuero et al., 2010).

MAGED1: this gene encodes for a protein member of the melanoma antigen gene family. Although this protein is not expressed in normal adult tissue it should be underlined that the molecule is a cell-death inducer involved in neuronal development. Pharmacological inhibition of MAGED1 activity has been shown to reduce Aβ-mediated toxicity in cortical neurons (Di Certo et al., 2007).

MED12: the protein encoded by this gene is involved in neuronal development. MED12 is a new component of APP-dependent nuclear-signalling pathway (Xu et al., 2011) and MED12 mutations are associated with cognitive and behavioural dysfunction in humans (Turner et al., 2011).

MT2A: (described above in the Aβ-Zn section).

NDOR1-NR1: this gene encodes for a NADPH-dependent diflavin reductase. NR1 levels decrease in the frontal cortex and hippocampus of AD patients (Amada et al., 2005).

NFKBIA: the molecule encoded by this gene is involved in the inhibition of NF-κB-mediated inflammatory responses. NF-κB is one of the major pathways activated during Aβ-driven inflammation occurring in AD (Couturier et al., 2011).

PER1/CSNK1A1: these are two genes involved in circadian rhythms. Circadian rhythms are altered in dementia. Thus, changes in PER1 mRNA expression fit with the alterations of the sleep/awake cycle found in AD; however, significant differences in PER1 expression have not observed in a recent study on AD patients (Etchegaray et al., 2009;Tseng et al., 2010).

PHB: this gene encodes for prohibitin, a protein involved in a variety of functions in many cell types. The functions of prohibitin in neurons remain largely unknown; however, recent findings suggest a possible protective role against ROS-mediated neuronal death (Zhou et al., 2012).

PTRH2 (as known as BIT1): this gene encodes for Bit1, an effector of anoikis (Jan et al., 2004). Overexpression of Bit1 has been reported to mediate cell survival in adherent cells through activation of NF-κB pathways (Griffiths et al., 2011).

SIVA1: the protein encoded by SIVA1 gene plays a role in the activation of apoptotic pathways. SIVA1 also negatively regulates NF-κB activity (Gudi et al., 2006).

SNAP23: the protein encoded by this gene is an important regulator of transport-vesicles docking and fusion. SNAP-23 is relevant for the functional regulation of post-synaptic glutamate receptors. Loss of SNAP-23 in transgenic mice leads to marked decrease in NMDA receptor surface expression and NMDA receptor–mediated currents (Suh et al., 2010).

WWOX: the molecule encoded by this gene, the WW domain containing oxidoreductase, is a pro-apoptotic protein. A correlation between down-regulation of WWOX and increased Tau phosphorylation has been observed in AD hippocampi (Sze et al., 2004;Mukaetova-Ladinska et al., 2009).

AD related down-regulated genes

ABCD3: the protein encoded by this gene belongs to the superfamily of ATP-binding cassette (ABC) transporters. A recent report indicates a significant increase in ABCD3 expression upon inflammatory conditions (Gray et al., 2011).

APBA2: this gene encodes for a member of the X11 family that interacts with APP and inhibits production of proteolytic APP fragments, thereby suppressing Aβ production (Saito et al., 2008).

BCL2A1: this gene encodes for a member of the Bcl-2 protein family. BCL2A1 over-expression reduces release of cytocrome c, thereby exerting potent anti-apoptotic activity. Bcl-2 is crucial to reduce caspase activation.

CHRNA3: this gene encodes for a member of the nicotinic acetylcholine receptor family proteins. An association between polymorphisms of this gene and AD development has been reported suggesting a role in the pathogenesis of sporadic AD (Kawamata and Shimohama, 2002).

FOXC2: the role of this gene is still elusive. The encoded protein, FOXC2, belongs to the forkhead family of transcriptor factors. Data indicate possible involvement of this gene in the NF-κB-activating signalsome as downstream effector of inflammatory or stress-like stimuli (Li et al., 2002).

GSTP1: glutathione-S-transferase P1 is encoded by this gene. A recent study indicates a protective role of the molecule against Cdk5-induced neuronal toxicity. GSTP1 is effective in inhibiting Cdk5 and reducing oxidative stress (Sun et al., 2011).

HIPK2: this gene encodes for a serine/threonine kinase crucial to maintain p53 wild-type activity. Homodomain interacting protein kinase 2 is involved in Aβ-driven toxicity although a study found no interactions between Aβ treatment and HIPK2 mRNA expression in HEK-293 cells as well as in fibroblasts from AD patients (Lanni et al., 2010).

HSPA1L: this gene encodes for a 70kDa heat shock protein. Similarly to HSPA4, Hsp70 has been reported to exert a protective role against intracellular Aβ-driven toxicity (Cui et al., 2011).

HTR1B: this gene encodes for the serotoninergic receptor subtype 5-HT1B, 5-HT1B is a putative target for antidepressants activity (Clark and Neumaier, 2001).

MDK: this gene encodes for a hepatin-binding growth factor. This factor is involved in repair and development of several tissues including neuronal ones (Sakakima et al., 2009).

PMAIP1: the molecule encoded by this gene is involved in pro-apoptotic mechanisms by interfering with p53/p73 signaling. As far as AD, alterations in APP function induce expression of several p53/p73 target genes including PMAIP1 (Benosman et al., 2011).

PTK2 (as known as FAK): this gene encodes for a tyrosine kinase involved in cell adhesion. Aβ-driven PTK2 activation has been reported as one of the earliest biochemical responses triggered by Aβ exposure in human and rat cortical cultures (Williamson et al., 2002).

1.4.4 Early and sustained altered expression of aging-related genes in young 3xTg-AD mice

Background

Aging is critical for sporadic AD and a lively debate on whether the disease is actually driven by aging is animating the field (Ferrer, 2012). The "age-based hypothesis" postulates that the aging brain represents the *conditio sine qua non* on which events like head trauma, infections, vascular alterations, diabetes, or even genetic mutations need to act to initiate the AD-related pathogenic cascade (Herrup, 2010). In other words, the aging brain is the required battlefield on which pro-AD events successfully initiate the disease.

The genetic aspects of AD have been intensively investigated for years [for one extensive review see (Tanzi, 2012)]; however, critical pieces of information are still missing to successfully compose the

puzzle. Accumulating evidence has revealed that a large number of gene products are involved in the development of late onset forms of AD (LOAD). To date, at least 9 LOAD-associated gene candidates have been identified: *ABCA7, BIN1, CD2AP, CD33, CLU, CR1, EPHA1, MS4A4/MS4A6E*, and *PICALM* (Harold et al., 2009;Lambert et al., 2009;Hollingworth et al., 2011;Naj et al., 2011). Variants of these genes, along with those occurring in APOE, account for approximately 32% of the genetic risk for AD (Corder et al., 1993;Raber et al., 2004).

It should be underlined that genetic variations are not always detrimental. For instance, a recent study has identified a protective role played by a specific genetic variant (A673T substitution) in the gene encoding for the β-amyloid precursor protein (*APP*). According to the study, this substitution helps to counteract the cognitive decline of AD patients, but also promotes the maintaining of cognitive competence in healthy elderly. The study is important because supports the notion that common molecular mechanisms can modulate cognition upon AD and aging and provides a rationale for the hypothesis that AD can be interpreted as a boosted variant of otherwise naturally occurring age-driven changes (Jonsson et al., 2012).

Microarray technology allows the simultaneous analysis of thousands transcripts in a single experiment and is a useful approach for the investigation of a wide range of gene-related pathologies. Gene expression studies in transgenic AD models have helped to unravel genetic factors influencing the disease progression at well-defined stages of the pathology and have disclosed their relationship and potential causative role in determining the development of defective cognitive phenotypes (Reddy and McWeeney, 2006).

Thus, in the present study we employed a whole genome microarray approach to investigate age-dependent gene expression profile changes in hippocampi obtained from young [3 months of age; (m.o.a.)] and old (12 m.o.a.) 3xTg-AD mice.

3xTg-AD mice (harboring human mutant *APP, PS1*, and hyperphosphorylated tau) offer the selective advantage of combining both Aβ- and tau-dependent pathology and is one of the most widely investigated animal model of AD (Oddo et al., 2003). To control for age-dependent transcript modifications, we also investigated profiles occurring in age-matched wild-type (WT) mice.

The major aim of the study was to provide a better understanding of whether common genetic mechanisms are shared by aging and an AD-like background and if overlapping pathogenic pathways can be identified in the two conditions.

RESULTS

In our analysis, we compared expression profiles of 3 and 12 month old (m.o.) 3xTg-AD mice with those of age-matched WT mice. To take in account changes purely driven by aging, we also evaluated profile modifications occurring in 3 m.o. WT mice *vs* 12 m.o. WT mice. Profiles were analyzed by gene clustering and the analysis revealed four different gene clusters (Fig. 20).

FIGURE 20 *UNSUPERVISED HIERARCHICAL CLUSTERING ANALYSIS RESULT.* THE FIGURE DEPICTS TRANSCRIPTS THAT ARE CLUSTERED ACCORDINGLY TO THEIR EXPRESSION VALUES (LOG RATIOS). EACH ROW REPRESENTS A TRANSCRIPT, EACH COLUMN THE 9 MICROARRAY EXPERIMENTAL CONDITIONS AS LISTED ON TOP. QUANTITATIVE CHANGES IN GENE EXPRESSION ARE DEPICTED IN COLOURS. RED AND GREEN INDICATE UPREGULATED AND DOWNREGULATED TRANSCRIPTS, RESPECTIVELY. BLACK INDICATES NO CHANGES IN EXPRESSION. MISSING DATA POINTS ARE DEPICTED IN GRAY.

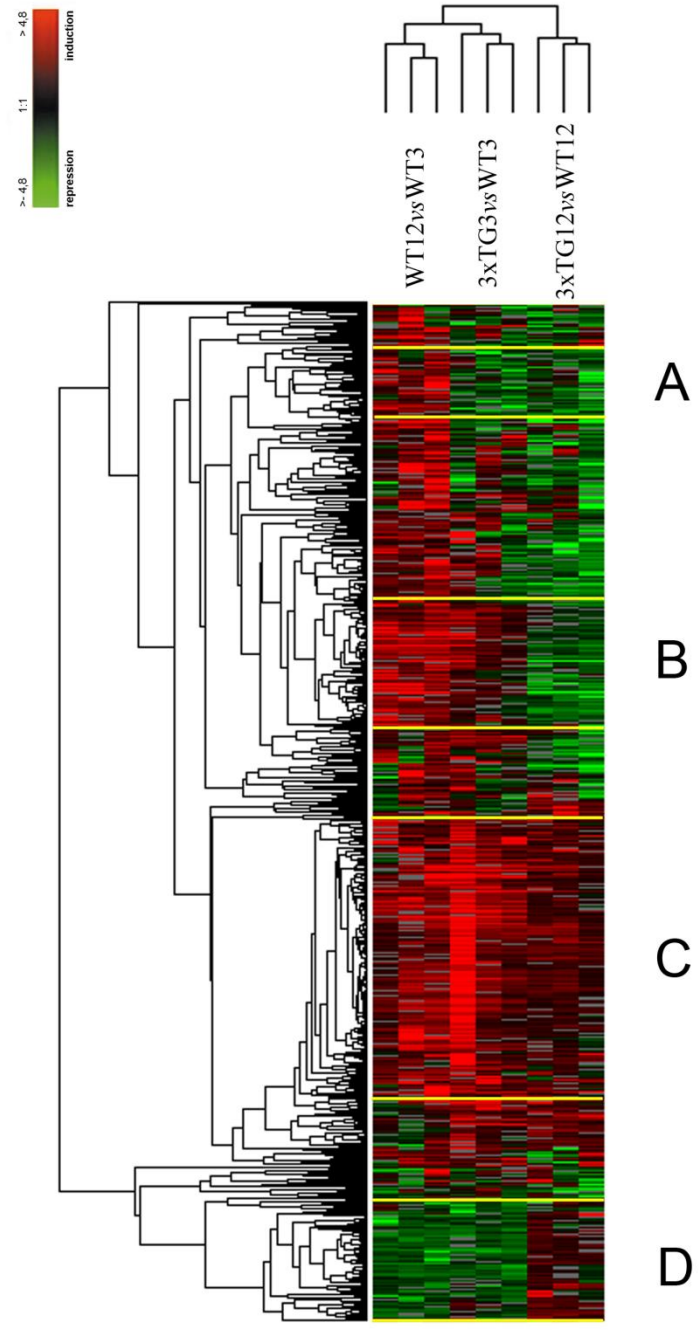

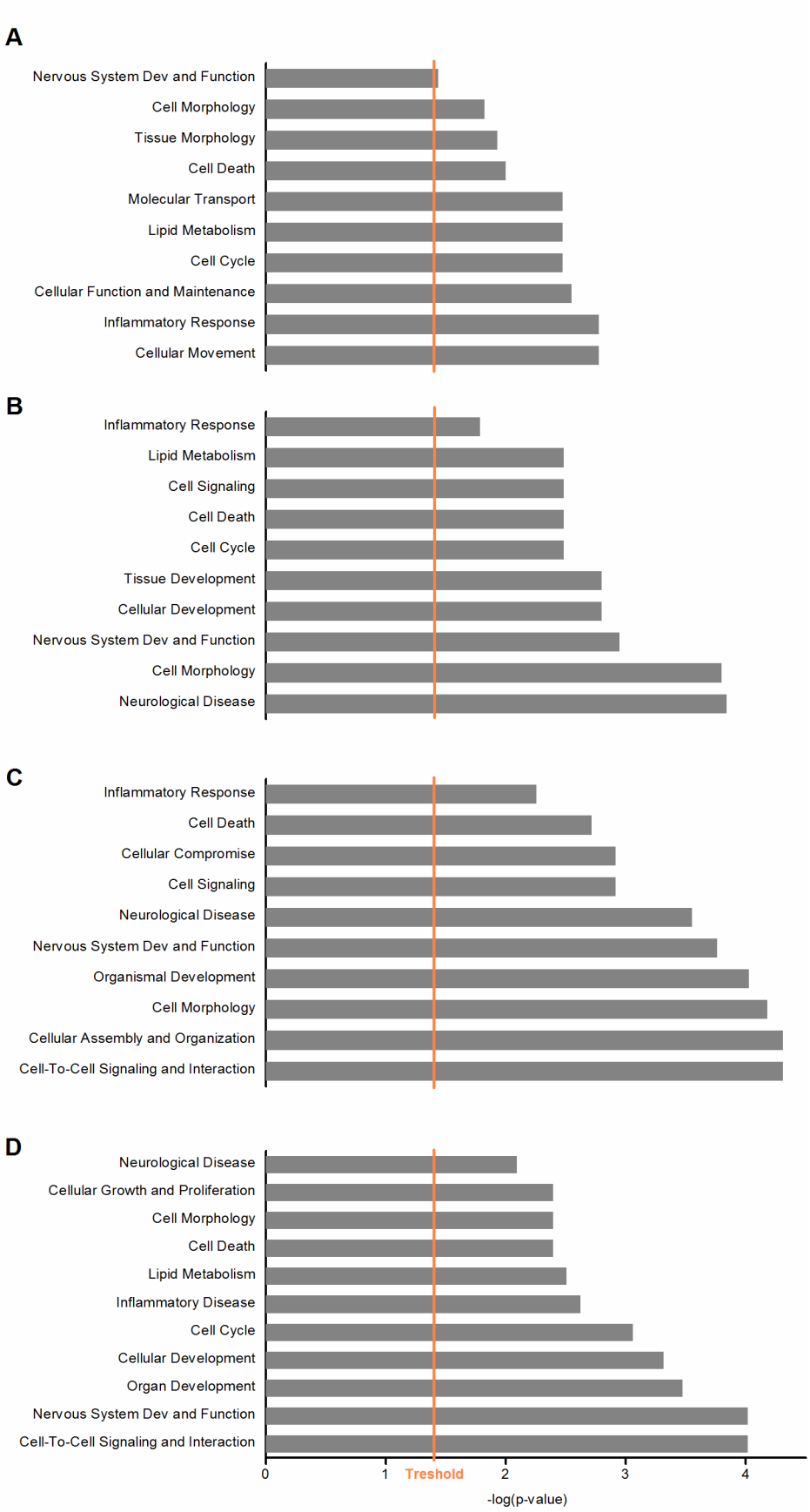

FIGURE 21. IPA BIOLOGICAL FUNCTION ANALYSIS. BAR CHARTS SHOW RESULTS OF IPA AND INDICATE KEY BIOLOGICAL FUNCTIONS MODULATED BY GENES SELECTED IN THE FOUR CLUSTERS DESCRIBED IN FIGURE 1. (A) CLUSTER A; (B) CLUSTER B; (C) CLUSTER C; (D) CLUSTER D.

Cluster A

Cluster A consists of 37 transcripts that, compared to age-matched WT mice, were found downregulated in both 3 m.o. and 12 m.o. 3xTg-AD mice. The same gene set was found upregulated in 12 m.o. WT mice when compared to 3 m.o. WT (Fig. 20A). IPA functional analysis indicated that the main biological functions associated with these genes belong to cellular movement, inflammatory response, cellular function and maintenance, cell cycle, lipid metabolism, molecular transport, cell death, tissue morphology, cell morphology, nervous system development and function (Fig. 21A, Tab. 2). Eight of these genes are involved in aging- and/or neurodegeneration-related functions as follows:

i) *Ckap2* and *DNASE1L3* (apoptotic death);

ii) *Dysferlin*, the *TMSB10/TMSB4X* complex and *Homer3* (Aβ processing and accumulation);

iii) *Complexin III*, *HCNP,* and *PEBP1* (neuronal development and differentiation)

Table 2. IPA functional analysis of genes of cluster A

Category	p-value	Molecules
Cellular Movement	1,69E-03-4,63E-02	*GPR182, PEBP1, CPLX3, TMSB10/TMSB4X, HAS1*
Inflammatory Response	1,69E-03-1,69E-03	*TMSB10/TMSB4X*
Cellular Function and Maintenance	2,84E-03-3,66E-02	*PEBP1, CPLX3, TMSB10/TMSB4X, CDC42EP2, HAS1*
Cell Cycle	3,38E-03-8,43E-03	*CKAP2*
Lipid Metabolism	3,38E-03-3,38E-03	*PEBP1*
Molecular Transport	3,38E-03-3,66E-02	*PEBP1, CPLX3*
Cell Death	1,01E-02-3,84E-02	*TMSB10/TMSB4X, CKAP2, DYSF, null*
Tissue Morphology	1,18E-02-1,18E-02	*HAS1*
Cell Morphology	1,51E-02-4,92E-02	*PEBP1, TMSB10/TMSB4X, ADCY6, VPS37C, HAS1*
Nervous System Development and Function	3,66E-02-3,66E-02	*CPLX3*

Cluster B

Cluster B consists of 62 transcripts that, compared to 3 m.o. WT mice, were found upregulated in 3 m.o. 3xTg-AD mice and 12 m.o. WT mice. The same set was downregulated in 12 m.o. 3xTg-AD mice when compared to 12 m.o. WT mice (Fig. 20B). IPA analysis showed that these genes are implicated in several key biological functions such as: neurological disease, cell morphology, nervous system development and function, cellular development, tissue development, cell cycle, cell death, cell signaling, lipid metabolism, and inflammatory response (Fig. 21B, Tab. 3). Several genes belonging to this cluster are also involved in aging- and/or neurodegeneration-related functions as follows:

i) *CD200, Neurod1, SOX9* (neuroglia quantity*), OPHN1* (dendritic spines), *SNAP25, EGR1, OPHN1* (memory) *OPHN1, ETV1, CDH2* (axon guidance), *GABRA1, Cadherin* (synapse formation), and *Spond1* (neuronal development);

ii) *SPIN1, JAK3, Neurod1, SOX9, YWHAE, DNAjB, EGR1, and HSPA1A/HSPA1B* (cell cycle arrest and cellular senescence);

iii) *Hsp70, IL10 receptor,* and *CD200* (inflammation);

iv) *Ndufs1 and TRAK1* (mitochondrial functioning)

Table 3. IPA functional analysis of genes of cluster B

Category	p-value	Molecules
Neurological Disease	1,45E-04-4,55E-02	*CTR9, NEUROD1, CD200, YWHAE, HSPA1A/HSPA1B, EGR1, F7, SSR1, SCOC, SNAP25, MFAP2, CDH2, SOX9, RSPO2, PROCR, GABRA1*
Cell Morphology	1,61E-04-4,87E-02	*NEUROD1, LDB3, YWHAE, PAM, HSPA1A/HSPA1B, EGR1, F7, OPHN1, SOX9, CDH2, NDUFS1, RSPO2, PROCR, GABRA1*
Nervous System Development and Function	1,14E-03-4,87E-02	*NEUROD1, CD200, YWHAE,RIT2, HSPA1A/HSPA1B, EGR1, ETV1, SNAP25, OPHN1, CDH2, SOX9, GABRA1, TACC1*
Cellular Development	1,6E-03-4,43E-02	*NEUROD1, SOX9, HSPA1A/HSPA1B, RIT2, EGR1, RSPO2, F7, JAK3, SPRED2*
Tissue Development	1,6E-03-4,75E-02	*NEUROD1, MFAP2, SOX9,CDH2, CD200, EGR1, F7, JAK3, CERCAM*
Cell Cycle	3,32E-03-3,64E-02	*NEUROD1, SOX9, YWHAE, HSPA1A/HSPA1B, EGR1, JAK3*
Cell Death	3,32E-03-4,95E-02	*NEUROD1, CD200, YWHAE, HSPA1A/HSPA1B, EGR1, F7, DNAJB9, DSG1, NDUFS1, CDH2, SOX9, UBA7, PROCR, JAK3, TACC1*
Cell Signaling	3,32E-03-3,59E-02	*SOX9, CDH2, YWHAE, RIT2, IL10RB, F7, DOK3, SNAP25*
Lipid Metabolism	3,32E-03-2,62E-02	*Rdh1 (*includes others*), F7*
Inflammatory Response	1,65E-02-4,55E-02	*CD200, EGR1, F7, DOK3, YTHDF2*

Cluster C

Cluster C consists of 193 transcripts that, compared to age-matched WT mice, were upregulated in 3 and 12 m.o. 3xTg-AD mice. The same set was upregulated in 12 m.o. WT mice compared to 3 m.o. WT mice (Fig. 20C). IPA-inferred functional analysis revealed that the overexpressed transcripts are associated to cellular assembly and organization, in cell-to-cell signaling and interaction, cell morphology, organismal development, nervous system development and function, neurological disease, cell signaling, cellular compromise, cell death, and inflammatory response (Fig. 21C, Tab. 4). Among these 193 transcripts, 62

belong to the "nervous system development and function" and "neurological disease" categories. Most of the cluster C transcripts are also involved in aging- and/or neurodegeneration-related mechanisms as follows:

i) *Hax1, NDUFA9, GDAP1, HADHB, KIF1B, PGAM1, Ppia,* and *DNM1L* (mitochondrial functioning);

ii) *ATP2B1, CACNB4, RYR2, PKD2,* and *NDUFA9* [homeostasis of intracellular calcium (Ca^{2+})];

iii) *IRF1, PPIA, VCAM1, TIMP2, HMGB1L1, PGAM1*, and *JAK1* (inflammatory response);

iv*) APBA2, APP, GABRA5, MAPK1, PMP22, SYBU, USP14*, and *VDAC3* (synaptic transmission); *APP, B2M, MAPK1, NPTN, VDAC3* [long-term potentiation (LTP)]; *APP, CST3, DCC, HES1, HEY1, HPRT1, SOX2,* and *YWHAH* (neurogenesis); *APBA2, APP, CRK, DCC, GPR12, HMGB1L1, MAPK1, STK38L, VCAM1*, and *YWHAZ* (neurite outgrowth);

v) *Beclin-1, MAP1LC3-B, HADHB, AK5, CyC1, SIRT7,* and *ENC1* (neuronal death);

vi) *HSPA12A, HIAT1, KIAA1409, NRP2, STARD13, UBB, PKIA* [AD-related single nucleotide polymorphisms (SNPs)];

vii) *APP, ATP6V1C1, BECN1, CST3, DCC, DNM1L, GABRA5, GABRB1, HIAT1, HSPA12A, KIAA1409, LPPR4, MAPK9, NRP2, PKIA, RYR2, STARD13, UBB,* and *YWHAZ* (AD pathogenesis)

Table 4. IPA functional analysis of genes of cluster C

Category	p-value	Molecules
Cell-To-Cell Signaling and Interaction	4,94E-05-2,9E-02	*B2M, APBA2, VCAM1, GABRA5, USP14, JAK1, NRP2, MAPK1, KIF1B, CACNB4, CRK, HES1 (*includes *EG:15205), VDAC3, App, IRF1 (*includes *EG:16362), SYBU, PMP22, DCC, RSU1*
Cellular Assembly and Organization	4,94E-05-2,9E-02	*B2M, APBA2, FHL1 (*includes *EG:14199), YWHAH, GPR12, MAPK1, KIF1B, HAX1, LPPR4, BOK, SNX3, CRK, BECN1, App, WASL, MYRIP, STARD13, DCC, MAP1LC3B, NRN1, VCAM1, NRP2, MED1 (*includes *EG:19014), RYR2, SEPT7, SMARCA5, YWHAZ, STK38L, MAPK9, GDAP1, VDAC3, TSG101, SYBU, PMP22, CETN3, Hmg1l1, HPRT1, DNM1L, ENC1*
Cell Morphology	6,66E-05-3,45E-02	*B2M, APBA2, VCAM1, MAPK1, GPR12, NRP2, SEPT7, RYR2, STK38L, YWHAZ, CRK, GDAP1, HES1 (*includes *EG:15205), BECN1, VDAC3, App, TSG101, PMP22, Hmg1l1, STARD13, DCC, MAP1LC3B, DNM1L, NRN1*
Organismal Development	9,48E-05-2,9E-02	*PAFAH1B2, VCAM1, JAK1, MAPK1, NRP2, MED1 (*includes *EG:19014), PKD2 (includes EG:18764), MAPK9, BECN1, App, H2AFZ, TSG101, WASL, Hmg1l1,CST3,TIMP2*
Nervous System Development and Function	1,75E-04-3,24E-02	*B2M, APBA2, USP14, GABRA5, GPR12, MAPK1, YWHAH, KIF1B, ITM2B, LPPR4, CRK, HES1 (includes EG:15205), App, SOX2, CST3,*

		*DCC, BPNT1, NRN1, HEY1, VCAM1, NRP2, MED1 (*includes *EG:19014), CACNB4, STK38L, YWHAZ, MAPK9, VDAC3, SYBU, PMP22, null, Hmg1l1, HPRT1, DNM1L, ENC1*
Neurological Disease	2,83E-04-3,34E-02	*GABRA5, YWHAH, MAPK1, ATP6V1C1, ATP2B1, KIF1B, LPPR4, SLMAP, SOX2, PDHA1, TTBK2, PGAM1, GABRB1, PKIA, PGRMC1, G3BP2, IMPA1, HIAT1, YWHAZ, SPARCL1, HPRT1, CYC1, TMEM66, RSU1, ORC4, ENC1, B2M, APBA2, CA2, FHL1 (*includes *EG:14199), ITM2B, PPP1CB, BECN1, App, UNC79, TBCEL, FARSB, HADHB, TMEFF1, PPP3CB, CST3, STARD13,* *DCC, null, JKAMP, VCAM1, NRP2, SLC2A13, CACNB4, RYR2, MAPK9, GDAP1, KIFAP3 (*includes *EG:16579), HSPA12A, PMP22, AK5, null, DOCK8, PPIA, GLT25D2, DNM1L*
Cell Signaling	1,23E-03-3,34E-02	*G3BP2, JAK1, MAPK1, ATP2B1, PKD2 (*includes *EG:18764), RYR2, CACNB4, STK38L, MAPK9, CRK, KIFAP3 (*includes *EG:16579), App, IRF1 (*includes *EG:16362), SOX2, CLK1, TRIM13, TTBK2, PPM1A, RSU1, TMEM9B, TIMP2*
Cellular Compromise	1,23E-03-3E-02	*VCAM1, MAPK1, SEPT7, PGAM1, CRK, GDAP1, DNM1L, TSG101, App, IRF1 (*includes *EG:16362)*
Cell Death	1,93E-03-3,45E-02	*PAFAH1B2, CA2, VCAM1, JAK1, MAPK1, KIF1B, MED1 (*includes *EG:19014), CUL1, YWHAZ, SMARCA5, MAPK9, BOK, HES1 (*includes *EG:15205), BECN1, KIFAP3 (*includes *EG:16579), TSG101, App, IRF1 (*includes *EG:16362), GNPTG, NT5C3, PMP22, AK5, Hmg1l1, DCC, PPM1A, TIMP2*
Inflammatory Response	5,57E-03-3E-02	*VCAM1, JAK1, Hmg1l1, PPIA, PGAM1, App, IRF1 (*includes *EG:16362), TIMP2*

Cluster D

Cluster D consists of 77 transcripts that, compared with 3 m.o. WT mice, were downregulated in 3 m.o. 3xTg-AD mice and 12 m.o. WT mice. These transcripts were upregulated in 12 m.o. 3xTg-AD mice when compared with 3 m.o. WT mice (Fig. 20D). IPA analysis of cluster D indicated transcripts involvement in cell-to-cell signaling and interaction, nervous system development and function, organ development, cellular development, cell cycle, inflammatory disease, lipid metabolism, cell death, cell morphology, cellular growth and proliferation, and neurological diseases (Fig. 21D, Tab. 5). Several transcripts are also involved in aging- and/or neurodegeneration-related functions as follows:

i) *BIN, ACTB, BAIAP2, EphB, KLK8, ARD1, PDE4, Ehmt2, Neurod2, STAT3, S100B,* and *CCND3* (neuronal proliferation, survival and differentiation, neuronal plasticity and synapse formation);

ii) *ARID1A, BRD4, CCND3, EHMT2, GPC1, LAS1L, MAP4, PA2G4, PTGES3, STAT3,* and *TRRAP* (cell division processes);

iii) *Atp6v1a* (mitochondrial activity)

Table 5. IPA functional analysis of genes of cluster D

Category	p-value	Molecules
Cell-To-Cell Signaling and Interaction	9,74E-05-4,89E-02	*ST5, EPHB1, ARID1A, CCND3, BAIAP2, RGS4, STAT3*
Nervous System Development and Function	9,74E-05-4,99E-02	*ISLR2, NEUROD2, EPHB1, PRPF19, CCND3, ACTB, S100B, BAIAP2, PDE4A, RGS4, STAT3, DIO2, KLK8, RNF6, HIP1R*
Organ Development	3,38E-04-4,59E-02	*EPHB1, CCND3, STAT3, DIO2*
Cellular Development	4,87E-04-4,78E-02	*PRPF19, PA2G4, ELAVL3, PDE4A, RGS4, STAT3, DIO2, BIN1, GPC1, NEUROD2, LSMD1, CCND3, S100B, BAIAP2, BRD4, UBTF, TRRAP, SCAND1*
Cell Cycle	8,76E-04-4,78E-02	*GPC1, MAP4, ARID1A, null, CCND3, PA2G4, EHMT2 (*includes *EG:10919), LAS1L, BRD4, STAT3, TRRAP*
Inflammatory Disease	2,39E-03-3,47E-02	*CCND3, PDE4A, STAT3*
Lipid Metabolism	3,14E-03-3,6E-02	*GPC1, MAP4, null, COTL1, HIP1R*
Cell Death	4,07E-03-3,21E-02	*PRPF19, ARID1A, PA2G4, ACTB, PDE4A, RGS4, STAT3, CAPN10, KLK8, BIN1, ITPK1, GPC1, MAP4, LSMD1, CCND3, S100B, VCP, UBTF, TEX261*
Cell Morphology	4,07E-03-4,39E-02	*ISLR2, MAP4, ACTB, BAIAP2, VCP, S100B, PDE4A, BRD4, RGS4, STAT3, TRRAP, RNF6*
Cellular Growth and Proliferation	4,07E-03-4,99E-02	*PRPF19, PA2G4, ACTB, RGS4, STAT3, NAA10, BIN1, GPC1, LSMD1, CCND3, EIF4A1, S100B, BRD4, PTPRS, LAS1L, UBTF, TRRAP*
Neurological Disease	8,12E-03-3,21E-02	*S100B, STAT3*

TaqMan qRT-PCR: microarray data validation

In order to validate the microarray results, qRT-PCR analysis was performed on RNA extracted from the same hippocampal samples employed for microarray experiments. Analysis was performed on three upregulated genes (*BECN1, CST3, GABRA5*) belonging to cluster C. In all cases, qRT-PCR confirmed the microarray results (Fig. 3). Interestingly, with the limitation associated with the low number of genes investigated by qRT-PCR, we observed that the assayed transcripts are undergoing statistical significant overexpression upon aging in WT mice while 3xTg-AD animals already reached maximal expression in young mice compared with the old 3xTg-AD animals. In particular, young 3xTg-AD showed expression values overcoming those of old WT mice.

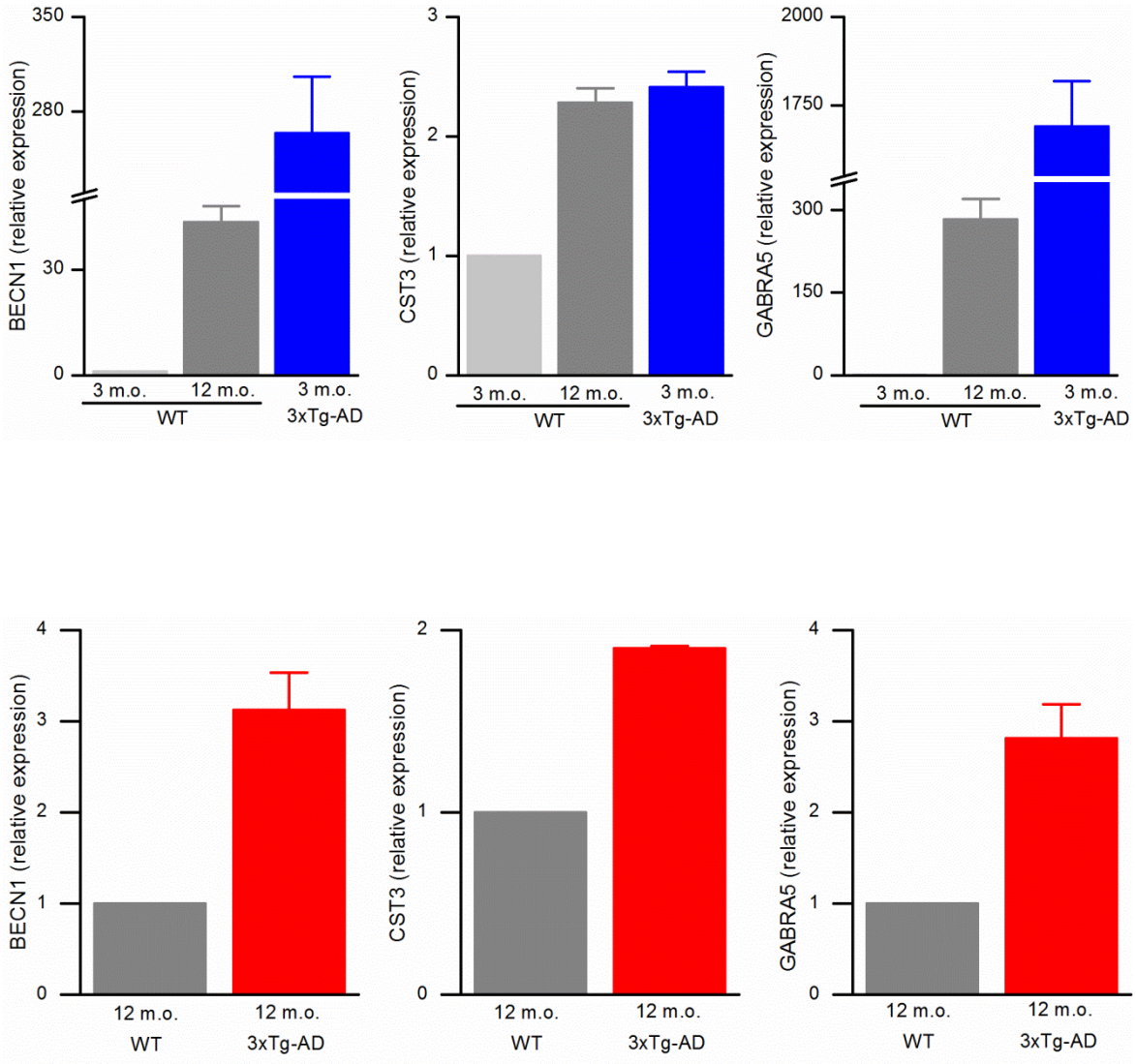

FIGURE 22 BAR GRAPH SHOW MRNA LEVELS OF CST3, GABRA5, AND BECN1 MEASURED BY REAL TIME PCR IN YOUNG AND OLD WT MICE AND 3XTG-AD MICE AS WELL AS IN OLD WT MICE AND 3XTG-AD MICE. DATA ARE EXPRESSED AS MEAN VALUE OF RELATIVE FOLD CHANGES ± SD OF THREE INDEPENDENT EXPERIMENTS PERFORMED IN TRIPLICATE.

1.5 DISCUSSIONS

1.5.1 RESVERATROL IN AB AND AB-METAL CONJUGATES AGGREGATION AND TOXICITY

It has been demonstrated by several laboratories that resveratrol has the capability to extend lifespan in several organisms (Wood et al., 2004;Gruber et al., 2007). Consequently this natural compound aroused great interest as possible nutritional supplement to prevent aging effects.

As demonstrated by MTT assay (Fig. 3C) resveratrol reduced not only Aβ [as already demonstrated in different models by (Xue et al., 2009;Gandy et al., 2010;Manczak et al., 2010)] but also reduces Aβ-metal complexes toxicity on neuroblastoma cells. It has been previously reported by this laboratory that metal ions (such as Al, Cu, Fe and Zn) influence heterogeneously Aβ aggregation properties *in vitro* and its toxicity towards neuroblastoma cells (Drago et al., 2008a).

Several papers have highlighted resveratrol capability to be a potent anti-amyloidogenic and fibril-destabilizing polyphenol (Ono et al., 2003;Riviere et al., 2007;Vingtdeux et al., 2008;Ladiwala et al., 2010). In our opinion the supposed mechanism of action is unsatisfactory for two reasons: 1) in accordance with Hudson et al. (2009) resveratrol biases the thioflavin T fluorescence assay for amyloid fibril detection through nonspectral interferences. 2) Anti-aggregative drugs for the treatment of AD could be more dangerous than beneficial as oligomers are more toxic than fibrils (Pratico, 2008;Wan et al., 2011). As suggested by Hudson and colleagues (2009), CR assay was performed to detect the presence of amyloid fibrils in the presence of resveratrol. As shown in Fig. 1, resveratrol does not influence Aβ-metal complexes aggregative pathway, except for Aβ-Cu. In this case we observed an increase in fibrillization. We could speculate that resveratrol has the capability of stabilizing Aβ-Cu complex into well ordered structures. This is probably due to the tendency of resveratrol to chelate Cu (Fig. 2). In agreement with CR assay, also TEM micrographs do not show an anti-amyloidogenic effect of resveratrol in any tested condition.

After excluding an anti-amyloidogenic role played by resveratrol, its antioxidant properties were investigated to explain the neuroprotective activity. It has been widely demonstrated that AD brain showed damages caused by ROS (Behl et al., 1994;Hensley et al., 1994;Milton, 2004). ROS in AD are the byproduct of several pathological events. Among these is the production of hydrogen peroxide by Aβ (Huang et al., 2004;Stoltenberg et al., 2007;Duce and Bush, 2010) and the accumulation of transition metals (such as Fe^{3+}, Cu^{2+} and Zn^{2+}) (Alscher et al., 2002;Zatta et al., 2002;Verstraeten et al., 2008). Aβ-metals complexes cause the coexistence of these two by-products exacerbating damages due to cellular oxidative stress. Accordingly with this hypothesis we observed an increase in super-oxide dismutase (SOD) activity in neuroblastoma cells treated with Aβ-Fe, Aβ-Cu and Aβ-Zn compared with non treated cells (Fig. 5B). SOD (both as SOD1 and SOD2) act as an antioxidant, protecting cells from being damaged by free radical species (Kumar and Gill, 2009); their increase is an indication of cellular oxidative stress due to ROS overproduction. Neuroblastoma cells treated simultaneously with Aβ-metal complexes and resveratrol showed negligible differences in SOD activity if compared with controls. Altogether these data suggest that

Aβ-Fe and Aβ-Zn complexes exerted their toxicity mainly through oxidative stress involved in SOD expression (e.g.: production of radical species); while Aβ-Cu seemed to exert its toxicity through different mechanisms; in fact this complex was still toxic, even in the presence of resveratrol.

Aβ and especially Aβ-Al resulted significantly toxic on neuroblastoma cells without increasing SOD activity, suggesting that Aβ and Aβ-Al were not directly involved in free radical species production in our experimental conditions; in fact Al^{3+} is neither a redox metal nor taking part in oxidative stress processes alone or in the conditions we used (Atwood et al., 2003;Hureau and Faller, 2009), meanwhile Aβ, not complexed with metals, is involved in H_2O_2 production but it seems not involved in that of free radical species (Huang et al., 2004). Aβ and Al capacity to produce free radicals is linked to the presence of transition metals such as Fe and Cu (Lovell et al., 1998;Atwood et al., 2003;Stoltenberg et al., 2007;Verstraeten et al., 2008). Nevertheless, resveratrol resulted neuroprotective also against Aβ and Aβ-Al suggesting that it can act through other mechanisms not necessarily involving SOD activity. It is noteworthy that resveratrol plays its neuroprotective role through several activities including: activation of protein kinase C, reduction of malondialdehyde levels, blocking COX-2 expression, reduction of neuroinflammatory responses and scavenging (Fremont, 2000;Vingtdeux et al., 2008;Kim et al., 2010).

Despite these chemopreventive properties, Aβ-Al and Aβ-Cu retained toxic activity on neuroblastoma cells even after treatment with resveratrol; this suggests that these two Aβ-metal complexes exert their toxicity through mechanisms that cannot be prevented by resveratrol. In agreement, it has been previously demonstrated by this laboratory that Aβ-Al could damage cell membranes thanks to its high superficial hydrophobicity (Suwalsky et al., 2009), acting as a bullet hitting cell surface. Similarly, Aβ-Cu exerts its toxicity through mechanisms that are not only oxidative stress dependent (Dahlgren et al., 2002).

In conclusion, results herein presented highlight four main findings: we did not observed in our experimental conditions any anti-amyloidogenic and fibril-destabilizing effect played by resveratrol, as proposed by other groups; resveratrol exerts its neuroprotective activity not only against Aβ but also against Aβ-metal complexes; resveratrol acts as a scavenger against Aβ-Fe, Aβ-Cu and Aβ-Zn free radicals production, reducing their toxicity; eventually, resveratrol is not sufficient to fully prevent Aβ-Al and Aβ-Cu toxicity.

1.5.2 Physiological cholesterol concentration is neuroprotective against Ab and Ab-metal conjugates toxicity

One of the toughest challenges in the study of AD is to establish the pathological primum movens of the disease. The difficulty is due to the multifactorial character of this syndrome; a recent review underlines the complexity of this pathology and caused by the huge amount of variables that could interact with its development (Querfurth and LaFerla, 2010). Within all the possible variables influencing the course of AD, metal ions seemed to play a critical role on Aβ aggregation and consequently its toxicity. It has been demonstrated by this laboratory that aluminum is the most effective metal ion able of influencing

Aβ toxicity (i.e.: on neuroblastoma cells), while other metals tested (i.e.: Fe, Cu and Zn) showed minor or negligible effects (Drago et al., 2008a;Zatta et al., 2009). The aim of this study was to investigate the role of cholesterol on Aβ and Aβ-metal complexes aggregation and in influencing their interaction with lipid model of cellular membrane. The role of high levels of cholesterol, as AD aggravating factor, has been largely demonstrated (Cossec et al., 2010;McGuinness and Passmore, 2010;Vestergaard et al., 2010) and its ability to influence Aβ aggregation has received considerable attention despite some inconsistencies in the literature (see Table 1) (Frears et al., 1999;Harris, 2002;Ricchelli et al., 2005;Ferreira et al., 2007). We have previously hypothesized that the toxicity of Aβ-metal complexes is related to their ability in perturbing cellular membranes (Suwalsky et al., 2009). In this connection there is a huge body of evidences supporting Aβ role in disrupting membrane structure (McLaurin and Chakrabartty, 1997;Chauhan et al., 2000). The ability of Aβ-metal complexes to alter membrane structures is linked to their ability to retain the oligomeric state and to expose hydrophobic clusters that interact with the lipid bilayer (Kremer et al., 2001). Aβ-Al was the most effective Aβ-metal complex to combine these features even in the presence of cholesterol (Fig. 1 and 2). In agreement, we demonstrated Aβ-Al was the most effective agent in perturbing cell membrane models as well as a cause of neuronal death (Drago et al., 2008a;Suwalsky et al., 2009).

In our experimental conditions, cholesterol (at the same molar ratio used on cell cultures, 1:10) seemed to balance the increased membrane disorder caused by the presence of Aβ-Al. As shown in Fig. 5B, cholesterol alone did not induce changes on DMPC bilayer structure. On the contrary, the presence of cholesterol in solution, together with Aβ-Al, drastically reduced alterations on DMPC bilayer produced by this metal complex. This result could be explained on the basis of the role played by cholesterol in membrane structure. It has been consistently demonstrated that cholesterol modulates the properties of lipid bilayers, making them less deformable and thereby less permeable to small water-soluble molecules. These results appeared coherent with data obtained from cell viability assay (Fig. 3) observing a significant decrease in Aβ-Al toxicity in the presence of cholesterol. Aβ alone also resulted less toxic even not significantly in the presence of cholesterol. Only Aβ-Cu in the presence of cholesterol resulted more toxic if compared with Aβ-Cu alone. We could speculate that this result is most likely due to oxidative stress properties of Cu emphasized by the presence of cholesterol; however further and more specific investigations are required. Meanwhile, treatment with Aβ-Fe and Aβ-Zn in the presence or in the absence of cholesterol exerted only negligible effects, both in cell viability and X-ray diffraction essays. As for cell viability, Aβ-Fe showed a higher reproducibility in cells treated with Aβ-Fe in the presence of cholesterol (SD ±0,14%) unlike those treated with Aβ-Fe alone (SD ±5,9%); we can hypothesize this result is related to an increased stabilization of the Aβ-Fe complex in the presence of cholesterol. Even in this case, further investigations are required to confirm this speculation and clarify the interaction between Aβ-Fe and cholesterol.

One aim of our study was to investigate the effect of Aβ and Aβ-metal complexes on a lipid model of cellular membrane. We found that Aβ-Al complex was the most effective in perturbing DMPC bilayer

(Fig. 5A) compared to the other metal complexes. Considerably less pronounced was the effect of Aβ-Al complex on DMPE bilayer (Fig. 6A). This result can be explained on the basis of their different structures. DMPC and DMPE differ only in their terminal amino groups, these being $^{+}N(CH_3)_3$ in DMPC and $^{+}NH_3$ in DMPE. Moreover, both molecular conformations are very similar in their dry crystalline phases (Suwalsky et al., 1996) with the hydrocarbon chains mostly parallel and extended, and the polar head groups lying perpendicularly to them. However, the gradual hydration of DMPC results in water filling the highly polar interbilayer spaces with the resulting increase of their width. This phenomenon allows for the incorporation of the Aβ-Al complex into DMPC bilayers disrupting their arrangement and consequently the whole of the bilayer structure. Moreover, DMPE molecules pack tighter than those of DMPC due to their smaller polar groups and higher effective charge, resulting in a very stable bilayer system that is not significantly affected by water (Suwalsky et al., 1996). On the other hand, the Al complexed with Aβ may induce a change in the net charge of the peptide which can promote abnormal lipid-peptide interactions, thus promoting pathological oligomerization of Aβ. Recently, our group has demonstrated that when Al was bound to Aβ, forming a stable metallorganic complex, the surface hydrophobicity of the peptide dramatically increased as a consequence of metal-induced conformational changes, favouring misfolding/aggregation phenomena (Mizuno et al., 1999). Aβ-Al, thanks to its higher lypophilicity compared to the other Aβ-metal complexes, could intercalate with the acyl chain region altering the bilayer arrangement. In accordance, we showed that Aβ-Al was able to promote a greater increase in membrane fluidity mostly in the lipid tail/polar heads border areas of cell membrane with respect to the other Aβ-metal complexes (Suwalsky et al., 2009).

Collectively, our results indicate that cholesterol seems to slow down Aβ and Aβ-metal complexes aggregation pathway without blocking it, with the exception of Aβ-Al (see above). In addition, our results indicate that physiological concentrations of cholesterol avoid external lipid bilayer leaflet disruption caused by Aβ-Al. In agreement we also observed a decrease in Aβ and Aβ-metal complexes toxicity, with the not significant exception discussed above. These data could suggest a protective role played by cholesterol at concentrations closed to those physiological, highlighting once more the thin limit between positive or negative effects caused by cholesterol. Nevertheless future studies will be required to fully understand the mechanisms that underlie these results.

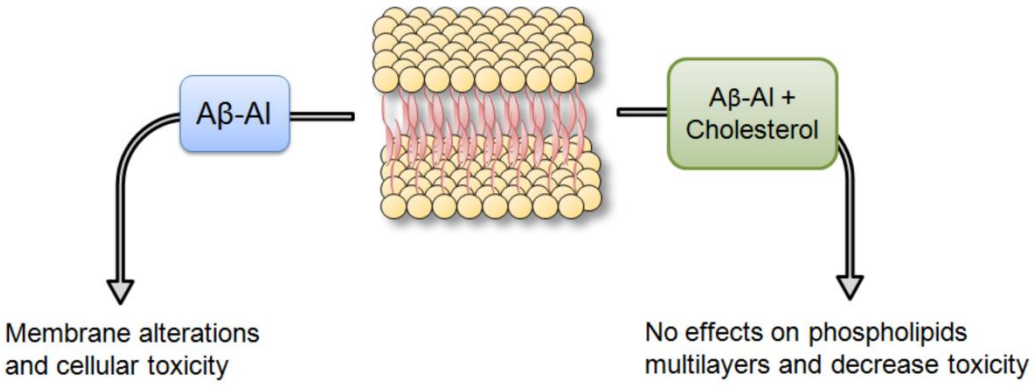

1.5.3 MICROARRAY ANALYSIS OF GENE EXPRESSION PROFILES IN HUMAN NEUROBLASTOMA CELLS EXPOSED TO AB-ZN AND AB-CU CONJUGATES

In recent years, great attention has been focused on how changes in Aβ conformation can affect the neurotoxic properties of the peptide and it is now established that oligomers are the most toxic species. Thus, factors promoting Aβ capability to retain its oligomeric structure strongly influence the pathogenic weight of the peptide. Several endogenous factors alter Aβ folding and, among these, metals appear to have a primary role in the process. We have previously shown (Drago et al., 2008a;Bolognin et al., 2011) that several metals when conjugated with Aβ modified cell viability most likely by changing the peptide folding. However, it must be noted that oligomerization is not the only pathogenic factor in AD as Aβ (in any aggregation form) favor the detrimental destabilization of brain metal homeostasis (Duce and Bush, 2010;Faller and Hureau, 2012;Roberts et al., 2012).

As with results, discussion is divided in two sub-sections.

Aβ-Zn

Zinc greatly affects brain physiopathology (Sensi et al., 2009). In AD, loss of zinc homeostasis triggers a series of downstream harmful events (Corona et al., 2011). We have previously shown that Aβ-Zn promotes rapid formation of amorphous aggregates (Bolognin et al., 2011) (a phenomenon confirmed in this set of experiments; see Supplementary Figure 2) and induces some levels of SH-SY5Y toxicity (Drago et al., 2008a). Microarray analysis shows that exposure to Aβ-Zn evokes a complex network of responses that can exert compensatory and protective actions. Unfortunately, the number of transcripts we have found to be changed is too low and heterogeneous to obtain a Ingenuity Pathway Analysis-generated pathway. Nevertheless, it is reasonable to speculate that Aβ-Zn promotes gene expression changes that belong to a potential pathway centered on cell death modulation. This hypothesis is supported by the coexistence of down-regulation of pro-apoptotic transcripts (ACIN1, CAST, CITED2, and ZNF148). Moreover, the metal peptide complex is likely to promote an additional pathway centered on compensatory and protective responses as we observed down-regulation of AD-related genes that are usually over-expressed in the disease (ACE, C5, IL1RN, and NR4A1) along with up-regulation of

cytoprotective genes (EIF5A, ENO1, HSPA4, PSIP1, RPS3, and WNT3A). Interestingly, two of the up-regulated transcripts (HSPA4 and WNT3A) are reported to counteract Aβ toxicity. MT2A over-expression is also important and potentially a key component of this hypothesized protective pathway as MTs are crucial in providing Zn and Cu homeostasis, reducing oxidative stress, and regulating authophagy (Lee and Koh, 2010).

Taken together, microarray results, together with previous data, support the hypothesis that Aβ-Zn (when not forming oligomeric structures) is unable to induce the expression of pro-apoptotic pathways but, on the contrary, activates compensatory and protective mechanisms counteracting its toxicity (Duce et al., 2010).

Aβ-Cu

Brain Cu levels undergo significant changes with aging (Squitti and Salustri, 2009). In AD, data indicate that cortical Cu levels in AD are decreased (Deibel et al., 1996), a process due to sequestration of the cation in amyloid plaques (Miller et al., 2006). Cu can promote oxidative stress (Bonda et al., 2011;Roberts et al., 2012); however, the metal is also involved in synaptic inhibition of glutamatergic neurotransmission (Schlief and Gitlin, 2006) and its decreased availability can promote excitotoxicity. Furthermore, decreased intracellular levels of Cu favor the internalization of Aβ and Cu in cholesterol rich lipid rafts of the plasmamembrane, thereby facilitating the formation of Aβ -Cu complexes(Hung et al., 2009). Thus, the issue of age- and AD-related loss of Cu homeostasis is critical in the theoretical framework of the metal hypothesis of AD (Zatta et al., 2009;Roberts et al., 2012).

Aβ-Cu shows many commonalities with Aβ-Zn. This is probably due to high biophysical similarities as well as vicariant possibilities of the two metal ions. They have the same ionic charge ($^{2+}$), a similar ionic radius (≈87pm) which likely promotes similar changes in structural Aβ conformation. As with Aβ-Zn, Cu conjugated with Aβ generates amorphous aggregates of high molecular weight [12,97]. However, Aβ-Cu has a selective feature: the complex shows less pronounced exposure of hydrophobic clusters and is more soluble. It is important to underline that Cu^{2+}, even when still bound to Aβ, can be reduced to Cu^{+} and promote oxidative stress (Tougu et al., 2011;Roberts et al., 2012) by generating hydrogen peroxide (Huang et al., 1999). This Cu-mediated oxidative stress has been shown to be significant in neuronal cultures and has an important role in AD (Roberts et al., 2012). Reduced Cu also generates hydroxyl radicals by Fenton reaction, an upstream event leading to harmful molecular modifications (i.e.: protein carbonyl modifications, DNA damage, lipid peroxidation) found in AD (Roberts et al., 2012).

We have previously shown that Aβ-Cu conjugates exert moderate levels of SH-SY5Y toxicity most likely by promoting ROS production (Granzotto and Zatta, 2011). Our microarray data show that Aβ-Cu interferes with NF-κB a transcription factor involved in cellular response against several stressors, including ROS, and in AD-related inflammatory responses (Camandola and Mattson, 2007). Our findings indicate an

indirect action on NF-κB. In fact, the complex promotes up-regulation of two genes that negatively control its activity (NFKBIA and SIVA1). It must be noted that this negative modulation is potentially counteracted by simultaneous over-expression of PTRH2, a gene that is cytoprotective through activation of NF-κB related pathways (Griffiths et al., 2011).

As with Aβ-Zn, the number of changed transcripts triggered by Aβ-Cu exposure is too low and heterogeneous to obtain a Ingenuity Pathway Analysis-generated pathway. However, some speculative pathways can be hypothesized.

On the contrary to what we have found in the case of Aβ-Zn (where anti-apoptotic and compensatory/protective pathways seem to prevail) Aβ-Cu appears to produce an overall homeostatic response in which expression of pro- and anti-apoptotic genes reaches a balance. Indeed, along with up-regulation of pro-apoptotic genes (MAGED1 and WWOX), we found a simultaneous under-expression of anti-apoptotic transcripts (BCL2A1, GSTP1, and MDK).

A speculative pathway that can be proposed is centered on proteins that counteract oxidative stress. Supporting that hypothesis we report over-expression of transcripts like PHB and MT2A that encode for scavenger molecules. In the case of MT2A, it is possible that free radicals generated by Aβ-Cu promote intracellular Zn and Cu release from MTs, a process that further induces MT2A expression (as the gene is controlled by the Cu/Zn sensitive metal-responsive transcription factor-1) (Heuchel et al., 1994).

Conclusions

To describe how up- or down-regulated transcripts modulate AD pathogenic pathways is still not completely understood and warrant further investigation. However, present data along with previous findings (Drago et al., 2008b;Bolognin et al., 2011;Gatta et al., 2011) lend support to the idea that metal ions play a critical role in shaping Aβ conformation, a process that in the case of Zn or Cu activates complex biological responses that appear to modulate apoptotic cell death and handling of oxidative stress. Further unraveling of the pathogenic implications of these Aβ/metal-driven changes offers a challenge and an opportunity in AD-related research.

1.5.4 Early and sustained altered expression of aging-related genes in young 3xTg-AD mice

In the present study we performed an expression profile study aimed at assessing transcriptome modifications occurring in the hippocampus of 3 and 12 m.o. 3xTg-AD mice. Changes were compared with those of age-matched WT mice and with age-dependent modifications occurring in 3 and 12 m.o. WT mice. Our purpose was to verify differences or commonalities between changes occurring in an AD-like Tg model and those occurring upon physiological aging. The aim was to compare gene effects promoted by the pro-AD environment offered by the 3xTg-AD mice with those evoked by senescence in WT mice.

The most relevant finding of the study is the identification of changes occurring in young 3xTg-AD mice that are similar to the ones shown by old WT mice upon aging. Profile modifications detected in young 3xTg-AD

mice closely resembled those occurring upon physiological aging in WT animals, thereby suggesting that 3 m.o 3xTg-AD mice undergo a premature modulation of aging-related genes (Fig. 4). For clarity and to improve readability of the results, we separately discuss the gene data of the three experimental conditions as follows:

1- 3 m.o. 3xTg-AD *vs* 3 m.o. WT mice
2- 12 m.o. 3xTg-AD *vs* 12 m.o. WT mice
3- 12 m.o. WT *vs* 3 m.o. WT mice

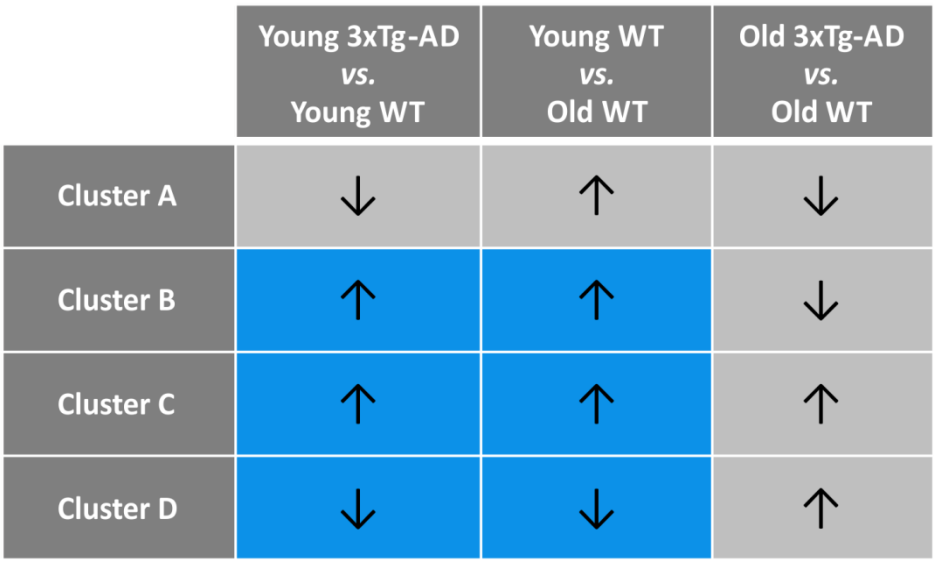

FIGURE 23 GRAPHICAL SYNOPSIS OF CLUSTER ANALYSIS RESULTS. CHART OFFERS A SYNOPTIC VIEW OF ALL THE TRANSCRIPTOME PROFILES ALTERED IN THE THREE EXPERIMENTAL CONDITIONS AS LISTED ON THE CHART TOP. NOTE THAT, AS DEPICTED BY THE BLUE BOXES, 3 M.O. 3XTG-AD *VS* 3 M.O. WT MICE AS WELL AS 12 M.O. WT *VS* 3 M.O. WT MICE SHOW A SIMILAR PATTERN OF EXPRESSION CHANGES IN CLUSTER B,C, AND D. ALSO NOTE THAT, ONLY IN THE CASE OF GENES OF CLUSTER C, A COMMON PATTERN OF EXPRESSION PROFILES IS OBSERVED ACROSS ALL THE THREE EXPERIMENTAL CONDITIONS.

3 M.O. 3XTG-AD VS 3 M.O. WT MICE

The comparison between expression profiles in young 3xTg-AD mice *vs* 3 m.o. WT mice revealed overexpression of several genes grouped in clusters B and C (Fig. 1, 4). Many of these transcripts are known to serve a role in AD pathogenesis by modulating mechanisms like intracellular Ca^{2+} ($[Ca^{2+}]_i$) homeostasis, mitochondrial functioning, inflammatory response, dendrites, synaptic plasticity and memory, neuronal death, cell cycle and autophagy.

$[Ca^{2+}]_i$ homeostasis

Deregulation of $[Ca^{2+}]_i$ is a key contributing factor for AD development and progression (Querfurth and LaFerla, 2010;Corona et al., 2011). The maintenance of low levels of $[Ca^{2+}]_i$ results from the combined activity of complex mechanisms involving influx/efflux of the cation through the plasma membrane as well as its buffering by intracellular stores like the endoplasmic reticulum (ER) and mitochondria (Carafoli, 1987;Rizzuto et al., 2012). Perturbations in Ca^{2+} handling by these organelles as well as impaired intra/extracellular cation exchange contribute to the neuronal dysfunction and degeneration occurring in brain aging and AD (Mattson, 2007;Camandola and Mattson, 2011). In cluster C we found five genes involved in $[Ca^{2+}]_i$ homeostasis (*ATP2B1, CACNB4, RYR2, PKD2, NDUFA9*). ATP2B1 encodes for the plasma membrane Ca^{2+}-ATPase, a key system controlling high capacitance/low affinity Ca^{2+} extrusion while *CACNB4* encodes for the voltage-dependent L-type calcium channel subunit beta-4, a critical route for Ca^{2+} influx. Altered expression and functionality of these proteins correlate with defective Ca^{2+} handling as well as with development of a seizure-prone phenotype (Ketelaars et al., 2004). *CACNB4* is also associated with neuroprotection in animal models of ischemic brain injury (Jin et al., 2001). As for intracellular organelles controlling Ca^{2+} homeostasis, we found changes in the expression of *RYR2*, the gene that encodes for the ryanodine receptor 2, a major system controlling Ca^{2+} release from the ER. *RYR2* overexpression found in 3xTg-AD mice is in line with previous findings supporting an important role for the ryanodine receptor type 2 in promoting altered ER-Ca^{2+} release in pre-symptomatic 3xTg-AD mice, a mechanism that leads to aberrant Ca^{2+} signaling (Chakroborty et al., 2009;Goussakov et al., 2010;Chakroborty et al., 2012). This dataset suggests a complex scenario in which enhanced $[Ca^{2+}]_i$ extrusion (mediated by *ATP2B1*) may serve as a compensatory role to the impaired $[Ca^{2+}]_i$ buffering system and excessive ER-Ca^{2+} release mediated by *RYR2*.

Mitochondrial functioning

Alterations of mitochondrial functioning are crucial in physiological aging as well as in neurodegenerative conditions (Lin and Beal, 2006;Lezi and Swerdlow, 2012). In clusters B and C we found transcripts involved in the modulation of mitochondrial morphology and metabolism [*TRAK1 and Ndufs1* (cluster B); *Hax1, NDUFA9, GDAP1, KIF1B*, *HADBH, PGAM1, Ppia,* and *DNM1L* (cluster C)]. *GDAP1* and *DNM1L* encode for proteins that promote mitochondrial fission; *PGAM1* encodes for an enzyme of the glycolytic pathway that is involved in mitochondrial-mediated neuroprotective effects against Aβ-induced cell death; *TRAK1* plays a critical role in axonal transport of mitochondria (Pedrola et al., 2005;Brickley and Stephenson, 2011;Miyamae et al., 2011;Zhang et al., 2012). Finally, *Ndufs1* encodes for the NADH-ubiquinone oxidoreductase 75 kD, a subunit that regulates the activity of mitochondrial complex I.

The early and sustained overexpression of transcripts involved in mitochondrial fission (*GDAP1, DNML1*) and neuroprotection (*PGAM1*) is in line with recent findings indicating that mitochondrial fission is neuroprotective through reduction of oxidative damage (Zhang et al., 2012).

Inflammatory response

Chronic, discrete and microlocalized areas of inflammation as well as the appearance of activated microglia and reactive astrocytes in the vicinity of senile plaques are hallmarks of the AD brain (Akiyama et al., 2000). Moreover, neuroinflammation plays a detrimental role in brain aging and age-related cognitive decline (Salvioli et al., 2006;Ownby, 2010). Cluster C revealed the presence of some transcripts (*APP, IRF1, PPIA, VCAM1, TIMP2, HMGB1L1, PGAM1, JAK1*) that encode for proteins critically involved in the modulation of the inflammatory response. Of note, in analogy with what found for mitochondrial functioning, in 3xTg-AD mice, we observed an early activation of upstream (IRF1) and downstream (*JAK1*) pro-inflammatory transcripts. Interestingly, other genes involved in the inflammatory response (*Hsp70, IL10 receptor, CD200*) were also found (cluster D). However, these transcripts were downregulated (instead of upregulated when comparing 3 m.o. 3xTg-AD mice *vs* 3 m.o. WT mice). Among these, *Hsp70* and *CD200* are known to play an anti-inflammatory role. Thus, the overexpression of inflammatory genes appears to be coupled with simultaneous decrease in the expression of anti-inflammatory transcripts, thereby suggesting an overall pro-inflammatory status.

Dendrites, synaptic plasticity, and memory

Age- and AD-related cognitive decline is associated with synaptic dysfunction (Coleman and Flood, 1987;Selkoe, 2002). In that respect, we found overexpression of several transcripts [*CD200, Neurod1, SOX9, SNAP25, EGR1, OPHN1, ETV1, CDH2, GABRA1, Spond1,* (cluster B) and *APBA2, APP, GABRA5, MAPK1, PMP22, SYBU, USP14, VDAC3, CST3, DCC, HES1, HEY1, HPRT1, SOX2, YWHAH, CRK, GPR12, HMGB1L1, STK38L, VCAM1;* (cluster C)] that are implicated in dendritic spine formation, modulation of synaptic functioning and cognitive decline. The overexpression of transcripts encoding for proteins involved in promoting synaptic activity and neurotransmission can be interpreted as a protective event against AD-related synaptic dysfunctions.

Overexpression of transcripts present in cluster C suggests a bimodal set of activities. One set of actions may counteract neuronal damage and promote protective effects aimed at maintaining cognitive abilities. For instance, *APBA2* is known to bind to *APP* and reduce Aβ production, thereby counteracting memory deficits and promoting LTP in Tg AD mice (Mitchell et al., 2009). Similarly, *CST3* upregulation is protective against the neurotoxic effects of Aβ oligomers and oxidative stress damage. This phenomenon has been reported in Tg AD models, in brains of AD patients and those of elderly individuals (Kaur and Levy, 2012). The *GABRA5* transcript increase found in our 3xTg-AD mice lends support to the compensatory hypothesis as *GABRA5* has been reported to be downregulated with aging and this process has been linked to defective spatial memory performance (Haberman et al., 2012).

These protective actions are counteracted by the concurrent upregulation of transcripts that, on the contrary, are associated with neuronal dysfunction. This is the case of *APP* and *ERK2* transcripts. Given the aminoacidic composition of murine Aβ, murine *APP* is marginally involved in the formation of toxic Aβ species but some studies have also proposed that the protein can favor *ERK1,2* activation, tau phosphorylation, and the formation of neurofibrillary tangles (Nizzari et al., 2007). Chronic *ERK2* activation

by Aβ oligomers can also play important detrimental actions as the early and sustained *ERK2* stimulation has been shown to promote cognitive decline in Tg AD mouse models (Dineley et al., 2001;Giovannini et al., 2008) and induce neuronal toxicity through caspase-3 activation (Chong et al., 2006).

It is interesting to note that in cluster A and D we found downregulation of other transcripts [*PEBP1* and *Complexin III* (cluster A) and *BIN*, *ACTB, BAIAP2, EphB, KLK8, ARD1, PDE4, Ehmt2, Neurod2, STAT3, S100B, CCND3* (cluster D)] involved in dendritic spine formation, modulation of synaptic functioning, and cognitive decline. In this respect, *PEBP1* and *Complexin III* downregulation is linked to impaired cholinergic neurotransmission [*PEBP1* (Maki et al., 2002)] in the hippocampus as well as to synaptic transmission deficits [*Complexin III* (Landgraf et al., 2012)], two mechanisms largely impaired in AD and in mild cognitive impairment (Rogers et al., 1998;Haense et al., 2012).

BAIAP2, EphB1, BIN1, and *KLK8* are involved in excitatory synaptic transmission and synaptic plasticity. *BAIAP2* (also known as *IRSp53*) modulates NMDA receptor-related synaptic transmission, LTP, as well as learning and memory. *BAIAP2* knock-out mice show impaired spatial learning and novel object recognition (Kim et al., 2009). Thus, *BAIAP2* downregulation might be involved in the development of cognitive deficits affecting this model. Dysfunction in NMDAR activity has been associated to *EphB* (a family of ligand proteins) receptor deficits and linked to the appearance of neurological disorders including AD (Sheffler-Collins and Dalva, 2012). Still in the set of synaptic plasticity-related genes that we found underexpressed, *KLK8* seems important as the gene is involved in brain development, neuronal plasticity, and stress response (Yousef et al., 2003). Thus, *KLK8* downregulation can favor aberrant CNS development. *S100B* is a calcium-binding protein released by astroglial cells. The protein exerts trophic functions in neighbouring neurons under physiological conditions. Compelling evidence shows that transgenic animals overexpressing S100B present neuronal loss and increased expression of the pro-apoptotic protein clusterin, a protein that is increased in hippocampi and frontal cortices of AD patients (Shapiro et al., 2010).

In summary, our findings suggest that 3xTg-AD mice present an early modulation of transcripts that exert detrimental effects on synaptic functioning but also develop changes that counteract this impairment. The process appears to go on chronically as the same pattern is present in 12 m.o. 3xTg-AD mice.

Neuronal death, cell cycle, and autophagy

Aberrant expression of cell cycle- and authophagy-related molecules plays a pivotal role in the neuronal loss associated with AD and brain aging (Bowser and Smith, 2002;Snape et al., 2009;Nixon and Yang, 2012). Our analysis revealed the overexpression of a groups of transcripts [*SPIN1, JAK3, Neurod1, SOX9, YWHAE, EGR1, HSPA1A/HSPA1B* (cluster B); *Beclin-1, MAP1LC3-B, HADHB, AK5, CyC1, SIRT7* and *ENC1* (cluster C)] involved in autophagy, cell cycle, and cell death, thereby suggesting the activation of a complex network of neuronal death-related responses occurring in young 3xTg-AD.

Early *EGR1* upregulation has been reported in AD patients (Gomez Ravetti et al., 2010) and can contribute, along with other cell cycle-related genes, to NFTs formation, a phenomenon that is also

mediated by the increased expression of cell cycle proteins (Bowser and Smith, 2002;Lu et al., 2011). Furthermore, overexpression of *SPIN1*, a gene involved in cell cycle impairment, promotes chromosome instability, a process leading to cellular senescence and apoptosis (Yuan et al., 2008). *Sirt7*, a less investigated member of the sirtuin family, is a nuclear protein expressed in the brain with cellular distribution and functions that are still unknown (Liszt et al., 2005;Michishita et al., 2005). Combined experiments employing *Sirt7* knockout mice and *Sirt7* overexpressing cells have indicated the anti-proliferative role of the protein and suggested that *Sirt7* activity can improve tissue integrity in aging animals (Vakhrusheva et al., 2008).

Beclin-1 and *MAP1LC3-B* are two autophagy-related genes whose overexpression might serve a compensatory mechanism to counteract pathology in 3 m.o. 3xTg-AD mice. This hypothesis is consistent with recent findings indicating that early induction of autophagy reduces cognitive decline in 3xTg-AD mice (Khandelwal et al., 2011;Majumder et al., 2011). Autophagy can, in fact, clear out damaged proteins that are prone to aggregation (Ma et al., 2011) and this process can be neuroprotective by mediating the degradation of misfolded proteins (Metcalf et al., 2012). Intriguingly, in AD, autophagy can play a dual role. On one hand it is protective by promoting the removal of Aβ and tau aggregates, on the other hand, autophagosomes are nevertheless sites of choice for pathogenic accumulation and production of Aβ (Yu et al., 2005;Levine and Kroemer, 2008;Tung et al., 2012).

Analysis of networks of genes involved in neuronal death also showed several transcripts that, compared with young WT mice, were found downregulated in young 3xTg-AD mice [*ARID1A, BRD4, CCND3, EHMT2, GPC1, LAS1L, MAP4, PA2G4, PTGES3, STAT3, TRRAP* (cluster D)]. Interestingly, aberrant expression of *CCND3* has been reported to be closely associated with AD-related neuronal death occurring in specific hippocampal regions (Busser et al., 1998).

12 M.O. 3XTG-AD VS 12 M.O. WT MICE

In order to evaluate how AD-like progression affects gene expression, we investigated profiles of 12 m.o. 3xTg-AD mice compared to 12 m.o. WT mice and matched this set of data with profiles of 3 m.o. 3xTg-AD mice compared with age-matched WT mice. This analysis revealed a similar overexpression of all transcripts of cluster C and downexpression of cluster A transcripts. Interesting differences appeared when analyzing transcripts belonging to cluster B and D (Fig. 1, 4).

Transcripts of cluster B, overexpressed in young 3xTg-AD mice, were downregulated in 12 m.o. 3xTg-AD mice when compared to age-matched WT mice, a finding that supports the hypothesis that aged 3xTg-AD mice may show deficits in counteracting the disease progression. Underexpression of many transcripts found in cluster B has been previously reported in several models of aging and AD as well as in AD patients. This is the case for *SNAP25* (encoding for a key protein involved in synaptic vesicle cycle and neurotransmission modulation) (VanGuilder et al., 2010), *GABRA1* (encoding for a GABA receptor subunit downregulated in AD brains) (Limon et al., 2012), *CDH2* (encoding for N-cadherin, whose deregulation

triggers apoptotic pathway activation) (Ando et al., 2011), and *OPHN1* (encoding for a Rho-GTPase involved in controlling excitatory synapses maturation and plasticity) (Nadif Kasri et al., 2009).

Transcripts of cluster D downexpressed in 3 m.o. 3xTg-AD, and previously discussed, are instead overexpressed in aged 3xTg-AD. The upregulation of transcripts that are involved in the modulation of synaptic plasticity, neuronal proliferation, survival, differentiation, and regulation of cell division process might reflect a compensatory neuroprotective response (*BAIAP2*) although the net result suggests a more complex framework (see for instance the role of *KLK8*). *BAIAP2* downregulation is related to altered synaptic plasticity as observed in BAIAP2-deficient mice while its overexpression increases dendritic spine density and postsynaptic potentiation, ultimately enhancing cognition (Choi et al., 2005). KLK8 deficiency promotes decreased synaptic plasticity while, on the contrary, gain in *KLK8* mRNA levels has been observed in AD brains and equally associated to detrimental effects on hippocampal functioning (Shimizu-Okabe et al., 2001). Inhibition of *S100B* has positive effects on Aβ loads and gliosis observed in AD patients (Mori et al., 2010) while *S100B* overexpression has been associated with exacerbation of AD clinical signs (Bialowas-McGoey et al., 2008;Michetti et al., 2012). Finally, altered expression of cell cycle proteins (i.e.: *CCND3*) in post-mitotic neurons has been observed both in aging and in AD.

Collectively, over and underexpression of the aforementioned transcipts confirm a complex pattern of responses in which some genes exert detrimental effects that are in line with the development of AD-like pathology. At the same time others transcripts appear to counteract these effects. Interestingly, this process appears to progress chronically as a similar pattern has been reported in 3 m.o. and in 12 m.o. 3xTg-AD mice.

12 M.O. WT VS 3 M.O. WT MICE

Finally, we compared expression profiles of 12 m.o. WT mice *vs* 3 m.o. WT mice to analyze effects of physiological aging.

Interestingly, changes driven by aging were largely overlapping with those observed in 3 m.o. 3xTg-AD mice when compared to 3 m.o. WT mice. We, in fact, observed overexpression of several transcripts belonging to cluster B and C and downregulation of a gene data set present in cluster D (Fig. 1, 4). Functional correlates of these changes have been discussed above.

Overall, these data support the hypothesis that the pro-AD environment offered by the 3xTg-AD mice accelerates and promotes early modifications of genes that are otherwise changed by aging in old WT mice.

Moreover, comparison between 12 m.o. WT mice and age-matched 3xTg-AD mice showed expression changes that were similar only for genes belonging to cluster C.

Interestingly, IPA analysis of this cluster revealed transcripts (*HSPA12A, HIAT1, KIAA1409, NRP2, STARD13, UBB, PKIA*) that genome wide association studies have recently shown to be involved in AD-related SNPs as well as transcripts (*APP, ATP6V1C1, BECN1, CST3, DCC, DNM1L, GABRA5, GABRB1, HIAT1, HSPA12A,*

KIAA1409, LPPR4, MAPK9, NRP2, PKIA, RYR2, STARD13, UBB, YWHAZ) that are closely related to AD development.

Finally, cluster A is the only one showing a unique behavior in 3xTg-AD mice, likely indicating changes that are specifically triggered by the pro-AD genetic background of these mice.

It is intriguing to hypothesize that these genes have a functional role in AD progression and represent potential AD biomarkers. Among these, we observed a downregulation of *Homer3* and *Dysferlin*. Homer3 interacts with APP and inhibits Aβ production. Thus, *Homer3* downregulation can lead to enhanced Aβ production (Parisiadou et al., 2008). Accumulation of Dysferlin (a protein involved in membrane repair) within senile plaques, thereby leading to defective neuronal repair (Galvin et al., 2006). Thus, it is conceivable that the *Dysferlin* downregulation that we find in the 3xTg-AD mice can exert a similar detrimental effect.

Collectively, our data support the hypothesis that aging and AD share some mechanistic similarities. In our Tg-AD model, the pro-AD environment promotes and accelerates changes that are otherwise occurring upon aging in WT animals. These data are in agreement with recent findings indicating the presence of a group of so-called BioAge genes that are considered biomarkers for brain aging and associated with neuronal loss, glial activation, and lipid dysmetabolism. Intriguingly, in close analogy with our results, the same genes are also differentially expressed in AD patients (Podtelezhnikov et al., 2011).

Our transcript expression data lend support to the age-based hypothesis for AD (Herrup, 2010), a theory that postulates that the early expression of sets of aging-related genes can favor AD development and progression. Our findings in a pre-clinical model also indicate some novel gene candidates that may be linked to AD and warrant further studies to fully understand their role in the disease.

2. CALCIUM DYSHOMEOSTASIS IN NEURODEGENERATION

2.1 INTRACELLULAR CALCIUM HOMEOSTASIS

Calcium (Ca^{2+}) is one of the most versatile metal ions. It takes part in a large amount of cellular processes in almost all types of cells, from bacteria to higher organisms (Dominguez, 2004).

Ca^{2+}-triggered cellular responses result from temporally and spatially localized variations in Ca^{2+} concentrations within the cell. For instance, at immunological synapse, the site where an antigen presenting cell comes into contact with a T cell, lymphocytes undergo relevant, fast, and highly localized intracellular Ca^{2+} ($[Ca^{2+}]_i$) transients. At the same time, a Ca^{2+} wave can diffuse within the cell and elicit an effect far from the site of entry (Rizzuto et al., 2012).

At resting state free $[Ca^{2+}]_i$ is kept at very low concentration, ≈100 nM. Most of the Ca^{2+} useful for biological activities is kept both outside the cell, thereby representing the major reservoir of the cation (≈1 mM), or is stored in intracellular compartments such as mitochondria and the endoplasmic reticulum (ER), where it reaches $[Ca^{2+}] > 100$ μM.

To maintain low level of $[Ca^{2+}]_i$ at rest and to allow rapid buffering of $[Ca^{2+}]_i$ transients, cells developed highly efficient and sophisticated mechanisms of Ca^{2+} influx/efflux through the plasma membrane and buffering systems mediated by intracellular stores.

As for Ca^{2+} handling through the plasma membrane two major sets of Ca^{2+} permeable channels are involved. A set of channels allow Ca^{2+} influx and include voltage-sensitive channels, store-operated channels and receptor-operated channels (i.e.: glutamate receptors). The latter are the route of choice for Ca^{2+} entry in the CNS. Cytosolic Ca^{2+} efflux takes advantage of two major extruders: a Na^{+}-Ca^{2+} exchanger (NCX) and a plasma-membrane Ca^{2+}-ATPase (PMCA). NCX uses the electrochemical gradient to remove a single Ca^{2+} ion in exchange of three Na^{+}, thereby representing an electrogenic phenomenon. PMCA, instead, hydrolyze ATP to extrude Ca^{2+} from the cell, with a stoichiometry of one Ca^{2+} ion removed for each molecule of ATP hydrolyzed.

On the intracellular side two organelles work synergistically to buffer excessive Ca^{2+} entry in order to avoid detrimental Ca^{2+} overload: the mitochondrion and the ER (or the sarcoplasmic reticulum in the case of myocytes). The latter uptakes Ca^{2+} through a sarco/endoplasmic reticulum Ca^{2+}-ATPase, while Ca^{2+} release occurs through two major receptor-operated channels: the ryanodine receptor (RYR) and the inositol triphosphate receptor (InsP3R).

Mitochondria ability to uptake Ca^{2+} has already been demonstrated several years ago (Carafoli, 2012). However, molecular determinants of mitochondrial Ca^{2+} handling have been only recently unraveled, although some pieces are still missing to complete the puzzle. Mitochondria Ca^{2+} uptake mechanism takes advantage of a highly selective ion transporter, the mitochondrial calcium uniporter (Kirichok et al., 2004). Because aberrant mitochondrial Ca^{2+} uptake results in mitochondrial membrane potential dissipation (Δψ), organelles swelling and ROS generation, mitochondria developed efficient mechanisms for Ca^{2+} extrusion. This occurs through two major antiporter, a Na^{+}-Ca^{2+} exchanger [NCLX;

resembling that of the plasma membrane; (Palty et al., 2010)] and a putative H^+-Ca^{2+} exchanger, whose molecular identity has not been yet defined.

Overall, maintenance of physiological Ca^{2+} levels requires the concerted activity of several organelles, transporters, exchangers and pumps, whose role has been herein briefly and partially described.

2.2 Calcium dyshomeostasis in aging and disease: a lay summary

As previously reported Ca^{2+} is involved in several physiological mechanisms within the CNS. Proper Ca^{2+} signaling in neurons is involved in neurite outgrowth, synaptogenesis, synaptic transmission and plasticity, metabolic processes, and cell survival (Mattson, 2007).

During aging, and especially in aged-brains affected by neurodegenerative disorders, cellular Ca^{2+} homeostasis results significantly impaired, thereby representing a nexus between cellular life and death. One of the major causes of altered Ca^{2+} homeostasis in aging is an alteration in Ca^{2+}-regulating protein activity. Physiologically, $[Ca^{2+}]_i$ increases only transiently, however pathological conditions or normal aging as well, may alter the cellular ability of handling Ca^{2+} transients, thereby resulting in aberrant $[Ca^{2+}]_i$ rises. Reported constitutive proteins that result impaired in aging/neurodegeneration and closely related with detrimental Ca^{2+} homeostasis are: ligand- and voltage-gated Ca^{2+} channels, Ca^{2+}-ATPases, and glutamate transporters, on the plasma-membrane side; Ca^{2+}-binding proteins (i.e.: calbindin, calmodulin) on the cytoplasmic side; presenilin-1, RYRs, and InsP3Rs, on the ER side; electron transport chain proteins, Bcl-2 family members, and uncoupling proteins, on mitochondrial side.

In the case of neurodegenerative disorders, aberrant or altered functioning of the aforementioned proteins, is triggered or coupled with detrimental production, folding and deposition of the so-called disease-related proteins: Aβ in AD, huntingtin in Huntington's disease (HD), α-synuclein in Parkinson's disease (PD), and τ-protein in tauopathies. Alterations in such disease-related proteins correlate with brain areas in which Ca^{2+} dyshomeostasis occur, and are involved in exacerbating aging-related Ca^{2+} deregulation, thereby representing an instrumental explanation for the early and massive neuronal loss occurring in these neurodegenerative pathologies.

2.3 Materials and methods

2.3.1 Chemicals

Tissue culture media and sera were purchased from GIBCO (Life Technologies). Fluorescent calcium (fura-2 AM, and fluo-4FF AM) and ROS (dihydrorhodamine, DHR) indicators were purchased from Molecular Probes (Life Technologies). All other chemicals, unless otherwise specified, were purchased from Sigma-Aldrich.

2.3.2 NEURONAL STRIATAL CULTURES

Striatal cell cultures were prepared from fetal (E15 or E16) Swiss-Webster or CD1 mice. Striatal tissues were dissected in ice-cold dissecting medium and then placed in trypsin (0.25%) for 10 min at 37° C. Tissues were centrifuged, supernatant discarded, and pellet mechanically dissociated with a glass Pasteur pipette. Cells were then resuspended in plating medium containing either: (1) Eagle's Minimal Essential Medium (with 20 mM glucose, 26.2 mM $NaHCO_3$) supplemented with L-glutamine (2 mM), 5% fetal calf serum, and 5% horse serum (Hyclone), or (2) Neurobasal Medium supplemented with L-Glutamine (0.5 mM), 5% fetal bovine serum, 5% horse serum, 1x B27, and 0.2% penicillin/streptomycin.

To prepare mixed cultures (1), cell suspensions were diluted and plated onto an astrocytes layer on 35 mm culture dishes with a glass bottom (Mat-Tek). Cells were fed twice a week with a growth medium (containing 10% horse serum, and 2 mM L-glutamine) and after 12 days in vitro (DIV) with a serum-free medium supplemented with 2 mM L-glutamine.

For near-pure neuronal cultures (2), cells suspensions were diluted and plated onto laminin/poly-DL-lysine coated glass coverslips. Three days after plating, non-neuronal cell growth was inhibited by adding 10µM of cytosine arabinofuranoside. Twice a week, 25% of the medium was replaced with equal amounts of fresh Neurobasal medium.

Striatal neurons were used between 12 to 17 DIV.

2.3.3 IMAGING STUDIES

Ca^{2+} imaging employing fura-2 was performed using a Nikon Diaphot inverted microscope equipped with a Xenon lamp, a 40x Nikon epifluorescence oil immersion objective (N.A.: 1.3), and a CCD camera (Quantex). Fluo-4FF experiments were instead performed using a Nikon Eclipse TE300 inverted microscope equipped with a Xenon lamp, a 40x Nikon epifluorescence oil immersion objective (N.A.: 1.3) and a 12-bit Orca CCD camera (Hamamatsu). DHR experiments were performed with a confocal microscope (Noran Odyssey) equipped with an argon-ion laser, an inverted microscope (Nikon Diaphot), and a 60x Nikon oil-immersion objective (N.A.: 1.4). Fura-2 ratios and DHR confocal images (and relative bright field images) were digitized and analyzed using Image-1 system (Universal Imaging) or Metamorph imaging software (Universal Imaging), respectively. Fluo-4FF images were acquired and analyzed with Metafluor 6.0 software (Molecular Devices).

2.3.3.1 $[Ca^{2+}]_i$ MEASUREMENTS

Striatal cultures were loaded for 30 min in the dark with fura-2 AM (5 µM), or fluo-4FF AM (5 µM), plus 0.2% Pluronic F-127 in HEPES-buffered saline solution (HCSS) (120mM NaCl, 5.4mM KCl, 0.8mM $MgCl_2$, 20mM HEPES, 15mM glucose, 1.8mM $CaCl_2$, 10mM NaOH, pH 7.4), washed, and incubated for further 30 min in HCSS. In fura-2 experiments $[Ca^{2+}]_i$ was determined using the ratio method described by Grynkiewicz et al. (1985). Fura-2 (Ex λ: 340, 380 nm, Em λ: 510 nm) calibrated values were obtained by determining R_{min} and R_{max} using: EGTA (10 mM) and ionomycin (10 µM) in 0 Ca^{2+} buffer for R_{min}, and Ca^{2+}

(10 mM) with ionomycin (10 µM) for R_{max}. Fura-2 K_d was set at 225 nM. Results are reported as mean $[Ca^{2+}]_i$ nM ± SEM. In fluo-4FF (Ex λ: 490 nm, Em λ: 510 nm) fluorescence changes of each cell (F_x) were normalized to basal fluorescence intensity (F_0). Results are expressed as mean F_x/F_0± SEM values. In all experiments, NMDA (50 µM + 10 µM glycine) was applied for 20 seconds and then removed through a rapid perfusion system.

2.3.3.2 ROS PRODUCTION MEASUREMENTS

Cells were loaded with DHR (5 µM) in the dark in a 37° C/5% CO_2 incubator for 30 min and then studied with confocal imaging. DHR was excited at 488 nm and emission collected at >515 nm. In order to minimize DHR photo-oxidation, laser beam was used to less than 5% of full power and image acquisition intervals minimized to ≤ 2 seconds every 5 minutes. DHR was maintained in the buffer throughout all the imaging session to allow the probe equilibration between inside and outside the cells.

NMDA exposure was performed by adding NMDA (50 µM + 10 µM glycine) to the baseline HCSS solution for 5 minutes. NMDA receptors activation was then halted by addition of 10 µM MK-801 and neurons imaged for additional 25 minutes.

2.3.4 NADPH-DIAPHORASE STAINING

To identify nNOS(+) neurons we employed the following NADPH-diaphorase staining procedure (Fig. 24). After Ca^{2+}_i or DHR experiments, cultures were rinsed three times in ice-cold TBS and fixed for 30 min at 4° C in 4% paraformaldehyde/0.1 M PBS buffer. After fixation, dishes were washed with TBS and staining solution applied for 1h at 37° C. NADPH-diaphorase staining solution contained: 0.1 mM Tris/HCl, 0.2% Triton X-100, 1.2 mM sodium azide, 0.2 mM nitrotetrazolium blue, and 1 mM NADPH, pH 7.2. The staining solution was removed and cultures rinsed with TBS. After staining, dishes were re-inserted in the microscope stage and fields re-matched with those previously imaged with fura-2, fluo-4FF, and DHR. nNOS(+) neurons identified as NADPH-diaphorase (+) under bright-field illumination were then evaluated for their responses in the imaging experiments.

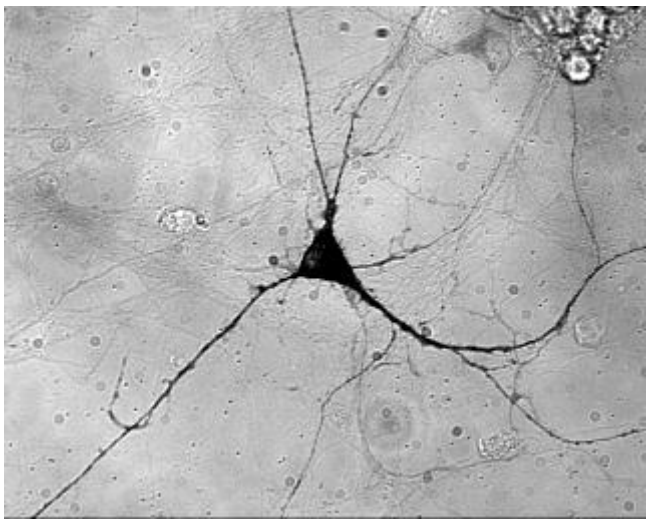

FIGURA 24 NNOS(+) PYRAMIDAL NEURON FOLLOWING NADPH-D STAINING.

2.3.5 Statistical analysis

Grubbs' test was performed to detect outliers, the significance level was set at α=0.05 (no nNOS(+) were found to be significant outliers). Statistical analysis was performed using the Student's *t*-test for unpaired data. Results were considered statistically significant at $p<0.05$.

2.4 Results

2.4.1 nNOS(+) striatal neurons possess functional NMDA receptors but fail to generate mitochondrial ROS in response to an excitotoxic challenge

Background

Excitotoxicity is a major pathogenic component of several neurodegenerative disorders, including Alzheimer's disease, Parkinson's disease, amyotrophic lateral sclerosis, and Huntington's disease (HD) (Choi, 2005;Lau and Tymianski, 2010;Spalloni et al., 2013). HD is an autosomal dominant neurodegenerative condition characterized by severe behavioral, cognitive, and movement disorders (Ross and Tabrizi, 2011). Inheritance of the huntingtin (Htt) protein showing a pathogenic expansion of a glutamine stretch (polyQ repeats >35) (MacDonald et al., 1993) leads to massive cortical and striatal neuronal loss (Halliday et al., 1998;Cattaneo et al., 2005;Guo et al., 2012). Reasons for this subregional selectivity of the neurodegenerative process are not completely understood, although several mechanisms have been proposed. In that respect, evidence indicates that polyQ Htt promotes HD pathology through dysregulation of vesicle trafficking (DiFiglia et al., 1995;Qin et al., 2004), alteration of BDNF transport (Gauthier et al., 2004), disruption of microtubules (Trushina et al., 2003), interference with NMDA receptors (NMDARs) and synaptic activity (Zeron et al., 2004) as well as alteration of organelle morphology (Costa and Scorrano, 2012).

Excitotoxicity is a phenomenon driven by excessive synaptic accumulation of glutamate and associated with dysregulation of intraneuronal Ca^{2+} ($[Ca^{2+}]_i$) homeostasis (Choi, 2005). A major feature of excitotoxicity is the NMDAR/Ca^{2+}-dependent enhanced generation of nitric oxide (NO) and other reactive oxygen species (ROS) (Forder and Tymianski, 2009).

A subpopulation of striatal neurons (accounting for less than 1% of the overall population) expresses high levels of the enzyme nicotinamide adenine dinucleotide phosphate diaphorase (NADPH-d) that is the neuronal isoform of nitric oxide synthase (nNOS) (Hope et al., 1991). Intriguingly, nNOS positive neurons [nNOS(+)] are not affected by NMDAR-dependent toxicity and are spared in the striatum of HD patients (Ferrante et al., 1985;Koh et al., 1986;Koh and Choi, 1988). The molecular and biochemical determinants of this decreased vulnerability are still not completely known. A possible simple explanation for the phenomenon is that nNOS(+) neurons have fewer or less active NMDARs. To test this hypothesis, in

the present study, we employed single cell Ca^{2+} imaging and assessed differences in NMDAR-evoked rises in $[Ca^{2+}]_i$ in striatal cultures, and compared responses obtained in nNOS(+) and (-) neurons.

Mitochondrial function is critical to maintaining $[Ca^{2+}]_i$ homeostasis (Pizzo et al., 2012). Mutant Htt promotes mitochondrial dysfunction and we have previously shown that specific Htt domains are crucial to drive its mitochondrial localization and promote dysfunction (Rockabrand et al., 2007).

Ca^{2+} overload in mitochondria promotes generation of free radicals in the organelles (Dugan et al., 1995;Reynolds and Hastings, 1995), a step that has been shown to be instrumental in the initiation of the excitotoxic cascade (Stout et al., 1998). Thus, we also tested whether exposure to NMDA in striatal cultures generated different levels of mitochondrial ROS (mt-ROS) in nNOS(+) neurons compared to the overall population of nNOS(-) cells.

RESULTS

$[Ca^{2+}]_i$ rises upon NMDA exposure in nNOS(+) and (-) striatal neurons: in this set of experiment, we tested whether nNOS(+) possess less functional NMDARs and evaluated NMDAR-dependent $[Ca^{2+}]_i$ increases as an indirect parameter of receptor activity. $[Ca^{2+}]_i$ rises upon NMDA exposure were investigated with single cell Ca^{2+} imaging. This indirect assay is the only possible way to study NMDAR activity in specific nNOS(+) neurons. A more direct approach would have been to investigate NMDAR-evoked currents with patch clamp electrophysiology. Unfortunately, this approach is highly unfeasible given the extremely low density (<1 %) of nNOS(+) neurons in our striatal cultures along with the absence of any suitable marker to identify these neurons when in culture, two factors making very unlikely the possibility of successfully patching on to these cells in adequate numbers.

Striatal cultures loaded with fura-2, a high affinity Ca^{2+} probe (K_d=225 nM), were exposed to NMDA (50 µM + 10 µM glycine) and $[Ca^{2+}]_i$ elevation assessed during and after the challenge. In this set of experiments, we observed that NMDAR-dependent $[Ca^{2+}]_i$ rises occurring in nNOS(+) were not statistically different from those found in the overall population of nNOS(-) neurons (Fig. 1A-B). To dissect and possibly reveal more subtle differences in $[Ca^{2+}]_i$ handling between nNOS(+) and (-) neurons, we analyzed peak amplitudes, areas under the curve (an index of the overall cytosolic Ca^{2+} load) and recovery phase time (τ) of the $[Ca^{2+}]_i$ changes (Fig. 1C-E). None of these parameters showed statistically significant differences between the two neuronal populations. Analysis of baseline $[Ca^{2+}]_i$ levels also showed no differences between nNOS(+) and (-) neurons at rest (data not shown).

In the fura-2 data set we noticed that some neurons showed $[Ca^{2+}]_i$ responses in the micromolar range. Fura-2 is a high affinity Ca^{2+} probe, a technical limitation that leads to underestimating peak $[Ca^{2+}]_i$ rises for values above 1 µM (Hyrc et al., 1997). We therefore repeated the same set of experiments with the low affinity Ca^{2+} indicator fluo-4FF, a probe that, with a K_d of 9.7 µM, is suitable for the detection of $[Ca^{2+}]_i$ changes occurring in the 1 µM to 1 mM range. Fluo-4FF experiments confirmed that NMDAR-dependent $[Ca^{2+}]_i$ increases are identical in nNOS(+) and (-) neurons (Fig. 2A-E). Of note, different from

fura-2 experiments, in the fluo-4FF data set we observed a decreased recovery time in all neurons, a phenomenon that likely reflects the lower affinity of the probe for Ca^{2+}.

Finally, we assessed whether nNOS(+) neurons show any differences in calcium response via other glutamatergic ionotropic receptors (i.e.: AMPARs). To that aim, fura-2 loaded striatal neurons were exposed to kainate (50 µM) and $[Ca^{2+}]_i$ responses analyzed as agonist-evoked peak levels and cytosolic cation loads (as indicated by evaluation of the area under the curve). Even in this set of experiments, we did not observe significant differences between nNOS(+) and (-) striatal neurons (data not shown).

In summary, Ca^{2+} imaging experiments indicated that nNOS(+) neurons possess fully functional NMDARs.

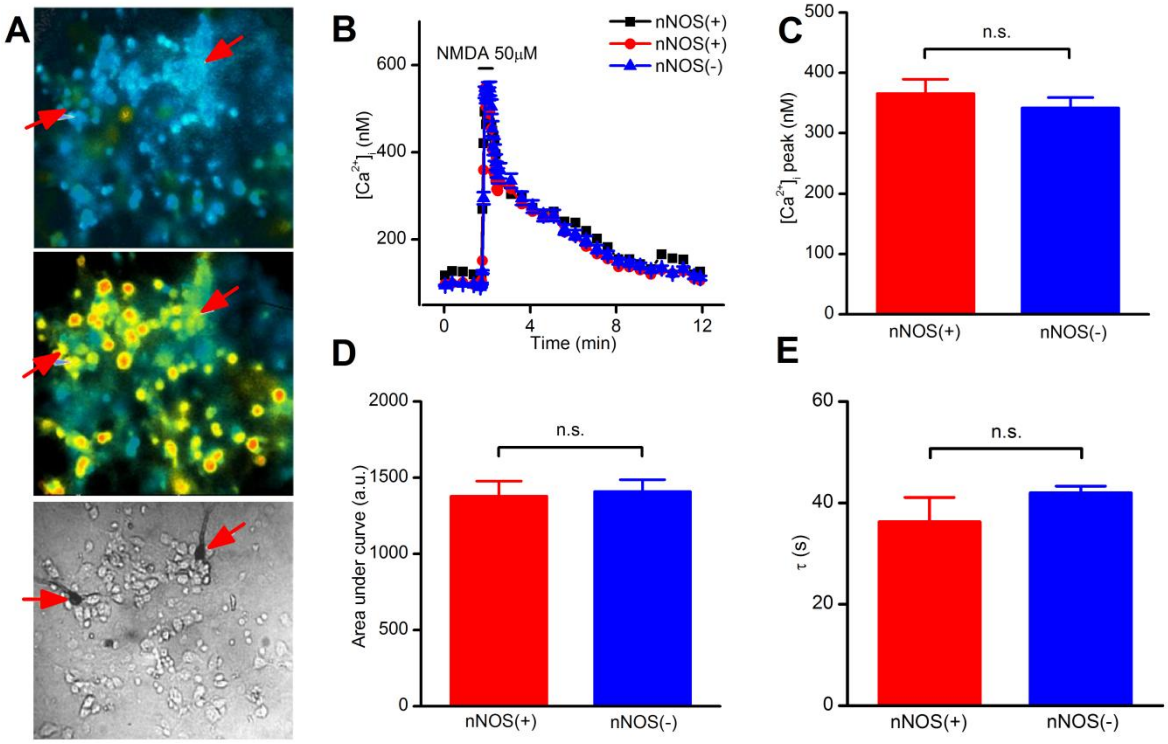

FIGURE 25 QUANTITATIVE FURA-2 $[Ca^{2+}]_i$ EXPERIMENTS ON STRIATAL CULTURED NEURONS. (A) 20X FLUORESCENCE IMAGES OF STRIATAL NEURONS BEFORE (ABOVE), DURING (MIDDLE) NMDA EXPOSURE, AND 20X BRIGHT FIELD IMAGE (BELOW) IDENTIFYING STAINED NNOS(+) NEURONS (ARROWS). (B) REPRESENTATIVE TRACES OF NNOS(+) (N=2) AND NNOS(-) (N=47) FOLLOWING NMDA EXPOSURE. (C) AVERAGE $[Ca^{2+}]_i$ PEAK AMPLITUDE IN THE TWO NEURONAL POPULATIONS (P=0.42). (D) EVALUATION OF $[Ca^{2+}]_i$ DYNAMICS EXPRESSED AS AREA UNDER THE CURVE (P=0.70). (E) ANALYSIS OF THE RECOVERY PHASE FOLLOWING NMDA EXPOSURE (P=0.43). RESULTS ARE EXPRESSED AS MEAN ± SEM; NNOS(+) N=22; NNOS(-) N=560.

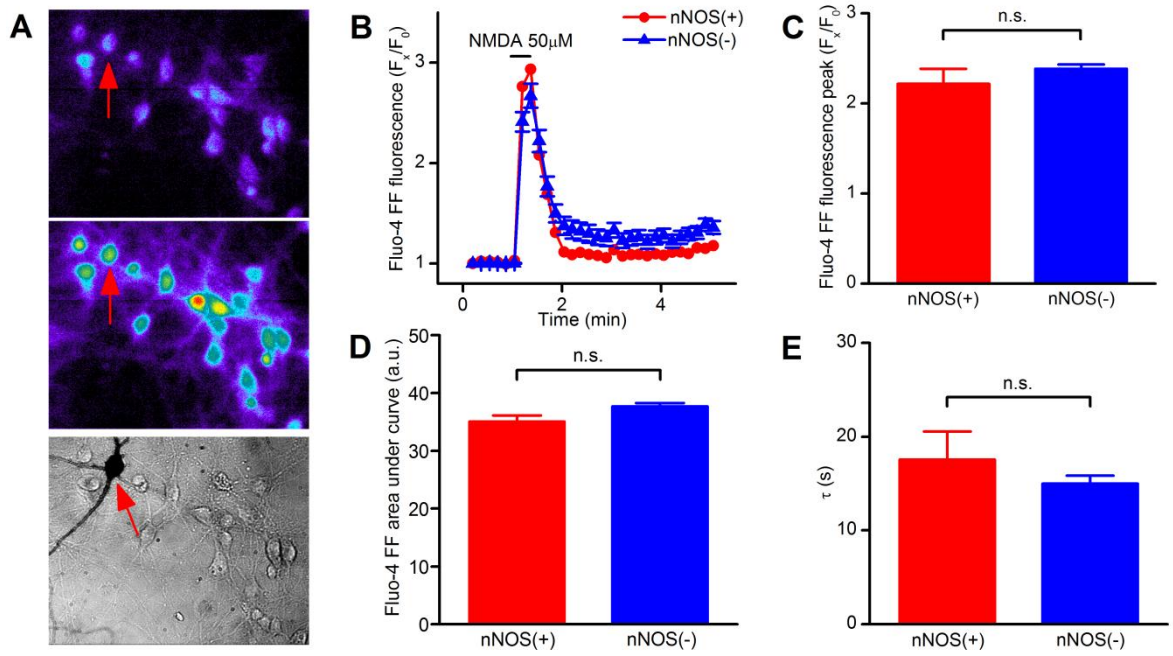

FIGURE 26 FLUO-4FF Ca^{2+}_i EXPERIMENTS ON STRIATAL CULTURED NEURONS. (A) FLUORESCENCE IMAGES OF STRIATAL NEURONS BEFORE (ABOVE), DURING (MIDDLE) NMDA EXPOSURE, AND BRIGHT FIELD IMAGE (BELOW) IDENTIFYING THE STAINED NNOS(+) NEURON (ARROWS). (B) REPRESENTATIVE TRACES OF NNOS(+) (N=1) AND NNOS(-) (N=18) FOLLOWING NMDA EXPOSURE. (C) AVERAGE Ca^{2+}_i PEAK AMPLITUDE IN THE TWO NEURONAL POPULATIONS (P=0.36). (D) EVALUATION OF $[Ca^{2+}]_i$ DYNAMICS EXPRESSED AS AREA UNDER THE CURVE (P=0.24). (E) ANALYSIS OF THE RECOVERY PHASE FOLLOWING NMDA EXPOSURE (P=0.43). RESULTS ARE EXPRESSED AS MEAN ± SEM; NNOS(+) N=13; NNOS(-) N=165.

ROS generation upon NMDA exposure in nNOS(+) and (-) neurons: aberrant Ca^{2+} entry through NMDARs results in cytosolic Ca^{2+} overload, dissipation of the mitochondrial inner membrane potential, opening of the permeability transition pore, and production of mt-ROS (Rizzuto et al., 2012). ROS are major contributors to excitotoxicity (Choi, 1992;Sayre et al., 2008). As mentioned above, NADPH diaphorase is the neuronal isoform of nitric oxide synthase enzyme (Hope et al., 1991). Thus, nNOS(+) neurons are likely to be chronically exposed to an intracellular environment that is constantly confronted (and needs to be equipped to deal) with the presence of high NO levels.

To investigate mt-ROS levels generated by NMDAR activation, striatal neurons were first loaded with the ROS sensitive probe DHR (Henderson and Chappell, 1993) and fluorescent changes evaluated before, during, and after NMDA exposure with confocal microscopy. Native DHR is uncharged and not fluorescent and passively diffuses through membranes. Once in the presence of ROS, DHR is oxidized to the cationic fluorescent product, rhodamine 123, allowing the investigation of mitochondrial ROS production (Dugan et al., 1995).

In this set of experiments DHR-loaded neurons, after acquisition of baseline fluorescence levels, were exposed to NMDA (50 µM + 10 µM glycine) for five minutes, NMDAR activation was then halted by addition of the receptor antagonist (MK-801; 10 µM) and fluorescence changes evaluated up to thirty minutes. Confocal DHR imaging revealed that NMDA application failed to promote significant fluorescence changes in nNOS(+) neurons while (-) neurons showed significant signal rises (Fig. 3).

Thus, DHR experiments revealed that NMDA exposure fails to elicit production of mitochondrial ROS in nNOS(+) striatal neurons.

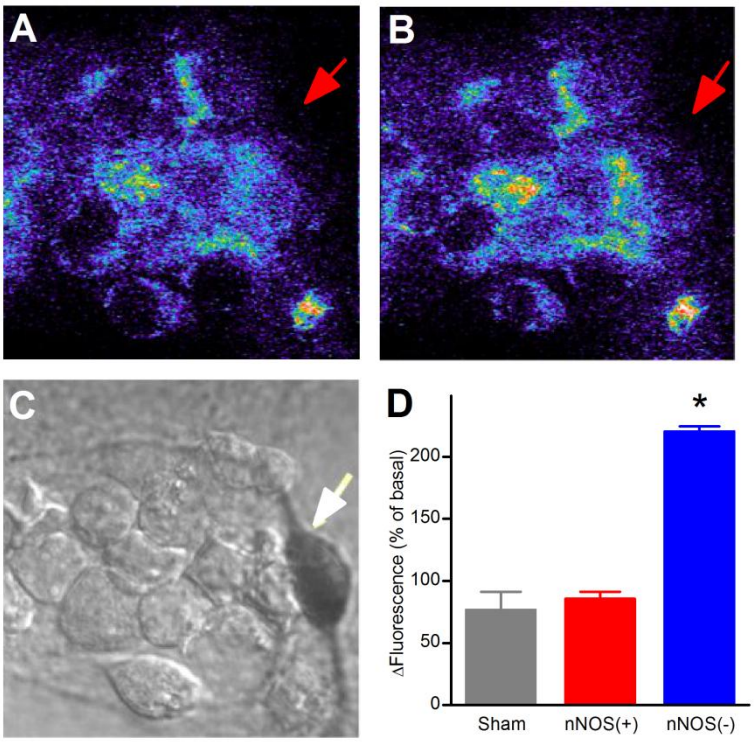

↑ **Figure 27** Confocal images of striatal cultures loaded with the ROS sensitive dye DHR. (A) Basal levels of DHR fluorescence prior to NMDA stimulation. (B) Same field showing DHR fluorescence 25 min after a 5 min NMDA exposure. (C) Same field under bright field illumination in which is clearly stained a nNOS(+) neuron (arrow). (D) Quantification of DHR fluorescence increase 25 min after NMDA exposure (as % of basal; *p<0.001). Results are expressed as mean ± SEM; nNOS(+) n=19; nNOS(-) n=142.

2.5 DISCUSSION

nNOS(+) neurons are spared from NMDAR-driven excitotoxicity, a phenomenon that has puzzled the field for many years (Beal et al., 1986;Koh and Choi, 1988;Kumar, 2004;El Ghazi et al., 2012). Our study offers two major findings that may help to unravel the mechanisms underlying the decreased vulnerability of these neurons.

Firstly, nNOS(+) striatal neurons possess fully functional NMDARs and respond to receptor activation with $[Ca^{2+}]_i$ rises that do not differ for amplitude and temporal dynamics to the ones observed in the overall population of nNOS(-) neurons. Secondly, in nNOS(+) neurons, NMDAR activation does not lead to generation of mt-ROS, thereby occluding a critical downstream event of their excitotoxic cascade.

NMDAR-dependent deregulation of intraneuronal $[Ca^{2+}]_i$ levels upon prolonged or excessive glutamate exposure is the event that starts excitotoxicity (Choi, 1992; 2005). Thus, the reduced vulnerability of nNOS(+) neurons to excitotoxic challenges could have been easily explained by reduced expression or functioning of NMDARs in this subpopulation.

Our data support an alternative view and finally demonstrate that these neurons are most likely resistant not because their difference in number or functionality of NMDARs but, on the contrary, because they are able to set in motion protective events acting downstream to NMDAR activation.

ROS play important roles in several biological functions and are critical mediators of physiological or death signaling (Huang and McNamara, 2012;Ray et al., 2012). Upon excitotoxic conditions, NMDAR-driven production of high levels of cytosolic and mitochondrial ROS as well as nitrosative species leads to neuronal death (Floyd, 1999;Droge, 2002;Lau and Tymianski, 2010). Neurons maintain a redox homeostasis and counteract these oxidative and nitrosative hits by employing several endogenous scavenging mechanisms (Greenlund et al., 1995) like superoxide dismutases, catalases, and glutathione peroxidases.

As nNOS(+) neurons express high levels of nNOS (Hope et al., 1991) and are thereby producing large amounts of NO, it is conceivable that they are primed to deal with an oxidizing intracellular environment and possess a boosted capability to neutralize this challenge.

Landmark findings support this idea and, in fact, indicate that nNOS(+) express high levels of manganese superoxide dismutase (MnSOD) (Gonzalez-Zulueta et al., 1998). MnSOD, a mitochondrial enzyme, neutralizes free radicals. The enzyme confers resistance against NMDA- and NO-mediated toxicity both *in vivo* and *in vitro* by preventing the generation of toxic peroxynitrite originating from the NO and $O_2^{\bullet-}$ interaction (Beckman and Koppenol, 1996;Gonzalez-Zulueta et al., 1998;Brown, 2010). Thus, enhanced MnSOD activity in nNOS(+) neurons fits with the reduced ROS generation that we find upon NMDA exposure and provides a rationale for their decreased vulnerability to NMDAR-mediated neuronal death.

Our results are providing further proof to the ROS-dependent hypothesis. These findings support the idea that mitochondria play a strategic role in the phenomenon. We show that NMDA exposure produces $[Ca^{2+}]_i$ levels that are similar in nNOS(+) and (-) striatal neurons. We also show that these

excitotoxic Ca^{2+} rises fail to promote significant generation of ROS in the mitochondria of nNOS(+) neurons. Thus, in nNOS(+) neurons, the behavior of mitochondria, critical actors of the excitotoxic cascade, seems to differ.

We provide some arguments for this assumption. In the Ca^{2+} imaging experiments we have shown that nNOS(+) neurons face the same NMDAR-driven Ca^{2+} overload. If one has to fit these data and the DHR results in a comprehensive conceptual framework, it can be hypothesized that either: 1) mitochondria of nNOS(+) neurons are allowing less Ca^{2+} uptake (thereby decreasing the overall generation of Ca^{2+}-dependent mt-ROS) or 2) nNOS(+) neurons have developed ways to counteract the generation of mt-ROS.

When considering the first hypothesis, it should be underlined that our Ca^{2+} imaging experiments take in account and report changes of cation levels occurring in the cytosol, a phenomenon that is the net result of simultaneous and concerted activities of many Ca^{2+} homeostatic systems (Pizzo et al., 2012; Rizzuto et al., 2012). The fact that we observed similar NMDAR-driven Ca^{2+} loads in the two neuronal subpopulations could, in theory, be explained by compensatory mechanisms occurring in nNOS(+) neurons that prevent Ca^{2+} overloads in mitochondria. For this mechanism to work, one has to infer that these cells may have enhanced expression and/or functioning of the plasma-membrane Ca^{2+}-ATPases (PMCA), a key pathway for Ca^{2+} extrusion, a possibility that we have not tested yet. Differences in activity of the other major cellular system for Ca^{2+} extrusion, the plasmatic Na^{+}-Ca^{2+} exchanger (NCX), are unlikely as excitotoxic conditions (like the one used in our setting) favor either a NCX reverse operational mode (thereby leading the exchanger to serve as pathway for Ca^{2+} entry) (Orrenius et al., 2003) or NCX functional blockade by its calpain-mediated cleavage (Bano et al., 2005).

Enhanced functioning of intracellular Ca^{2+} stores (i.e.: the endoplasmic reticulum; ER) is also unlikely to work to decrease Ca^{2+} rises in nNOS(+) neurons. Accordingly to the “hot spot” hypothesis proposed by Rizzuto and colleagues (Rizzuto et al., 1998), Ca^{2+} overload in the ER is a detrimental source for ROS generation as the cation eventually exits the ER and is taken up by mitochondria located in the ER vicinity, thereby providing the driving force for production of mt-ROS. Thus, if nNOS(+) neurons overdrive the ER to maintain Ca^{2+} homeostasis such compensatory mechanism should be counterbalanced by enhanced generation of mt-ROS, the opposite of what we observed in our nNOS(+) neurons.

The idea that mitochondria of nNOS(+) sequester equal amounts of Ca^{2+} but respond to this hit with a decreased generation of ROS is substantiated by previous findings (Gonzalez-Zulueta et al., 1998) that indicate a major role for MnSOD, a mitochondrial enzyme, in promoting protection against NMDAR-mediated oxidative stress in nNOS(+) neurons. Within this framework, we speculate that the observed reduction of ROS generation in nNOS(+) neurons may be due to boosted scavenging capabilities embedded in this neuronal subpopulation.

In summary, our data offer complementary data that substantiate a major role for mitochondria in promoting the reduced vulnerability to NMDA in nNOS(+) striatal neurons. Given the role played by polyQ Htt in affecting mitochondrial functioning, this mechanism can be particularly relevant in the context of the neuronal loss occurring in the striatum of HD patients and provide targets for therapeutic intervention.

3. CONCLUSIONS

Collectively, data collected in this thesis highlight the critical role played by metal ions in neurodegenerative disorders development and progression. Notably, not only endogenous and biologically required metal ions (i.e.: iron, copper, zinc and calcium) are involved in the pathogenesis of neurodegenerative disorders, but also exogenous metals (i.e.: aluminum) could have a key and subtle, although still poorly investigated, role in neuronal degeneration.

In agreement, further investigations are required to: 1) fully elucidate how brain biometal metabolism, environmental metal exposure, and neurodegeneration are linked together, and 2) develop effective therapeutic strategies in order to reduce sequelae correlated with metals dyshomeostasis.

REFERENCES

Akatsu, H., Ogawa, N., Kanesaka, T., Hori, A., Yamamoto, T., Matsukawa, N., and Michikawa, M. (2011). Higher activity of peripheral blood angiotensin-converting enzyme is associated with later-onset of Alzheimer's disease. *J Neurol Sci* 300**,** 67-73.

Akiyama, H., Barger, S., Barnum, S., Bradt, B., Bauer, J., Cole, G.M., Cooper, N.R., Eikelenboom, P., Emmerling, M., Fiebich, B.L., Finch, C.E., Frautschy, S., Griffin, W.S., Hampel, H., Hull, M., Landreth, G., Lue, L., Mrak, R., Mackenzie, I.R., Mcgeer, P.L., O'banion, M.K., Pachter, J., Pasinetti, G., Plata-Salaman, C., Rogers, J., Rydel, R., Shen, Y., Streit, W., Strohmeyer, R., Tooyoma, I., Van Muiswinkel, F.L., Veerhuis, R., Walker, D., Webster, S., Wegrzyniak, B., Wenk, G., and Wyss-Coray, T. (2000). Inflammation and Alzheimer's disease. *Neurobiology of Aging* 21**,** 383-421.

Ali-Torres, J., Rodriguez-Santiago, L., Sodupe, M., and Rauk, A. (2011). Structures and stabilities of Fe2+/3+ complexes relevant to Alzheimer's disease: an ab initio study. *J Phys Chem A* 115**,** 12523-12530.

Alscher, R.G., Erturk, N., and Heath, L.S. (2002). Role of superoxide dismutases (SODs) in controlling oxidative stress in plants. *J Exp Bot* 53**,** 1331-1341.

Amada, N., Aihara, K., Ravid, R., and Horie, M. (2005). Reduction of NR1 and phosphorylated Ca2+/calmodulin-dependent protein kinase II levels in Alzheimer's disease. *Neuroreport* 16**,** 1809-1813.

Ando, K., Uemura, K., Kuzuya, A., Maesako, M., Asada-Utsugi, M., Kubota, M., Aoyagi, N., Yoshioka, K., Okawa, K., Inoue, H., Kawamata, J., Shimohama, S., Arai, T., Takahashi, R., and Kinoshita, A. (2011). N-cadherin regulates p38 MAPK signaling via association with JNK-associated leucine zipper protein: implications for neurodegeneration in Alzheimer disease. *Journal of Biological Chemistry* 286**,** 7619-7628.

Aston, C., Jiang, L., and Sokolov, B.P. (2005). Transcriptional profiling reveals evidence for signaling and oligodendroglial abnormalities in the temporal cortex from patients with major depressive disorder. *Mol Psychiatry* 10**,** 309-322.

Atwood, C.S., Obrenovich, M.E., Liu, T., Chan, H., Perry, G., Smith, M.A., and Martins, R.N. (2003). Amyloid-beta: a chameleon walking in two worlds: a review of the trophic and toxic properties of amyloid-beta. *Brain Res Brain Res Rev* 43**,** 1-16.

Banks, W.A., Niehoff, M.L., Drago, D., and Zatta, P. (2006). Aluminum complexing enhances amyloid beta protein penetration of blood-brain barrier. *Brain Res* 1116**,** 215-221.

Bano, D., Young, K.W., Guerin, C.J., Lefeuvre, R., Rothwell, N.J., Naldini, L., Rizzuto, R., Carafoli, E., and Nicotera, P. (2005). Cleavage of the plasma membrane Na+/Ca2+ exchanger in excitotoxicity. *Cell* 120**,** 275-285.

Beal, M.F., Kowall, N.W., Ellison, D.W., Mazurek, M.F., Swartz, K.J., and Martin, J.B. (1986). Replication of the neurochemical characteristics of Huntington's disease by quinolinic acid. *Nature* 321**,** 168-171.

Beckman, J.S., and Koppenol, W.H. (1996). Nitric oxide, superoxide, and peroxynitrite: the good, the bad, and ugly. *Am J Physiol* 271**,** C1424-1437.

Behl, C., Davis, J.B., Lesley, R., and Schubert, D. (1994). Hydrogen peroxide mediates amyloid beta protein toxicity. *Cell* 77**,** 817-827.

Benilova, I., Karran, E., and De Strooper, B. (2012). The toxic Abeta oligomer and Alzheimer's disease: an emperor in need of clothes. *Nat Neurosci* 15**,** 349-357.

Benosman, S., Meng, X., Von Grabowiecki, Y., Palamiuc, L., Hritcu, L., Gross, I., Mellitzer, G., Taya, Y., Loeffler, J.P., and Gaiddon, C. (2011). Complex regulation of p73 isoforms after alteration of amyloid precursor polypeptide (APP) function and DNA damage in neurons. *J Biol Chem* 286**,** 43013-43025.

Bialowas-Mcgoey, L.A., Lesicka, A., and Whitaker-Azmitia, P.M. (2008). Vitamin E increases S100B-mediated microglial activation in an S100B-overexpressing mouse model of pathological aging. *Glia* 56**,** 1780-1790.

Bibl, M., Esselmann, H., and Wiltfang, J. (2012). Neurochemical biomarkers in Alzheimer's disease and related disorders. *Ther Adv Neurol Disord* 5**,** 335-348.

Bolognin, S., Messori, L., Drago, D., Gabbiani, C., Cendron, L., and Zatta, P. (2011). Aluminum, copper, iron and zinc differentially alter amyloid-Abeta(1-42) aggregation and toxicity. *Int J Biochem Cell Biol* 43**,** 877-885.

Bolognin, S., and Zatta, P. (2011). "Chapter 10 Aluminium in Neurodegenerative Diseases," in *Neurodegeneration: Metallostasis and Proteostasis*. The Royal Society of Chemistry), 212-225.

Bonda, D.J., Lee, H.G., Blair, J.A., Zhu, X., Perry, G., and Smith, M.A. (2011). Role of metal dyshomeostasis in Alzheimer's disease. *Metallomics* 3**,** 267-270.

Boocock, D.J., Faust, G.E., Patel, K.R., Schinas, A.M., Brown, V.A., Ducharme, M.P., Booth, T.D., Crowell, J.A., Perloff, M., Gescher, A.J., Steward, W.P., and Brenner, D.E. (2007). Phase I dose escalation pharmacokinetic study in healthy volunteers of resveratrol, a potential cancer chemopreventive agent. *Cancer Epidemiol Biomarkers Prev* 16**,** 1246-1252.

Bowser, R., and Smith, M.A. (2002). Cell cycle proteins in Alzheimer's disease: plenty of wheels but no cycle. *J Alzheimers Dis* 4**,** 249-254.

Brickley, K., and Stephenson, F.A. (2011). Trafficking kinesin protein (TRAK)-mediated transport of mitochondria in axons of hippocampal neurons. *Journal of Biological Chemistry* 286**,** 18079-18092.

Brown, G.C. (2010). Nitric oxide and neuronal death. *Nitric Oxide* 23**,** 153-165.

Bush, A.I. (2003). The metallobiology of Alzheimer's disease. *Trends Neurosci* 26**,** 207-214.

Bush, A.I. (2012). The Metal Theory of Alzheimer's Disease. *J Alzheimers Dis*.

Busser, J., Geldmacher, D.S., and Herrup, K. (1998). Ectopic cell cycle proteins predict the sites of neuronal cell death in Alzheimer's disease brain. *Journal of Neuroscience* 18**,** 2801-2807.

Butterfield, D.A., Poon, H.F., St Clair, D., Keller, J.N., Pierce, W.M., Klein, J.B., and Markesbery, W.R. (2006). Redox proteomics identification of oxidatively modified hippocampal proteins in mild cognitive impairment: insights into the development of Alzheimer's disease. *Neurobiol Dis* 22**,** 223-232.

Camandola, S., and Mattson, M.P. (2007). NF-kappa B as a therapeutic target in neurodegenerative diseases. *Expert Opin Ther Targets* 11**,** 123-132.

Camandola, S., and Mattson, M.P. (2011). Aberrant subcellular neuronal calcium regulation in aging and Alzheimer's disease. *Biochimica et Biophysica Acta* 1813**,** 965-973.

Carafoli, E. (1987). Intracellular calcium homeostasis. *Annu Rev Biochem* 56**,** 395-433.

Carafoli, E. (2012). The interplay of mitochondria with calcium: an historical appraisal. *Cell Calcium* 52**,** 1-8.

Cattaneo, E., Zuccato, C., and Tartari, M. (2005). Normal huntingtin function: an alternative approach to Huntington's disease. *Nat Rev Neurosci* 6**,** 919-930.

Chakroborty, S., Goussakov, I., Miller, M.B., and Stutzmann, G.E. (2009). Deviant Ryanodine Receptor-Mediated Calcium Release Resets Synaptic Homeostasis in Presymptomatic 3xTg-AD Mice. *Journal of Neuroscience* 29**,** 9458-9470.

Chakroborty, S., Kim, J., Schneider, C., Jacobson, C., Molgo, J., and Stutzmann, G.E. (2012). Early presynaptic and postsynaptic calcium signaling abnormalities mask underlying synaptic depression in presymptomatic Alzheimer's disease mice. *J Neurosci* 32**,** 8341-8353.

Chauhan, A., Ray, I., and Chauhan, V.P. (2000). Interaction of amyloid beta-protein with anionic phospholipids: possible involvement of Lys28 and C-terminus aliphatic amino acids. *Neurochem Res* 25**,** 423-429.

Chen, L., Kwong, M., Lu, R., Ginzinger, D., Lee, C., Leung, L., and Chan, J.Y. (2003). Nrf1 is critical for redox balance and survival of liver cells during development. *Mol Cell Biol* 23**,** 4673-4686.

Chen, W.T., Liao, Y.H., Yu, H.M., Cheng, I.H., and Chen, Y.R. (2011). Distinct effects of Zn2+, Cu2+, Fe3+, and Al3+ on amyloid-beta stability, oligomerization, and aggregation: amyloid-beta destabilization promotes annular protofibril formation. *J Biol Chem* 286**,** 9646-9656.

Chiti, F., and Dobson, C.M. (2006). Protein misfolding, functional amyloid, and human disease. *Annu Rev Biochem* 75**,** 333-366.

Choi, D.W. (1992). Excitotoxic cell death. *J Neurobiol* 23**,** 1261-1276.

Choi, D.W. (2005). Neurodegeneration: cellular defences destroyed. *Nature* 433**,** 696-698.

Choi, J., Ko, J., Racz, B., Burette, A., Lee, J.R., Kim, S., Na, M., Lee, H.W., Kim, K., Weinberg, R.J., and Kim, E. (2005). Regulation of dendritic spine morphogenesis by insulin receptor substrate 53, a downstream effector of Rac1 and Cdc42 small GTPases. *J Neurosci* 25**,** 869-879.

Chong, Y.H., Shin, Y.J., Lee, E.O., Kayed, R., Glabe, C.G., and Tenner, A.J. (2006). ERK1/2 activation mediates Abeta oligomer-induced neurotoxicity via caspase-3 activation and tau cleavage in rat organotypic hippocampal slice cultures. *Journal of Biological Chemistry* 281**,** 20315-20325.

Chylack, L.T., Jr., Fu, L., Mancini, R., Martin-Rehrmann, M.D., Saunders, A.J., Konopka, G., Tian, D., Hedley-Whyte, E.T., Folkerth, R.D., and Goldstein, L.E. (2004). Lens epithelium-derived growth factor (LEDGF/p75) expression in fetal and adult human brain. *Exp Eye Res* 79**,** 941-948.

Clark, M.S., and Neumaier, J.F. (2001). The 5-HT1B receptor: behavioral implications. *Psychopharmacol Bull* 35**,** 170-185.

Coleman, P.D., and Flood, D.G. (1987). Neuron numbers and dendritic extent in normal aging and Alzheimer's disease. *Neurobiology of Aging* 8**,** 521-545.

Corder, E.H., Saunders, A.M., Strittmatter, W.J., Schmechel, D.E., Gaskell, P.C., Small, G.W., Roses, A.D., Haines, J.L., and Pericak-Vance, M.A. (1993). Gene dose of apolipoprotein E type 4 allele and the risk of Alzheimer's disease in late onset families. *Science* 261**,** 921-923.

Corona, C., Pensalfini, A., Frazzini, V., and Sensi, S.L. (2011). New therapeutic targets in Alzheimer's disease: brain deregulation of calcium and zinc. *Cell Death Dis* 2**,** e176.

Cossec, J.C., Marquer, C., Panchal, M., Lazar, A.N., Duyckaerts, C., and Potier, M.C. (2010). Cholesterol changes in Alzheimer's disease: methods of analysis and impact on the formation of enlarged endosomes. *Biochim Biophys Acta* 1801**,** 839-845.

Costa, V., and Scorrano, L. (2012). Shaping the role of mitochondria in the pathogenesis of Huntington's disease. *EMBO J* 31**,** 1853-1864.

Couturier, J., Paccalin, M., Morel, M., Terro, F., Milin, S., Pontcharraud, R., Fauconneau, B., and Page, G. (2011). Prevention of the beta-amyloid peptide-induced inflammatory process by inhibition of double-stranded RNA-dependent protein kinase in primary murine mixed co-cultures. *J Neuroinflammation* 8**,** 72.

Cui, J., Wang, Y., Dong, Q., Wu, S., Xiao, X., Hu, J., Chai, Z., and Zhang, Y. (2011). Morphine protects against intracellular amyloid toxicity by inducing estradiol release and upregulation of Hsp70. *J Neurosci* 31**,** 16227-16240.

Cui, J.G., Li, Y.Y., Zhao, Y., Bhattacharjee, S., and Lukiw, W.J. (2010). Differential regulation of interleukin-1 receptor-associated kinase-1 (IRAK-1) and IRAK-2 by microRNA-146a and NF-kappaB in stressed human astroglial cells and in Alzheimer disease. *J Biol Chem* 285**,** 38951-38960.

Dahlgren, K.N., Manelli, A.M., Stine, W.B., Jr., Baker, L.K., Krafft, G.A., and Ladu, M.J. (2002). Oligomeric and fibrillar species of amyloid-beta peptides differentially affect neuronal viability. *J Biol Chem* 277**,** 32046-32053.

Darvesh, A.S., Carroll, R.T., Bishayee, A., Geldenhuys, W.J., and Van Der Schyf, C.J. (2010). Oxidative stress and Alzheimer's disease: dietary polyphenols as potential therapeutic agents. *Expert Rev Neurother* 10**,** 729-745.

Deibel, M.A., Ehmann, W.D., and Markesbery, W.R. (1996). Copper, iron, and zinc imbalances in severely degenerated brain regions in Alzheimer's disease: possible relation to oxidative stress. *J Neurol Sci* 143**,** 137-142.

Di Certo, M.G., Corbi, N., Bruno, T., Iezzi, S., De Nicola, F., Desantis, A., Ciotti, M.T., Mattei, E., Floridi, A., Fanciulli, M., and Passananti, C. (2007). NRAGE associates with the anti-apoptotic factor Che-1 and regulates its degradation to induce cell death. *J Cell Sci* 120**,** 1852-1858.

Dickson, D.W., Crystal, H.A., Bevona, C., Honer, W., Vincent, I., and Davies, P. (1995). Correlations of synaptic and pathological markers with cognition of the elderly. *Neurobiol Aging* 16**,** 285-298; discussion 298-304.

Difiglia, M., Sapp, E., Chase, K., Schwarz, C., Meloni, A., Young, C., Martin, E., Vonsattel, J.P., Carraway, R., Reeves, S.A., and Et Al. (1995). Huntingtin is a cytoplasmic protein associated with vesicles in human and rat brain neurons. *Neuron* 14**,** 1075-1081.

Dijkmans, T.F., Van Hooijdonk, L.W., Schouten, T.G., Kamphorst, J.T., Fitzsimons, C.P., and Vreugdenhil, E. (2009). Identification of new Nerve Growth Factor-responsive immediate-early genes. *Brain Res* 1249**,** 19-33.

Dineley, K.T., Westerman, M., Bui, D., Bell, K., Ashe, K.H., and Sweatt, J.D. (2001). Beta-amyloid activates the mitogen-activated protein kinase cascade via hippocampal alpha7 nicotinic acetylcholine receptors: In vitro and in vivo mechanisms related to Alzheimer's disease. *Journal of Neuroscience* 21**,** 4125-4133.

Dobson, C.M. (2003). Protein folding and misfolding. *Nature* 426**,** 884-890.

Dobson, C.M. (2006). Protein aggregation and its consequences for human disease. *Protein Pept Lett* 13**,** 219-227.

Dominguez, D.C. (2004). Calcium signalling in bacteria. *Mol Microbiol* 54**,** 291-297.

Drago, D., Bettella, M., Bolognin, S., Cendron, L., Scancar, J., Milacic, R., Ricchelli, F., Casini, A., Messori, L., Tognon, G., and Zatta, P. (2008a). Potential pathogenic role of beta-amyloid(1-42)-aluminum complex in Alzheimer's disease. *Int J Biochem Cell Biol* 40**,** 731-746.

Drago, D., Bolognin, S., and Zatta, P. (2008b). Role of metal ions in the abeta oligomerization in Alzheimer's disease and in other neurological disorders. *Curr Alzheimer Res* 5**,** 500-507.

Droge, W. (2002). Free radicals in the physiological control of cell function. *Physiol Rev* 82**,** 47-95.

Duce, J.A., and Bush, A.I. (2010). Biological metals and Alzheimer's disease: implications for therapeutics and diagnostics. *Prog Neurobiol* 92**,** 1-18.

Duce, J.A., Tsatsanis, A., Cater, M.A., James, S.A., Robb, E., Wikhe, K., Leong, S.L., Perez, K., Johanssen, T., Greenough, M.A., Cho, H.H., Galatis, D., Moir, R.D., Masters, C.L., Mclean, C., Tanzi, R.E., Cappai, R., Barnham, K.J., Ciccotosto, G.D., Rogers, J.T., and Bush, A.I. (2010). Iron-export ferroxidase activity of beta-amyloid precursor protein is inhibited by zinc in Alzheimer's disease. *Cell* 142**,** 857-867.

Dugan, L.L., Sensi, S.L., Canzoniero, L.M., Handran, S.D., Rothman, S.M., Lin, T.S., Goldberg, M.P., and Choi, D.W. (1995). Mitochondrial production of reactive oxygen species in cortical neurons following exposure to N-methyl-D-aspartate. *J Neurosci* 15**,** 6377-6388.

El Ghazi, F., Desfeux, A., Brasse-Lagnel, C., Roux, C., Lesueur, C., Mazur, D., Remy-Jouet, I., Richard, V., Jegou, S., Laudenbach, V., Marret, S., Bekri, S., Prevot, V., and Gonzalez, B.J. (2012). NO-dependent protective effect of VEGF against excitotoxicity on layer VI of the developing cerebral cortex. *Neurobiol Dis* 45**,** 871-886.

Etchegaray, J.P., Machida, K.K., Noton, E., Constance, C.M., Dallmann, R., Di Napoli, M.N., Debruyne, J.P., Lambert, C.M., Yu, E.A., Reppert, S.M., and Weaver, D.R. (2009). Casein kinase 1 delta regulates the pace of the mammalian circadian clock. *Mol Cell Biol* 29**,** 3853-3866.

Evans, B.A., Evans, J.E., Baker, S.P., Kane, K., Swearer, J., Hinerfeld, D., Caselli, R., Rogaeva, E., St George-Hyslop, P., Moonis, M., and Pollen, D.A. (2009). Long-term statin therapy and CSF cholesterol levels: implications for Alzheimer's disease. *Dement Geriatr Cogn Disord* 27**,** 519-524.

Faller, P. (2009). Copper and Zinc Binding to Amyloid-beta: Coordination, Dynamics, Aggregation, Reactivity and Metal-Ion Transfer. *Chembiochem* 10**,** 2837-2845.

Faller, P., and Hureau, C. (2012). A bioinorganic view of Alzheimer's disease: when misplaced metal ions (re)direct the electrons to the wrong target. *Chemistry* 18**,** 15910-15920.

Fasman, G.D. (1996). Aluminum and Alzheimer's disease: Model studies. *Coordination Chemistry Reviews* 149**,** 125-165.

Ferrante, R.J., Kowall, N.W., Beal, M.F., Richardson, E.P., Jr., Bird, E.D., and Martin, J.B. (1985). Selective sparing of a class of striatal neurons in Huntington's disease. *Science* 230**,** 561-563.

Ferreira, S.T., Vieira, M.N., and De Felice, F.G. (2007). Soluble protein oligomers as emerging toxins in Alzheimer's and other amyloid diseases. *IUBMB Life* 59**,** 332-345.

Ferrer, I. (2012). Defining Alzheimer as a common age-related neurodegenerative process not inevitably leading to dementia. *Progress in Neurobiology* 97**,** 38-51.

Fischer, D.F., Van Dijk, R., Sluijs, J.A., Nair, S.M., Racchi, M., Levelt, C.N., Van Leeuwen, F.W., and Hol, E.M. (2005). Activation of the Notch pathway in Down syndrome: cross-talk of Notch and APP. *FASEB J* 19**,** 1451-1458.

Floyd, R.A. (1999). Antioxidants, oxidative stress, and degenerative neurological disorders. *Proc Soc Exp Biol Med* 222**,** 236-245.

Forder, J.P., and Tymianski, M. (2009). Postsynaptic mechanisms of excitotoxicity: Involvement of postsynaptic density proteins, radicals, and oxidant molecules. *Neuroscience* 158**,** 293-300.

Frears, E.R., Stephens, D.J., Walters, C.E., Davies, H., and Austen, B.M. (1999). The role of cholesterol in the biosynthesis of beta-amyloid. *Neuroreport* 10**,** 1699-1705.

Fremont, L. (2000). Biological effects of resveratrol. *Life Sci* 66**,** 663-673.

Galvin, J.E., Palamand, D., Strider, J., Milone, M., and Pestronk, A. (2006). The muscle protein dysferlin accumulates in the Alzheimer brain. *Acta Neuropathol* 112**,** 665-671.

Gandy, S., Simon, A.J., Steele, J.W., Lublin, A.L., Lah, J.J., Walker, L.C., Levey, A.I., Krafft, G.A., Levy, E., Checler, F., Glabe, C., Bilker, W.B., Abel, T., Schmeidler, J., and Ehrlich, M.E. (2010). Days to

criterion as an indicator of toxicity associated with human Alzheimer amyloid-beta oligomers. *Ann Neurol* 68**,** 220-230.

Gatta, V., Drago, D., Fincati, K., Valenti, M.T., Dalle Carbonare, L., Sensi, S.L., and Zatta, P. (2011). Microarray analysis on human neuroblastoma cells exposed to aluminum, beta(1-42)-amyloid or the beta(1-42)-amyloid aluminum complex. *PLoS One* 6**,** e15965.

Gauthier, L.R., Charrin, B.C., Borrell-Pages, M., Dompierre, J.P., Rangone, H., Cordelieres, F.P., De Mey, J., Macdonald, M.E., Lessmann, V., Humbert, S., and Saudou, F. (2004). Huntingtin controls neurotrophic support and survival of neurons by enhancing BDNF vesicular transport along microtubules. *Cell* 118**,** 127-138.

Giovannini, M.G., Cerbai, F., Bellucci, A., Melani, C., Grossi, C., Bartolozzi, C., Nosi, D., and Casamenti, F. (2008). Differential activation of mitogen-activated protein kinase signalling pathways in the hippocampus of CRND8 transgenic mouse, a model of Alzheimer's disease. *Neuroscience* 153**,** 618-633.

Gomez Ravetti, M., Rosso, O.A., Berretta, R., and Moscato, P. (2010). Uncovering molecular biomarkers that correlate cognitive decline with the changes of hippocampus' gene expression profiles in Alzheimer's disease. *PLoS One* 5**,** e10153.

Gonzalez-Zulueta, M., Ensz, L.M., Mukhina, G., Lebovitz, R.M., Zwacka, R.M., Engelhardt, J.F., Oberley, L.W., Dawson, V.L., and Dawson, T.M. (1998). Manganese superoxide dismutase protects nNOS neurons from NMDA and nitric oxide-mediated neurotoxicity. *J Neurosci* 18**,** 2040-2055.

Gonzalez, Y.R., Zhang, Y., Behzadpoor, D., Cregan, S., Bamforth, S., Slack, R.S., and Park, D.S. (2008). CITED2 signals through peroxisome proliferator-activated receptor-gamma to regulate death of cortical neurons after DNA damage. *J Neurosci* 28**,** 5559-5569.

Gotz, J., Ittner, L.M., and Kins, S. (2006). Do axonal defects in tau and amyloid precursor protein transgenic animals model axonopathy in Alzheimer's disease? *J Neurochem* 98**,** 993-1006.

Goussakov, I., Miller, M.B., and Stutzmann, G.E. (2010). NMDA-mediated Ca(2+) influx drives aberrant ryanodine receptor activation in dendrites of young Alzheimer's disease mice. *Journal of Neuroscience* 30**,** 12128-12137.

Granzotto, A., Bolognin, S., Scancar, J., Milacic, R., and Zatta, P. (2011). Beta-amyloid toxicity increases with hydrophobicity in the presence of metal ions. *Monatshefte fur Chemie* 142**,** 421-430.

Granzotto, A., and Zatta, P. (2011). Resveratrol acts not through anti-aggregative pathways but mainly via its scavenging properties against Abeta and Abeta-metal complexes toxicity. *PLoS One* 6**,** e21565.

Granzotto, A., and Zatta, P. (2012). Metal ions and beta amyloid: conformational modifications and biological aspects. *Metal Ions in Neurological Systems***,** 77-83.

Gray, E., Ginty, M., Kemp, K., Scolding, N., and Wilkins, A. (2011). Peroxisome proliferator-activated receptor-alpha agonists protect cortical neurons from inflammatory mediators and improve peroxisomal function. *Eur J Neurosci* 33**,** 1421-1432.

Greenlund, L.J., Deckwerth, T.L., and Johnson, E.M., Jr. (1995). Superoxide dismutase delays neuronal apoptosis: a role for reactive oxygen species in programmed neuronal death. *Neuron* 14**,** 303-315.

Griffiths, G.S., Grundl, M., Leychenko, A., Reiter, S., Young-Robbins, S.S., Sulzmaier, F.J., Caliva, M.J., Ramos, J.W., and Matter, M.L. (2011). Bit-1 mediates integrin-dependent cell survival through activation of the NFkappaB pathway. *J Biol Chem* 286**,** 14713-14723.

Gruber, J., Tang, S.Y., and Halliwell, B. (2007). Evidence for a trade-off between survival and fitness caused by resveratrol treatment of Caenorhabditis elegans. *Ann N Y Acad Sci* 1100**,** 530-542.

Gudi, R., Barkinge, J., Hawkins, S., Chu, F., Manicassamy, S., Sun, Z., Duke-Cohan, J.S., and Prasad, K.V. (2006). Siva-1 negatively regulates NF-kappaB activity: effect on T-cell receptor-mediated activation-induced cell death (AICD). *Oncogene* 25**,** 3458-3462.

Guo, Z., Rudow, G., Pletnikova, O., Codispoti, K.E., Orr, B.A., Crain, B.J., Duan, W., Margolis, R.L., Rosenblatt, A., Ross, C.A., and Troncoso, J.C. (2012). Striatal neuronal loss correlates with clinical motor impairment in Huntington's disease. *Mov Disord* 27**,** 1379-1386.

Haberman, R.P., Quigley, C.K., and Gallagher, M. (2012). Characterization of CpG island DNA methylation of impairment-related genes in a rat model of cognitive aging. *Epigenetics* 7**,** 1008-1019.

Haense, C., Kalbe, E., Herholz, K., Hohmann, C., Neumaier, B., Krais, R., and Heiss, W.D. (2012). Cholinergic system function and cognition in mild cognitive impairment. *Neurobiol Aging* 33**,** 867-877.

Halliday, G.M., Mcritchie, D.A., Macdonald, V., Double, K.L., Trent, R.J., and Mccusker, E. (1998). Regional specificity of brain atrophy in Huntington's disease. *Exp Neurol* 154**,** 663-672.

Hardy, J.A., and Higgins, G.A. (1992). Alzheimer's disease: the amyloid cascade hypothesis. *Science* 256**,** 184-185.

Harold, D., Abraham, R., Hollingworth, P., Sims, R., Gerrish, A., Hamshere, M.L., Pahwa, J.S., Moskvina, V., Dowzell, K., Williams, A., Jones, N., Thomas, C., Stretton, A., Morgan, A.R., Lovestone, S., Powell, J., Proitsi, P., Lupton, M.K., Brayne, C., Rubinsztein, D.C., Gill, M., Lawlor, B., Lynch, A., Morgan, K., Brown, K.S., Passmore, P.A., Craig, D., Mcguinness, B., Todd, S., Holmes, C., Mann, D., Smith, A.D., Love, S., Kehoe, P.G., Hardy, J., Mead, S., Fox, N., Rossor, M., Collinge, J., Maier, W., Jessen, F., Schurmann, B., Van Den Bussche, H., Heuser, I., Kornhuber, J., Wiltfang, J., Dichgans, M., Frolich, L., Hampel, H., Hull, M., Rujescu, D., Goate, A.M., Kauwe, J.S., Cruchaga, C., Nowotny, P., Morris, J.C., Mayo, K., Sleegers, K., Bettens, K., Engelborghs, S., De Deyn, P.P., Van Broeckhoven, C., Livingston, G., Bass, N.J., Gurling, H., Mcquillin, A., Gwilliam, R., Deloukas, P., Al-Chalabi, A., Shaw, C.E., Tsolaki, M., Singleton, A.B., Guerreiro, R., Muhleisen, T.W., Nothen, M.M., Moebus, S., Jockel, K.H., Klopp, N., Wichmann, H.E., Carrasquillo, M.M., Pankratz, V.S., Younkin, S.G., Holmans, P.A., O'donovan, M., Owen, M.J., and Williams, J. (2009). Genome-wide association study identifies variants at CLU and PICALM associated with Alzheimer's disease. *Nature Genetics* 41**,** 1088-1093.

Harris, J.R. (2002). In vitro fibrillogenesis of the amyloid beta 1-42 peptide: cholesterol potentiation and aspirin inhibition. *Micron* 33**,** 609-626.

Hawtin, S.R., Dobbins, A.C., Tailor, V.J., and Shearman, M.S. (1995). Beta-amyloid inhibition of MTT reduction is not mimicked by inhibitors of mitochondrial respiration. *Biochem Soc Trans* 23**,** 56S.

Henderson, L.M., and Chappell, J.B. (1993). Dihydrorhodamine 123: a fluorescent probe for superoxide generation? *Eur J Biochem* 217**,** 973-980.

Hensley, K., Carney, J.M., Mattson, M.P., Aksenova, M., Harris, M., Wu, J.F., Floyd, R.A., and Butterfield, D.A. (1994). A model for beta-amyloid aggregation and neurotoxicity based on free radical generation by the peptide: relevance to Alzheimer disease. *Proc Natl Acad Sci U S A* 91**,** 3270-3274.

Herrup, K. (2010). Reimagining Alzheimer's disease--an age-based hypothesis. *Journal of Neuroscience* 30**,** 16755-16762.

Heuchel, R., Radtke, F., Georgiev, O., Stark, G., Aguet, M., and Schaffner, W. (1994). The transcription factor MTF-1 is essential for basal and heavy metal-induced metallothionein gene expression. *EMBO J* 13**,** 2870-2875.

Higuero, A.M., Sanchez-Ruiloba, L., Doglio, L.E., Portillo, F., Abad-Rodriguez, J., Dotti, C.G., and Iglesias, T. (2010). Kidins220/ARMS modulates the activity of microtubule-regulating proteins and controls neuronal polarity and development. *J Biol Chem* 285**,** 1343-1357.

Hollingworth, P., Harold, D., Sims, R., Gerrish, A., Lambert, J.C., Carrasquillo, M.M., Abraham, R., Hamshere, M.L., Pahwa, J.S., Moskvina, V., Dowzell, K., Jones, N., Stretton, A., Thomas, C., Richards, A., Ivanov, D., Widdowson, C., Chapman, J., Lovestone, S., Powell, J., Proitsi, P., Lupton, M.K., Brayne, C., Rubinsztein, D.C., Gill, M., Lawlor, B., Lynch, A., Brown, K.S., Passmore, P.A., Craig, D., Mcguinness, B., Todd, S., Holmes, C., Mann, D., Smith, A.D., Beaumont, H., Warden, D., Wilcock, G., Love, S., Kehoe, P.G., Hooper, N.M., Vardy, E.R., Hardy, J., Mead, S., Fox, N.C., Rossor, M., Collinge, J., Maier, W., Jessen, F., Ruther, E., Schurmann, B., Heun, R., Kolsch, H., Van Den Bussche, H., Heuser, I., Kornhuber, J., Wiltfang, J., Dichgans, M., Frolich, L., Hampel, H., Gallacher, J., Hull, M., Rujescu, D., Giegling, I., Goate, A.M., Kauwe, J.S., Cruchaga, C., Nowotny, P., Morris, J.C., Mayo, K., Sleegers, K., Bettens, K., Engelborghs, S., De Deyn, P.P., Van Broeckhoven, C., Livingston, G., Bass, N.J., Gurling, H., Mcquillin, A., Gwilliam, R., Deloukas, P., Al-Chalabi, A., Shaw, C.E., Tsolaki, M., Singleton, A.B., Guerreiro, R., Muhleisen, T.W., Nothen, M.M., Moebus, S., Jockel, K.H., Klopp, N., Wichmann, H.E., Pankratz, V.S., Sando, S.B., Aasly, J.O., Barcikowska, M., Wszolek, Z.K., Dickson, D.W., Graff-Radford, N.R., Petersen, R.C., et al. (2011). Common variants at ABCA7, MS4A6A/MS4A4E, EPHA1, CD33 and CD2AP are associated with Alzheimer's disease. *Nature Genetics* 43**,** 429-435.

Hope, B.T., Michael, G.J., Knigge, K.M., and Vincent, S.R. (1991). Neuronal NADPH diaphorase is a nitric oxide synthase. *Proc Natl Acad Sci U S A* 88**,** 2811-2814.

House, E., Collingwood, J., Khan, A., Korchazkina, O., Berthon, G., and Exley, C. (2004). Aluminium, iron, zinc and copper influence the in vitro formation of amyloid fibrils of Abeta42 in a manner which may

have consequences for metal chelation therapy in Alzheimer's disease. *J Alzheimers Dis* 6**,** 291-301.

Huang, X., Cuajungco, M.P., Atwood, C.S., Hartshorn, M.A., Tyndall, J.D., Hanson, G.R., Stokes, K.C., Leopold, M., Multhaup, G., Goldstein, L.E., Scarpa, R.C., Saunders, A.J., Lim, J., Moir, R.D., Glabe, C., Bowden, E.F., Masters, C.L., Fairlie, D.P., Tanzi, R.E., and Bush, A.I. (1999). Cu(II) potentiation of alzheimer abeta neurotoxicity. Correlation with cell-free hydrogen peroxide production and metal reduction. *J Biol Chem* 274**,** 37111-37116.

Huang, X., Moir, R.D., Tanzi, R.E., Bush, A.I., and Rogers, J.T. (2004). Redox-active metals, oxidative stress, and Alzheimer's disease pathology. *Ann N Y Acad Sci* 1012**,** 153-163.

Huang, Y., Higginson, D.S., Hester, L., Park, M.H., and Snyder, S.H. (2007). Neuronal growth and survival mediated by eIF5A, a polyamine-modified translation initiation factor. *Proc Natl Acad Sci U S A* 104**,** 4194-4199.

Huang, Y.Z., and Mcnamara, J.O. (2012). Neuroprotective effects of reactive oxygen species mediated by BDNF-independent activation of TrkB. *J Neurosci* 32**,** 15521-15532.

Hudson, S.A., Ecroyd, H., Kee, T.W., and Carver, J.A. (2009). The thioflavin T fluorescence assay for amyloid fibril detection can be biased by the presence of exogenous compounds. *FEBS J* 276**,** 5960-5972.

Hung, Y.H., Robb, E.L., Volitakis, I., Ho, M., Evin, G., Li, Q.X., Culvenor, J.G., Masters, C.L., Cherny, R.A., and Bush, A.I. (2009). Paradoxical condensation of copper with elevated beta-amyloid in lipid rafts under cellular copper deficiency conditions: implications for Alzheimer disease. *J Biol Chem* 284**,** 21899-21907.

Hureau, C., and Faller, P. (2009). Abeta-mediated ROS production by Cu ions: structural insights, mechanisms and relevance to Alzheimer's disease. *Biochimie* 91**,** 1212-1217.

Hwang, I.K., Yoo, K.Y., Kim, D.W., Kim, S.Y., Park, J.H., Ryoo, Z.Y., Kim, J., Choi, S.Y., and Won, M.H. (2008). Ischemia-induced ribosomal protein S3 expressional changes and the neuroprotective effect against experimental cerebral ischemic damage. *J Neurosci Res* 86**,** 1823-1835.

Hyrc, K., Handran, S.D., Rothman, S.M., and Goldberg, M.P. (1997). Ionized intracellular calcium concentration predicts excitotoxic neuronal death: observations with low-affinity fluorescent calcium indicators. *J Neurosci* 17**,** 6669-6677.

Iqbal, K., Liu, F., Gong, C.X., Alonso Adel, C., and Grundke-Iqbal, I. (2009). Mechanisms of tau-induced neurodegeneration. *Acta Neuropathol* 118**,** 53-69.

Ittner, L.M., and Gotz, J. (2011). Amyloid-beta and tau--a toxic pas de deux in Alzheimer's disease. *Nat Rev Neurosci* 12**,** 65-72.

Jan, Y., Matter, M., Pai, J.T., Chen, Y.L., Pilch, J., Komatsu, M., Ong, E., Fukuda, M., and Ruoslahti, E. (2004). A mitochondrial protein, Bit1, mediates apoptosis regulated by integrins and Groucho/TLE corepressors. *Cell* 116**,** 751-762.

Ji, S.R., Wu, Y., and Sui, S.F. (2002). Cholesterol is an important factor affecting the membrane insertion of beta-amyloid peptide (A beta 1-40), which may potentially inhibit the fibril formation. *J Biol Chem* 277**,** 6273-6279.

Jin, K., Mao, X.O., Eshoo, M.W., Nagayama, T., Minami, M., Simon, R.P., and Greenberg, D.A. (2001). Microarray analysis of hippocampal gene expression in global cerebral ischemia. *Annals of Neurology* 50**,** 93-103.

Jonsson, T., Atwal, J.K., Steinberg, S., Snaedal, J., Jonsson, P.V., Bjornsson, S., Stefansson, H., Sulem, P., Gudbjartsson, D., Maloney, J., Hoyte, K., Gustafson, A., Liu, Y., Lu, Y., Bhangale, T., Graham, R.R., Huttenlocher, J., Bjornsdottir, G., Andreassen, O.A., Jonsson, E.G., Palotie, A., Behrens, T.W., Magnusson, O.T., Kong, A., Thorsteinsdottir, U., Watts, R.J., and Stefansson, K. (2012). A mutation in APP protects against Alzheimer's disease and age-related cognitive decline. *Nature* 488**,** 96-99.

Kalscheuer, V.M., Freude, K., Musante, L., Jensen, L.R., Yntema, H.G., Gecz, J., Sefiani, A., Hoffmann, K., Moser, B., Haas, S., Gurok, U., Haesler, S., Aranda, B., Nshedjan, A., Tzschach, A., Hartmann, N., Roloff, T.C., Shoichet, S., Hagens, O., Tao, J., Van Bokhoven, H., Turner, G., Chelly, J., Moraine, C., Fryns, J.P., Nuber, U., Hoeltzenbein, M., Scharff, C., Scherthan, H., Lenzner, S., Hamel, B.C., Schweiger, S., and Ropers, H.H. (2003). Mutations in the polyglutamine binding protein 1 gene cause X-linked mental retardation. *Nat Genet* 35**,** 313-315.

Kapetanovic, I.M., Muzzio, M., Huang, Z., Thompson, T.N., and Mccormick, D.L. (2011). Pharmacokinetics, oral bioavailability, and metabolic profile of resveratrol and its dimethylether analog, pterostilbene, in rats. *Cancer Chemother Pharmacol* 68**,** 593-601.

Karuppagounder, S.S., Pinto, J.T., Xu, H., Chen, H.L., Beal, M.F., and Gibson, G.E. (2009). Dietary supplementation with resveratrol reduces plaque pathology in a transgenic model of Alzheimer's disease. *Neurochem Int* 54**,** 111-118.

Katsaras, J. (1998). Adsorbed to a rigid substrate, dimyristoylphosphatidylcholine multibilayers attain full hydration in all mesophases. *Biophysical Journal* 75**,** 2157-2162.

Kaur, G., and Levy, E. (2012). Cystatin C in Alzheimer's disease. *Front Mol Neurosci* 5**,** 79.

Kawahara, M., and Kato-Negishi, M. (2011). Link between Aluminum and the Pathogenesis of Alzheimer's Disease: The Integration of the Aluminum and Amyloid Cascade Hypotheses. *Int J Alzheimers Dis* 2011**,** 276393.

Kawamata, J., and Shimohama, S. (2002). Association of novel and established polymorphisms in neuronal nicotinic acetylcholine receptors with sporadic Alzheimer's disease. *J Alzheimers Dis* 4**,** 71-76.

Ketelaars, S.O., Gorter, J.A., Aronica, E., and Wadman, W.J. (2004). Calcium extrusion protein expression in the hippocampal formation of chronic epileptic rats after kainate-induced status epilepticus. *Epilepsia* 45**,** 1189-1201.

Khandelwal, P.J., Herman, A.M., Hoe, H.S., Rebeck, G.W., and Moussa, C.E. (2011). Parkin mediates beclin-dependent autophagic clearance of defective mitochondria and ubiquitinated Abeta in AD models. *Human Molecular Genetics* 20**,** 2091-2102.

Kim, J., Lee, H.J., and Lee, K.W. (2010). Naturally occurring phytochemicals for the prevention of Alzheimer's disease. *J Neurochem* 112**,** 1415-1430.

Kim, M.H., Choi, J., Yang, J., Chung, W., Kim, J.H., Paik, S.K., Kim, K., Han, S., Won, H., Bae, Y.S., Cho, S.H., Seo, J., Bae, Y.C., Choi, S.Y., and Kim, E. (2009). Enhanced NMDA receptor-mediated synaptic transmission, enhanced long-term potentiation, and impaired learning and memory in mice lacking IRSp53. *Journal of Neuroscience* 29**,** 1586-1595.

Kirichok, Y., Krapivinsky, G., and Clapham, D.E. (2004). The mitochondrial calcium uniporter is a highly selective ion channel. *Nature* 427**,** 360-364.

Koh, J.Y., and Choi, D.W. (1988). Vulnerability of cultured cortical neurons to damage by excitotoxins: differential susceptibility of neurons containing NADPH-diaphorase. *J Neurosci* 8**,** 2153-2163.

Koh, J.Y., Peters, S., and Choi, D.W. (1986). Neurons containing NADPH-diaphorase are selectively resistant to quinolinate toxicity. *Science* 234**,** 73-76.

Kopito, R.R., and Ron, D. (2000). Conformational disease. *Nat Cell Biol* 2**,** E207-209.

Kremer, J.J., Sklansky, D.J., and Murphy, R.M. (2001). Profile of changes in lipid bilayer structure caused by beta-amyloid peptide. *Biochemistry* 40**,** 8563-8571.

Kumar, U. (2004). Characterization of striatal cultures with the effect of QUIN and NMDA. *Neurosci Res* 49**,** 29-38.

Kumar, V., and Gill, K.D. (2009). Aluminium neurotoxicity: neurobehavioural and oxidative aspects. *Arch Toxicol* 83**,** 965-978.

Ladiwala, A.R., Lin, J.C., Bale, S.S., Marcelino-Cruz, A.M., Bhattacharya, M., Dordick, J.S., and Tessier, P.M. (2010). Resveratrol selectively remodels soluble oligomers and fibrils of amyloid Abeta into off-pathway conformers. *J Biol Chem* 285**,** 24228-24237.

Lambert, J.C., Heath, S., Even, G., Campion, D., Sleegers, K., Hiltunen, M., Combarros, O., Zelenika, D., Bullido, M.J., Tavernier, B., Letenneur, L., Bettens, K., Berr, C., Pasquier, F., Fievet, N., Barberger-Gateau, P., Engelborghs, S., De Deyn, P., Mateo, I., Franck, A., Helisalmi, S., Porcellini, E., Hanon, O., De Pancorbo, M.M., Lendon, C., Dufouil, C., Jaillard, C., Leveillard, T., Alvarez, V., Bosco, P., Mancuso, M., Panza, F., Nacmias, B., Bossu, P., Piccardi, P., Annoni, G., Seripa, D., Galimberti, D., Hannequin, D., Licastro, F., Soininen, H., Ritchie, K., Blanche, H., Dartigues, J.F., Tzourio, C., Gut, I., Van Broeckhoven, C., Alperovitch, A., Lathrop, M., and Amouyel, P. (2009). Genome-wide association study identifies variants at CLU and CR1 associated with Alzheimer's disease. *Nature Genetics* 41**,** 1094-1099.

Landgraf, I., Muhlhans, J., Dedek, K., Reim, K., Brandstatter, J.H., and Ammermuller, J. (2012). The absence of Complexin 3 and Complexin 4 differentially impacts the ON and OFF pathways in mouse retina. *European Journal of Neuroscience* 36**,** 2470-2481.

Lanni, C., Nardinocchi, L., Puca, R., Stanga, S., Uberti, D., Memo, M., Govoni, S., D'orazi, G., and Racchi, M. (2010). Homeodomain interacting protein kinase 2: a target for Alzheimer's beta amyloid leading to misfolded p53 and inappropriate cell survival. *PLoS One* 5**,** e10171.

Lau, A., and Tymianski, M. (2010). Glutamate receptors, neurotoxicity and neurodegeneration. *Pflugers Arch* 460**,** 525-542.

Lee, H.P., Zhu, X., Casadesus, G., Castellani, R.J., Nunomura, A., Smith, M.A., Lee, H.G., and Perry, G. (2010). Antioxidant approaches for the treatment of Alzheimer's disease. *Expert Rev Neurother* 10**,** 1201-1208.

Lee, S.J., and Koh, J.Y. (2010). Roles of zinc and metallothionein-3 in oxidative stress-induced lysosomal dysfunction, cell death, and autophagy in neurons and astrocytes. *Mol Brain* 3**,** 30.

Leuba, G., Savioz, A., Vernay, A., Carnal, B., Kraftsik, R., Tardif, E., Riederer, I., and Riederer, B.M. (2008). Differential changes in synaptic proteins in the Alzheimer frontal cortex with marked increase in PSD-95 postsynaptic protein. *J Alzheimers Dis* 15**,** 139-151.

Levine, B., and Kroemer, G. (2008). Autophagy in the pathogenesis of disease. *Cell* 132**,** 27-42.

Lezi, E., and Swerdlow, R.H. (2012). Mitochondria in neurodegeneration. *Advances in Experimental Medicine and Biology* 942**,** 269-286.

Li, S., Jin, M., Koeglsperger, T., Shepardson, N.E., Shankar, G.M., and Selkoe, D.J. (2011). Soluble Abeta oligomers inhibit long-term potentiation through a mechanism involving excessive activation of extrasynaptic NR2B-containing NMDA receptors. *J Neurosci* 31**,** 6627-6638.

Li, X., Massa, P.E., Hanidu, A., Peet, G.W., Aro, P., Savitt, A., Mische, S., Li, J., and Marcu, K.B. (2002). IKKalpha, IKKbeta, and NEMO/IKKgamma are each required for the NF-kappa B-mediated inflammatory response program. *J Biol Chem* 277**,** 45129-45140.

Liang, B., Duan, B.Y., Zhou, X.P., Gong, J.X., and Luo, Z.G. (2010). Calpain activation promotes BACE1 expression, amyloid precursor protein processing, and amyloid plaque formation in a transgenic mouse model of Alzheimer disease. *J Biol Chem* 285**,** 27737-27744.

Limon, A., Reyes-Ruiz, J.M., and Miledi, R. (2012). Loss of functional GABA(A) receptors in the Alzheimer diseased brain. *Proceedings of the National Academy of Sciences of the United States of America* 109**,** 10071-10076.

Lin, M.T., and Beal, M.F. (2006). Mitochondrial dysfunction and oxidative stress in neurodegenerative diseases. *Nature* 443**,** 787-795.

Liszt, G., Ford, E., Kurtev, M., and Guarente, L. (2005). Mouse Sir2 homolog SIRT6 is a nuclear ADP-ribosyltransferase. *J Biol Chem* 280**,** 21313-21320.

Liu, B., Moloney, A., Meehan, S., Morris, K., Thomas, S.E., Serpell, L.C., Hider, R., Marciniak, S.J., Lomas, D.A., and Crowther, D.C. (2011a). Iron promotes the toxicity of amyloid beta peptide by impeding its ordered aggregation. *J Biol Chem* 286**,** 4248-4256.

Liu, W., Dou, F., Feng, J., and Yan, Z. (2011b). RACK1 is involved in beta-amyloid impairment of muscarinic regulation of GABAergic transmission. *Neurobiol Aging* 32**,** 1818-1826.

Livak, K.J., and Schmittgen, T.D. (2001). Analysis of relative gene expression data using real-time quantitative PCR and the 2(-Delta Delta C(T)) Method. *Methods* 25**,** 402-408.

Lovell, M.A., Robertson, J.D., Teesdale, W.J., Campbell, J.L., and Markesbery, W.R. (1998). Copper, iron and zinc in Alzheimer's disease senile plaques. *J Neurol Sci* 158**,** 47-52.

Lu, Y., Li, T., Qureshi, H.Y., Han, D., and Paudel, H.K. (2011). Early growth response 1 (Egr-1) regulates phosphorylation of microtubule-associated protein tau in mammalian brain. *Journal of Biological Chemistry* 286**,** 20569-20581.

Ma, Q., Qiang, J., Gu, P., Wang, Y., Geng, Y., and Wang, M. (2011). Age-related autophagy alterations in the brain of senescence accelerated mouse prone 8 (SAMP8) mice. *Exp Gerontol* 46**,** 533-541.

Macdonald, M.E., Ambrose, C.M., Duyao, M.P., Myers, R.H., Lin, C., Srinidhi, L., Barnes, G., Taylor, S.A., James, M., Groot, N., Macfarlane, H., Jenkins, B., Anderson, M.A., Wexler, N.S., Gusella, J.F., Bates, G.P., Baxendale, S., Hummerich, H., Kirby, S., North, M., Youngman, S., Mott, R., Zehetner, G., Sedlacek, Z., Poustka, A., Frischauf, A.-M., Lehrach, H., Buckler, A.J., Church, D., Doucette-Stamm, L., O'donovan, M.C., Riba-Ramirez, L., Shah, M., Stanton, V.P., Strobel, S.A., Draths, K.M., Wales, J.L., Dervan, P., Housman, D.E., Altherr, M., Shiang, R., Thompson, L., Fielder, T., Wasmuth, J.J., Tagle, D., Valdes, J., Elmer, L., Allard, M., Castilla, L., Swaroop, M., Blanchard, K., Collins, F.S., Snell, R., Holloway, T., Gillespie, K., Datson, N., Shaw, D., and Harper, P.S. (1993). A novel gene containing a trinucleotide repeat that is expanded and unstable on Huntington's disease chromosomes. *Cell* 72**,** 971-983.

Majumder, S., Richardson, A., Strong, R., and Oddo, S. (2011). Inducing autophagy by rapamycin before, but not after, the formation of plaques and tangles ameliorates cognitive deficits. *PLoS One* 6**,** e25416.

Maki, M., Matsukawa, N., Yuasa, H., Otsuka, Y., Yamamoto, T., Akatsu, H., Okamoto, T., Ueda, R., and Ojika, K. (2002). Decreased expression of hippocampal cholinergic neurostimulating peptide precursor protein mRNA in the hippocampus in Alzheimer disease. *Journal of Neuropathology and Experimental Neurology* 61**,** 176-185.

Manczak, M., Mao, P., Calkins, M.J., Cornea, A., Reddy, A.P., Murphy, M.P., Szeto, H.H., Park, B., and Reddy, P.H. (2010). Mitochondria-targeted antioxidants protect against amyloid-beta toxicity in Alzheimer's disease neurons. *J Alzheimers Dis* 20 Suppl 2**,** S609-631.

Marcello, E., Epis, R., Saraceno, C., and Di Luca, M. (2012). Synaptic dysfunction in Alzheimer's disease. *Adv Exp Med Biol* 970**,** 573-601.

Martin, R.B. (1992). Aluminium speciation in biology. 5-18.

Marubuchi, S., Wada, Y., Okuda, T., Hara, Y., Qi, M.L., Hoshino, M., Nakagawa, M., Kanazawa, I., and Okazawa, H. (2005). Polyglutamine tract-binding protein-1 dysfunction induces cell death of neurons through mitochondrial stress. *J Neurochem* 95**,** 858-870.

Mateos, L., Persson, T., Katoozi, S., Gil-Bea, F.J., and Cedazo-Minguez, A. (2012). Estrogen protects against amyloid-beta toxicity by estrogen receptor alpha-mediated inhibition of Daxx translocation. *Neurosci Lett* 506**,** 245-250.

Mattson, M.P. (2007). Calcium and neurodegeneration. *Aging Cell* 6**,** 337-350.

Mcguinness, B., and Passmore, P. (2010). Can statins prevent or help treat Alzheimer's disease? *J Alzheimers Dis* 20**,** 925-933.

Mclaurin, J., and Chakrabartty, A. (1997). Characterization of the interactions of Alzheimer beta-amyloid peptides with phospholipid membranes. *Eur J Biochem* 245**,** 355-363.

Metcalf, D.J., Garcia-Arencibia, M., Hochfeld, W.E., and Rubinsztein, D.C. (2012). Autophagy and misfolded proteins in neurodegeneration. *Experimental Neurology* 238**,** 22-28.

Michetti, F., Corvino, V., Geloso, M.C., Lattanzi, W., Bernardini, C., Serpero, L., and Gazzolo, D. (2012). The S100B protein in biological fluids: more than a lifelong biomarker of brain distress. *J Neurochem* 120**,** 644-659.

Michishita, E., Park, J.Y., Burneskis, J.M., Barrett, J.C., and Horikawa, I. (2005). Evolutionarily conserved and nonconserved cellular localizations and functions of human SIRT proteins. *Mol Biol Cell* 16**,** 4623-4635.

Miller, L.M., Wang, Q., Telivala, T.P., Smith, R.J., Lanzirotti, A., and Miklossy, J. (2006). Synchrotron-based infrared and X-ray imaging shows focalized accumulation of Cu and Zn co-localized with beta-amyloid deposits in Alzheimer's disease. *J Struct Biol* 155**,** 30-37.

Miller, Y., Ma, B., and Nussinov, R. (2010a). Polymorphism in Alzheimer Abeta amyloid organization reflects conformational selection in a rugged energy landscape. *Chem Rev* 110**,** 4820-4838.

Miller, Y., Ma, B., and Nussinov, R. (2010b). Zinc ions promote Alzheimer Abeta aggregation via population shift of polymorphic states. *Proc Natl Acad Sci U S A* 107**,** 9490-9495.

Milton, N.G. (2004). Role of hydrogen peroxide in the aetiology of Alzheimer's disease: implications for treatment. *Drugs Aging* 21**,** 81-100.

Milton, R.H., Abeti, R., Averaimo, S., Debiasi, S., Vitellaro, L., Jiang, L., Curmi, P.M., Breit, S.N., Duchen, M.R., and Mazzanti, M. (2008). CLIC1 function is required for beta-amyloid-induced generation of reactive oxygen species by microglia. *J Neurosci* 28**,** 11488-11499.

Mitchell, J.C., Ariff, B.B., Yates, D.M., Lau, K.F., Perkinton, M.S., Rogelj, B., Stephenson, J.D., Miller, C.C., and Mcloughlin, D.M. (2009). X11beta rescues memory and long-term potentiation deficits in Alzheimer's disease APPswe Tg2576 mice. *Human Molecular Genetics* 18**,** 4492-4500.

Miyamae, Y., Han, J., Sasaki, K., Terakawa, M., Isoda, H., and Shigemori, H. (2011). 3,4,5-tri-O-caffeoylquinic acid inhibits amyloid beta-mediated cellular toxicity on SH-SY5Y cells through the upregulation of PGAM1 and G3PDH. *Cytotechnology* 63**,** 191-200.

Mizuno, T., Nakata, M., Naiki, H., Michikawa, M., Wang, R., Haass, C., and Yanagisawa, K. (1999). Cholesterol-dependent generation of a seeding amyloid beta-protein in cell culture. *J Biol Chem* 274**,** 15110-15114.

Mocchegiani, E., Costarelli, L., Giacconi, R., Cipriano, C., Muti, E., and Malavolta, M. (2006). Zinc-binding proteins (metallothionein and alpha-2 macroglobulin) and immunosenescence. *Exp Gerontol* 41**,** 1094-1107.

Mori, T., Koyama, N., Arendash, G.W., Horikoshi-Sakuraba, Y., Tan, J., and Town, T. (2010). Overexpression of human S100B exacerbates cerebral amyloidosis and gliosis in the Tg2576 mouse model of Alzheimer's disease. *Glia* 58**,** 300-314.

Mucke, L., and Selkoe, D.J. (2012). Neurotoxicity of Amyloid beta-Protein: Synaptic and Network Dysfunction. *Cold Spring Harb Perspect Med* 2**,** a006338.

Mukaetova-Ladinska, E.B., Xuereb, J.H., Garcia-Sierra, F., Hurt, J., Gertz, H.J., Hills, R., Brayne, C., Huppert, F.A., Paykel, E.S., Mcgee, M.A., Jakes, R., Honer, W.G., Harrington, C.R., and Wischik, C.M. (2009). Lewy body variant of Alzheimer's disease: selective neocortical loss of t-SNARE proteins and loss of MAP2 and alpha-synuclein in medial temporal lobe. *ScientificWorldJournal* 9**,** 1463-1475.

Mulder, S.D., Hack, C.E., Van Der Flier, W.M., Scheltens, P., Blankenstein, M.A., and Veerhuis, R. (2010). Evaluation of intrathecal serum amyloid P (SAP) and C-reactive protein (CRP) synthesis in Alzheimer's disease with the use of index values. *J Alzheimers Dis* 22**,** 1073-1079.

Nadif Kasri, N., Nakano-Kobayashi, A., Malinow, R., Li, B., and Van Aelst, L. (2009). The Rho-linked mental retardation protein oligophrenin-1 controls synapse maturation and plasticity by stabilizing AMPA receptors. *Genes Dev* 23**,** 1289-1302.

Nair, N.G., Perry, G., Smith, M.A., and Reddy, V.P. (2010). NMR studies of zinc, copper, and iron binding to histidine, the principal metal ion complexing site of amyloid-beta peptide. *J Alzheimers Dis* 20**,** 57-66.

Naj, A.C., Jun, G., Beecham, G.W., Wang, L.S., Vardarajan, B.N., Buros, J., Gallins, P.J., Buxbaum, J.D., Jarvik, G.P., Crane, P.K., Larson, E.B., Bird, T.D., Boeve, B.F., Graff-Radford, N.R., De Jager, P.L., Evans, D., Schneider, J.A., Carrasquillo, M.M., Ertekin-Taner, N., Younkin, S.G., Cruchaga, C., Kauwe, J.S., Nowotny, P., Kramer, P., Hardy, J., Huentelman, M.J., Myers, A.J., Barmada, M.M., Demirci, F.Y., Baldwin, C.T., Green, R.C., Rogaeva, E., St George-Hyslop, P., Arnold, S.E., Barber, R., Beach, T., Bigio, E.H., Bowen, J.D., Boxer, A., Burke, J.R., Cairns, N.J., Carlson, C.S., Carney, R.M., Carroll, S.L., Chui, H.C., Clark, D.G., Corneveaux, J., Cotman, C.W., Cummings, J.L., Decarli, C., Dekosky, S.T., Diaz-Arrastia, R., Dick, M., Dickson, D.W., Ellis, W.G., Faber, K.M., Fallon, K.B., Farlow, M.R., Ferris, S., Frosch, M.P., Galasko, D.R., Ganguli, M., Gearing, M., Geschwind, D.H., Ghetti, B., Gilbert, J.R., Gilman, S., Giordani, B., Glass, J.D., Growdon, J.H., Hamilton, R.L., Harrell, L.E., Head, E., Honig, L.S., Hulette, C.M., Hyman, B.T., Jicha, G.A., Jin, L.W., Johnson, N., Karlawish, J., Karydas, A., Kaye, J.A., Kim, R., Koo, E.H., Kowall, N.W., Lah, J.J., Levey, A.I., Lieberman, A.P., Lopez, O.L., Mack, W.J., Marson, D.C., Martiniuk, F., Mash, D.C., Masliah, E., Mccormick, W.C., Mccurry, S.M., Mcdavid, A.N., Mckee, A.C., Mesulam, M., Miller, B.L., et al. (2011). Common variants at MS4A4/MS4A6E, CD2AP, CD33 and EPHA1 are associated with late-onset Alzheimer's disease. *Nature Genetics* 43**,** 436-441.

Newman, M., Tucker, B., Nornes, S., Ward, A., and Lardelli, M. (2009). Altering presenilin gene activity in zebrafish embryos causes changes in expression of genes with potential involvement in Alzheimer's disease pathogenesis. *J Alzheimers Dis* 16**,** 133-147.

Newman, S.J., Bond, B., Crook, B., Darker, J., Edge, C., and Maycox, P.R. (2000). Neuron-specific localisation of the TR3 death receptor in Alzheimer's disease. *Brain Res* 857**,** 131-140.

Nilsson, M.R. (2004). Techniques to study amyloid fibril formation in vitro. *Methods* 34**,** 151-160.

Nixon, R.A., and Yang, D.S. (2012). Autophagy and Neuronal Cell Death in Neurological Disorders. *Cold Spring Harb Perspect Biol*.

Nizzari, M., Venezia, V., Repetto, E., Caorsi, V., Magrassi, R., Gagliani, M.C., Carlo, P., Florio, T., Schettini, G., Tacchetti, C., Russo, T., Diaspro, A., and Russo, C. (2007). Amyloid precursor protein and Presenilin1 interact with the adaptor GRB2 and modulate ERK 1,2 signaling. *Journal of Biological Chemistry* 282**,** 13833-13844.

Oddo, S., Caccamo, A., Shepherd, J.D., Murphy, M.P., Golde, T.E., Kayed, R., Metherate, R., Mattson, M.P., Akbari, Y., and Laferla, F.M. (2003). Triple-transgenic model of Alzheimer's disease with plaques and tangles: intracellular Abeta and synaptic dysfunction. *Neuron* 39**,** 409-421.

Ono, K., Yoshiike, Y., Takashima, A., Hasegawa, K., Naiki, H., and Yamada, M. (2003). Potent anti-amyloidogenic and fibril-destabilizing effects of polyphenols in vitro: implications for the prevention and therapeutics of Alzheimer's disease. *J Neurochem* 87**,** 172-181.

Oprica, M., Hjorth, E., Spulber, S., Popescu, B.O., Ankarcrona, M., Winblad, B., and Schultzberg, M. (2007). Studies on brain volume, Alzheimer-related proteins and cytokines in mice with chronic overexpression of IL-1 receptor antagonist. *J Cell Mol Med* 11**,** 810-825.

Orrenius, S., Zhivotovsky, B., and Nicotera, P. (2003). Regulation of cell death: the calcium-apoptosis link. *Nat Rev Mol Cell Biol* 4**,** 552-565.

Ownby, R.L. (2010). Neuroinflammation and cognitive aging. *Curr Psychiatry Rep* 12**,** 39-45.

Palty, R., Silverman, W.F., Hershfinkel, M., Caporale, T., Sensi, S.L., Parnis, J., Nolte, C., Fishman, D., Shoshan-Barmatz, V., Herrmann, S., Khananshvili, D., and Sekler, I. (2010). NCLX is an essential component of mitochondrial Na+/Ca2+ exchange. *Proc Natl Acad Sci U S A* 107**,** 436-441.

Panza, F., Capurso, C., D'introno, A., Colacicco, A.M., Vasquez, F., Pistoia, G., Capurso, A., and Solfrizzi, V. (2006). Serum total cholesterol as a biomarker for Alzheimer's disease: mid-life or late-life determinations? *Exp Gerontol* 41**,** 805-806.

Parisiadou, L., Bethani, I., Michaki, V., Krousti, K., Rapti, G., and Efthimiopoulos, S. (2008). Homer2 and Homer3 interact with amyloid precursor protein and inhibit Abeta production. *Neurobiol Dis* 30**,** 353-364.

Pedrola, L., Espert, A., Wu, X., Claramunt, R., Shy, M.E., and Palau, F. (2005). GDAP1, the protein causing Charcot-Marie-Tooth disease type 4A, is expressed in neurons and is associated with mitochondria. *Human Molecular Genetics* 14**,** 1087-1094.

Perl, D.P., and Brody, A.R. (1980). Alzheimer's disease: X-ray spectrometric evidence of aluminum accumulation in neurofibrillary tangle-bearing neurons. *Science* 208**,** 297-299.

Pham, E., Crews, L., Ubhi, K., Hansen, L., Adame, A., Cartier, A., Salmon, D., Galasko, D., Michael, S., Savas, J.N., Yates, J.R., Glabe, C., and Masliah, E. (2010). Progressive accumulation of amyloid-beta

oligomers in Alzheimer's disease and in amyloid precursor protein transgenic mice is accompanied by selective alterations in synaptic scaffold proteins. *FEBS J* 277**,** 3051-3067.

Pizzo, P., Drago, I., Filadi, R., and Pozzan, T. (2012). Mitochondrial Ca(2)(+) homeostasis: mechanism, role, and tissue specificities. *Pflugers Arch* 464**,** 3-17.

Podtelezhnikov, A.A., Tanis, K.Q., Nebozhyn, M., Ray, W.J., Stone, D.J., and Loboda, A.P. (2011). Molecular insights into the pathogenesis of Alzheimer's disease and its relationship to normal aging. *PLoS One* 6**,** e29610.

Pratico, D. (2008). Oxidative stress hypothesis in Alzheimer's disease: a reappraisal. *Trends Pharmacol Sci* 29**,** 609-615.

Qin, Z.H., Wang, Y., Sapp, E., Cuiffo, B., Wanker, E., Hayden, M.R., Kegel, K.B., Aronin, N., and Difiglia, M. (2004). Huntingtin bodies sequester vesicle-associated proteins by a polyproline-dependent interaction. *J Neurosci* 24**,** 269-281.

Querfurth, H.W., and Laferla, F.M. (2010). Alzheimer's disease. *New England Journal of Medicine* 362**,** 329-344.

Raber, J., Huang, Y., and Ashford, J.W. (2004). ApoE genotype accounts for the vast majority of AD risk and AD pathology. *Neurobiology of Aging* 25**,** 641-650.

Ray, P.D., Huang, B.W., and Tsuji, Y. (2012). Reactive oxygen species (ROS) homeostasis and redox regulation in cellular signaling. *Cell Signal* 24**,** 981-990.

Reddy, P.H., and Mcweeney, S. (2006). Mapping cellular transcriptosomes in autopsied Alzheimer's disease subjects and relevant animal models. *Neurobiology of Aging* 27**,** 1060-1077.

Reichwald, J., Danner, S., Wiederhold, K.H., and Staufenbiel, M. (2009). Expression of complement system components during aging and amyloid deposition in APP transgenic mice. *J Neuroinflammation* 6**,** 35.

Reynolds, I.J., and Hastings, T.G. (1995). Glutamate induces the production of reactive oxygen species in cultured forebrain neurons following NMDA receptor activation. *J Neurosci* 15**,** 3318-3327.

Ricchelli, F., Drago, D., Filippi, B., Tognon, G., and Zatta, P. (2005). Aluminum-triggered structural modifications and aggregation of beta-amyloids. *Cell Mol Life Sci* 62**,** 1724-1733.

Riviere, C., Richard, T., Quentin, L., Krisa, S., Merillon, J.M., and Monti, J.P. (2007). Inhibitory activity of stilbenes on Alzheimer's beta-amyloid fibrils in vitro. *Bioorg Med Chem* 15**,** 1160-1167.

Rizzuto, R., De Stefani, D., Raffaello, A., and Mammucari, C. (2012). Mitochondria as sensors and regulators of calcium signalling. *Nat Rev Mol Cell Biol* 13**,** 566-578.

Rizzuto, R., Pinton, P., Carrington, W., Fay, F.S., Fogarty, K.E., Lifshitz, L.M., Tuft, R.A., and Pozzan, T. (1998). Close contacts with the endoplasmic reticulum as determinants of mitochondrial Ca2+ responses. *Science* 280**,** 1763-1766.

Roberts, B.R., Ryan, T.M., Bush, A.I., Masters, C.L., and Duce, J.A. (2012). The role of metallobiology and amyloid-beta peptides in Alzheimer's disease. *J Neurochem* 120 Suppl 1**,** 149-166.

Rockabrand, E., Slepko, N., Pantalone, A., Nukala, V.N., Kazantsev, A., Marsh, J.L., Sullivan, P.G., Steffan, J.S., Sensi, S.L., and Thompson, L.M. (2007). The first 17 amino acids of Huntingtin modulate its sub-cellular localization, aggregation and effects on calcium homeostasis. *Hum Mol Genet* 16**,** 61-77.

Rodriguez-Rodriguez, E., Mateo, I., Infante, J., Llorca, J., Garcia-Gorostiaga, I., Vazquez-Higuera, J.L., Sanchez-Juan, P., Berciano, J., and Combarros, O. (2009). Interaction between HMGCR and ABCA1 cholesterol-related genes modulates Alzheimer's disease risk. *Brain Res* 1280**,** 166-171.

Rogers, S.L., Doody, R.S., Mohs, R.C., and Friedhoff, L.T. (1998). Donepezil improves cognition and global function in Alzheimer disease: a 15-week, double-blind, placebo-controlled study. Donepezil Study Group. *Arch Intern Med* 158**,** 1021-1031.

Ross, C.A., and Tabrizi, S.J. (2011). Huntington's disease: from molecular pathogenesis to clinical treatment. *Lancet Neurol* 10**,** 83-98.

Sahara, S., Aoto, M., Eguchi, Y., Imamoto, N., Yoneda, Y., and Tsujimoto, Y. (1999). Acinus is a caspase-3-activated protein required for apoptotic chromatin condensation. *Nature* 401**,** 168-173.

Saito, Y., Sano, Y., Vassar, R., Gandy, S., Nakaya, T., Yamamoto, T., and Suzuki, T. (2008). X11 proteins regulate the translocation of amyloid beta-protein precursor (APP) into detergent-resistant membrane and suppress the amyloidogenic cleavage of APP by beta-site-cleaving enzyme in brain. *J Biol Chem* 283**,** 35763-35771.

Sakakima, H., Yoshida, Y., Yamazaki, Y., Matsuda, F., Ikutomo, M., Ijiri, K., Muramatsu, H., Muramatsu, T., and Kadomatsu, K. (2009). Disruption of the midkine gene (Mdk) delays degeneration and regeneration in injured peripheral nerve. *J Neurosci Res* 87**,** 2908-2915.

Sakono, M., and Zako, T. (2010). Amyloid oligomers: formation and toxicity of Abeta oligomers. *FEBS J* 277**,** 1348-1358.

Saldanha, A.J. (2004). Java Treeview--extensible visualization of microarray data. *Bioinformatics* 20**,** 3246-3248.

Salvioli, S., Capri, M., Valensin, S., Tieri, P., Monti, D., Ottaviani, E., and Franceschi, C. (2006). Inflamm-aging, cytokines and aging: state of the art, new hypotheses on the role of mitochondria and new perspectives from systems biology. *Current Pharmaceutical Design* 12**,** 3161-3171.

Santacruz, K., Lewis, J., Spires, T., Paulson, J., Kotilinek, L., Ingelsson, M., Guimaraes, A., Deture, M., Ramsden, M., Mcgowan, E., Forster, C., Yue, M., Orne, J., Janus, C., Mariash, A., Kuskowski, M., Hyman, B., Hutton, M., and Ashe, K.H. (2005). Tau suppression in a neurodegenerative mouse model improves memory function. *Science* 309**,** 476-481.

Sayre, L.M., Perry, G., and Smith, M.A. (2008). Oxidative stress and neurotoxicity. *Chem Res Toxicol* 21**,** 172-188.

Scheper, W., Zwart, R., Sluijs, P., Annaert, W., Gool, W.A., and Baas, F. (2000). Alzheimer's presenilin 1 is a putative membrane receptor for rab GDP dissociation inhibitor. *Hum Mol Genet* 9**,** 303-310.

Schlief, M.L., and Gitlin, J.D. (2006). Copper homeostasis in the CNS: a novel link between the NMDA receptor and copper homeostasis in the hippocampus. *Mol Neurobiol* 33**,** 81-90.

Schonknecht, P., Lutjohann, D., Pantel, J., Bardenheuer, H., Hartmann, T., Von Bergmann, K., Beyreuther, K., and Schroder, J. (2002). Cerebrospinal fluid 24S-hydroxycholesterol is increased in patients with Alzheimer's disease compared to healthy controls. *Neurosci Lett* 324**,** 83-85.

Selkoe, D.J. (1991). Amyloid protein and Alzheimer's disease. *Scientific American* 265**,** 68-71, 74-66, 78.

Selkoe, D.J. (2002). Alzheimer's disease is a synaptic failure. *Science* 298**,** 789-791.

Sensi, S.L., Paoletti, P., Bush, A.I., and Sekler, I. (2009). Zinc in the physiology and pathology of the CNS. *Nat Rev Neurosci* 10**,** 780-791.

Shapiro, L.A., Bialowas-Mcgoey, L.A., and Whitaker-Azmitia, P.M. (2010). Effects of S100B on Serotonergic Plasticity and Neuroinflammation in the Hippocampus in Down Syndrome and Alzheimer's Disease: Studies in an S100B Overexpressing Mouse Model. *Cardiovasc Psychiatry Neurol* 2010.

Sheffler-Collins, S.I., and Dalva, M.B. (2012). EphBs: an integral link between synaptic function and synaptopathies. *Trends in Neurosciences* 35**,** 293-304.

Shen, Y., Li, R., Mcgeer, E.G., and Mcgeer, P.L. (1997). Neuronal expression of mRNAs for complement proteins of the classical pathway in Alzheimer brain. *Brain Res* 769**,** 391-395.

Shimizu-Okabe, C., Yousef, G.M., Diamandis, E.P., Yoshida, S., Shiosaka, S., and Fahnestock, M. (2001). Expression of the kallikrein gene family in normal and Alzheimer's disease brain. *Neuroreport* 12**,** 2747-2751.

Shruster, A., Eldar-Finkelman, H., Melamed, E., and Offen, D. (2011). Wnt signaling pathway overcomes the disruption of neuronal differentiation of neural progenitor cells induced by oligomeric amyloid beta-peptide. *J Neurochem* 116**,** 522-529.

Simons, M., Keller, P., Dichgans, J., and Schulz, J.B. (2001). Cholesterol and Alzheimer's disease: is there a link? *Neurology* 57**,** 1089-1093.

Snape, M., Lee, H.G., Casadesus, G., and Smith, M.A. (2009). Cell cycle aberrations in Alzheimer's disease: a novel therapeutic opportunity. *Expert Rev Neurother* 9**,** 1579-1580.

Spalloni, A., Nutini, M., and Longone, P. (2013). Role of the N-methyl-d-aspartate receptors complex in amyotrophic lateral sclerosis. *Biochim Biophys Acta* 1832**,** 312-322.

Squitti, R., and Salustri, C. (2009). Agents complexing copper as a therapeutic strategy for the treatment of Alzheimer's disease. *Curr Alzheimer Res* 6**,** 476-487.

Stoltenberg, M., Bush, A.I., Bach, G., Smidt, K., Larsen, A., Rungby, J., Lund, S., Doering, P., and Danscher, G. (2007). Amyloid plaques arise from zinc-enriched cortical layers in APP/PS1 transgenic mice and are paradoxically enlarged with dietary zinc deficiency. *Neuroscience* 150**,** 357-369.

Stout, A.K., Raphael, H.M., Kanterewicz, B.I., Klann, E., and Reynolds, I.J. (1998). Glutamate-induced neuron death requires mitochondrial calcium uptake. *Nat Neurosci* 1**,** 366-373.

Suginta, W., Karoulias, N., Aitken, A., and Ashley, R.H. (2001). Chloride intracellular channel protein CLIC4 (p64H1) binds directly to brain dynamin I in a complex containing actin, tubulin and 14-3-3 isoforms. *Biochem J* 359**,** 55-64.

Suh, K.S., Mutoh, M., Nagashima, K., Fernandez-Salas, E., Edwards, L.E., Hayes, D.D., Crutchley, J.M., Marin, K.G., Dumont, R.A., Levy, J.M., Cheng, C., Garfield, S., and Yuspa, S.H. (2004). The organellular chloride channel protein CLIC4/mtCLIC translocates to the nucleus in response to cellular stress and accelerates apoptosis. *J Biol Chem* 279**,** 4632-4641.

Suh, Y.H., Terashima, A., Petralia, R.S., Wenthold, R.J., Isaac, J.T., Roche, K.W., and Roche, P.A. (2010). A neuronal role for SNAP-23 in postsynaptic glutamate receptor trafficking. *Nat Neurosci* 13**,** 338-343.

Sun, K.H., Chang, K.H., Clawson, S., Ghosh, S., Mirzaei, H., Regnier, F., and Shah, K. (2011). Glutathione-S-transferase P1 is a critical regulator of Cdk5 kinase activity. *J Neurochem* 118**,** 902-914.

Suwalsky, M., Benites, M., Villena, F., Aguilar, F., and Sotomayor, C.P. (1996). Interaction of 2,4-dichlorophenoxyacetic acid (2,4-D) with cell and model membranes. *Biochimica Et Biophysica Acta-Biomembranes* 1285**,** 267-276.

Suwalsky, M., Bolognin, S., and Zatta, P. (2009). Interaction between Alzheimer's amyloid-beta and amyloid-beta-metal complexes with cell membranes. *J Alzheimers Dis* 17**,** 81-90.

Syme, C.D., and Viles, J.H. (2006). Solution 1H NMR investigation of Zn2+ and Cd2+ binding to amyloid-beta peptide (Abeta) of Alzheimer's disease. *Biochim Biophys Acta* 1764**,** 246-256.

Sze, C.I., Su, M., Pugazhenthi, S., Jambal, P., Hsu, L.J., Heath, J., Schultz, L., and Chang, N.S. (2004). Down-regulation of WW domain-containing oxidoreductase induces Tau phosphorylation in vitro. A potential role in Alzheimer's disease. *J Biol Chem* 279**,** 30498-30506.

Takeo, C., Ikeda, K., Horie-Inoue, K., and Inoue, S. (2009). Identification of Igf2, Igfbp2 and Enpp2 as estrogen-responsive genes in rat hippocampus. *Endocr J* 56**,** 113-120.

Tamura, T., Horiuchi, D., Chen, Y.C., Sone, M., Miyashita, T., Saitoe, M., Yoshimura, N., Chiang, A.S., and Okazawa, H. (2010). Drosophila PQBP1 regulates learning acquisition at projection neurons in aversive olfactory conditioning. *J Neurosci* 30**,** 14091-14101.

Tanzi, R.E. (2012). The genetics of Alzheimer disease. *Cold Spring Harb Perspect Med* 2.

Terry, R.D., Masliah, E., Salmon, D.P., Butters, N., Deteresa, R., Hill, R., Hansen, L.A., and Katzman, R. (1991). Physical basis of cognitive alterations in Alzheimer's disease: synapse loss is the major correlate of cognitive impairment. *Ann Neurol* 30**,** 572-580.

Thanopoulou, K., Fragkouli, A., Stylianopoulou, F., and Georgopoulos, S. (2010). Scavenger receptor class B type I (SR-BI) regulates perivascular macrophages and modifies amyloid pathology in an Alzheimer mouse model. *Proc Natl Acad Sci U S A* 107**,** 20816-20821.

To, A.K., Chen, G.G., Chan, U.P., Ye, C., Yun, J.P., Ho, R.L., Tessier, A., Merchant, J.L., and Lai, P.B. (2011). ZBP-89 enhances Bak expression and causes apoptosis in hepatocellular carcinoma cells. *Biochim Biophys Acta* 1813**,** 222-230.

Tomljenovic, L. (2011). Aluminum and Alzheimer's disease: after a century of controversy, is there a plausible link? *J Alzheimers Dis* 23**,** 567-598.

Tougu, V., Tiiman, A., and Palumaa, P. (2011). Interactions of Zn(II) and Cu(II) ions with Alzheimer's amyloid-beta peptide. Metal ion binding, contribution to fibrillization and toxicity. *Metallomics* 3**,** 250-261.

Trushina, E., Heldebrant, M.P., Perez-Terzic, C.M., Bortolon, R., Kovtun, I.V., Badger, J.D., 2nd, Terzic, A., Estevez, A., Windebank, A.J., Dyer, R.B., Yao, J., and Mcmurray, C.T. (2003). Microtubule destabilization and nuclear entry are sequential steps leading to toxicity in Huntington's disease. *Proc Natl Acad Sci U S A* 100**,** 12171-12176.

Tseng, I.J., Liu, H.C., Yuan, R.Y., Sheu, J.J., Yu, J.M., and Hu, C.J. (2010). Expression of inducible nitric oxide synthase (iNOS) and period 1 (PER1) clock gene products in different sleep stages of patients with cognitive impairment. *J Clin Neurosci* 17**,** 1140-1143.

Tung, Y.T., Wang, B.J., Hu, M.K., Hsu, W.M., Lee, H., Huang, W.P., and Liao, Y.F. (2012). Autophagy: a double-edged sword in Alzheimer's disease. *J Biosci* 37**,** 157-165.

Turner, A.J., Belyaev, N.D., and Nalivaeva, N.N. (2011). Mediator: the missing link in amyloid precursor protein nuclear signalling. *EMBO Rep* 12**,** 180-181.

Turturici, G., Sconzo, G., and Geraci, F. (2011). Hsp70 and its molecular role in nervous system diseases. *Biochem Res Int* 2011**,** 618127.

Tyszkiewicz, J.P., and Yan, Z. (2005). beta-Amyloid peptides impair PKC-dependent functions of metabotropic glutamate receptors in prefrontal cortical neurons. *J Neurophysiol* 93**,** 3102-3111.

Uversky, V.N., Winter, S., and Lober, G. (1996). Use of fluorescence decay times of 8-ANS-protein complexes to study the conformational transitions in proteins which unfold through the molten globule state. *Biophysical Chemistry* 60**,** 79-88.

Vakhrusheva, O., Braeuer, D., Liu, Z., Braun, T., and Bober, E. (2008). Sirt7-dependent inhibition of cell growth and proliferation might be instrumental to mediate tissue integrity during aging. *J Physiol Pharmacol* 59 Suppl 9**,** 201-212.

Vanguilder, H.D., Yan, H., Farley, J.A., Sonntag, W.E., and Freeman, W.M. (2010). Aging alters the expression of neurotransmission-regulating proteins in the hippocampal synaptoproteome. *Journal of Neurochemistry* 113**,** 1577-1588.

Verstraeten, S.V., Aimo, L., and Oteiza, P.I. (2008). Aluminium and lead: molecular mechanisms of brain toxicity. *Arch Toxicol* 82**,** 789-802.

Vestergaard, M., Hamada, T., Morita, M., and Takagi, M. (2010). Cholesterol, lipids, amyloid Beta, and Alzheimer's. *Curr Alzheimer Res* 7**,** 262-270.

Vingtdeux, V., Dreses-Werringloer, U., Zhao, H., Davies, P., and Marambaud, P. (2008). Therapeutic potential of resveratrol in Alzheimer's disease. *BMC Neurosci* 9 Suppl 2**,** S6.

Walsh, D.M., Klyubin, I., Fadeeva, J.V., Cullen, W.K., Anwyl, R., Wolfe, M.S., Rowan, M.J., and Selkoe, D.J. (2002). Naturally secreted oligomers of amyloid beta protein potently inhibit hippocampal long-term potentiation in vivo. *Nature* 416**,** 535-539.

Wan, L., Nie, G., Zhang, J., Luo, Y., Zhang, P., Zhang, Z., and Zhao, B. (2011). beta-Amyloid peptide increases levels of iron content and oxidative stress in human cell and Caenorhabditis elegans models of Alzheimer disease. *Free Radic Biol Med* 50**,** 122-129.

Williamson, R., Scales, T., Clark, B.R., Gibb, G., Reynolds, C.H., Kellie, S., Bird, I.N., Varndell, I.M., Sheppard, P.W., Everall, I., and Anderton, B.H. (2002). Rapid tyrosine phosphorylation of neuronal proteins including tau and focal adhesion kinase in response to amyloid-beta peptide exposure: involvement of Src family protein kinases. *J Neurosci* 22**,** 10-20.

Wilquet, V., and De Strooper, B. (2004). Amyloid-beta precursor protein processing in neurodegeneration. *Curr Opin Neurobiol* 14**,** 582-588.

Wolozin, B. (2001). A fluid connection: cholesterol and Abeta. *Proc Natl Acad Sci U S A* 98**,** 5371-5373.

Wood, J.G., Rogina, B., Lavu, S., Howitz, K., Helfand, S.L., Tatar, M., and Sinclair, D. (2004). Sirtuin activators mimic caloric restriction and delay ageing in metazoans. *Nature* 430**,** 686-689.

Wu, S.H., Arevalo, J.C., Neubrand, V.E., Zhang, H., Arancio, O., and Chao, M.V. (2010). The ankyrin repeat-rich membrane spanning (ARMS)/Kidins220 scaffold protein is regulated by activity-dependent calpain proteolysis and modulates synaptic plasticity. *J Biol Chem* 285**,** 40472-40478.

Xu, X., Zhou, H., and Boyer, T.G. (2011). Mediator is a transducer of amyloid-precursor-protein-dependent nuclear signalling. *EMBO Rep* 12**,** 216-222.

Xue, W.F., Hellewell, A.L., Gosal, W.S., Homans, S.W., Hewitt, E.W., and Radford, S.E. (2009). Fibril fragmentation enhances amyloid cytotoxicity. *J Biol Chem* 284**,** 34272-34282.

Yasuhara, O., Matsuo, A., Terai, K., Walker, D.G., Berger, A.E., Akiguchi, I., Kimura, J., and Mcgeer, P.L. (1997). Expression of interleukin-1 receptor antagonist protein in post-mortem human brain tissues of Alzheimer's disease and control cases. *Acta Neuropathol* 93**,** 414-420.

Yin, Y.I., Bassit, B., Zhu, L., Yang, X., Wang, C., and Li, Y.M. (2007). {gamma}-Secretase Substrate Concentration Modulates the Abeta42/Abeta40 Ratio: IMPLICATIONS FOR ALZHEIMER DISEASE. *J Biol Chem* 282**,** 23639-23644.

Yokel, R.A. (2002). Brain uptake, retention, and efflux of aluminum and manganese. *Environ Health Perspect* 110 Suppl 5**,** 699-704.

Yousef, G.M., Kishi, T., and Diamandis, E.P. (2003). Role of kallikrein enzymes in the central nervous system. *Clinica Chimica Acta* 329**,** 1-8.

Yu, W.H., Cuervo, A.M., Kumar, A., Peterhoff, C.M., Schmidt, S.D., Lee, J.H., Mohan, P.S., Mercken, M., Farmery, M.R., Tjernberg, L.O., Jiang, Y., Duff, K., Uchiyama, Y., Naslund, J., Mathews, P.M., Cataldo, A.M., and Nixon, R.A. (2005). Macroautophagy--a novel Beta-amyloid peptide-generating pathway activated in Alzheimer's disease. *Journal of Cell Biology* 171**,** 87-98.

Yuan, H., Zhang, P., Qin, L., Chen, L., Shi, S., Lu, Y., Yan, F., Bai, C., Nan, X., Liu, D., Li, Y., Yue, W., and Pei, X. (2008). Overexpression of SPINDLIN1 induces cellular senescence, multinucleation and apoptosis. *Gene* 410**,** 67-74.

Yumoto, S., Kakimi, S., Ohsaki, A., and Ishikawa, A. (2009). Demonstration of aluminum in amyloid fibers in the cores of senile plaques in the brains of patients with Alzheimer's disease. *J Inorg Biochem* 103**,** 1579-1584.

Zatta, P., Drago, D., Bolognin, S., and Sensi, S.L. (2009). Alzheimer's disease, metal ions and metal homeostatic therapy. *Trends Pharmacol Sci* 30**,** 346-355.

Zatta, P., Kiss, T., Suwalsky, M., and Berthon, G. (2002). Aluminium(III) as a promoter of cellular oxidation. *Coordination Chemistry Reviews* 228**,** 271-284.

Zeron, M.M., Fernandes, H.B., Krebs, C., Shehadeh, J., Wellington, C.L., Leavitt, B.R., Baimbridge, K.G., Hayden, M.R., and Raymond, L.A. (2004). Potentiation of NMDA receptor-mediated excitotoxicity linked with intrinsic apoptotic pathway in YAC transgenic mouse model of Huntington's disease. *Mol Cell Neurosci* 25**,** 469-479.

Zhang, Y., Crouch, D.H., Yamamoto, M., and Hayes, J.D. (2006). Negative regulation of the Nrf1 transcription factor by its N-terminal domain is independent of Keap1: Nrf1, but not Nrf2, is targeted to the endoplasmic reticulum. *Biochem J* 399**,** 373-385.

Zhang, Y.W., Thompson, R., Zhang, H., and Xu, H. (2011). APP processing in Alzheimer's disease. *Mol Brain* 4**,** 3.

Zhang, Z., Kageyama, Y., and Sesaki, H. (2012). Mitochondrial division prevents neurodegeneration. *Autophagy* 8.

Zhong, P., Gu, Z., Wang, X., Jiang, H., Feng, J., and Yan, Z. (2003). Impaired modulation of GABAergic transmission by muscarinic receptors in a mouse transgenic model of Alzheimer's disease. *J Biol Chem* 278**,** 26888-26896.

Zhou, J., Fonseca, M.I., Pisalyaput, K., and Tenner, A.J. (2008). Complement C3 and C4 expression in C1q sufficient and deficient mouse models of Alzheimer's disease. *J Neurochem* 106**,** 2080-2092.

Zhou, P., Qian, L., D'aurelio, M., Cho, S., Wang, G., Manfredi, G., Pickel, V., and Iadecola, C. (2012). Prohibitin reduces mitochondrial free radical production and protects brain cells from different injury modalities. *J Neurosci* 32**,** 583-592.

PUBLICATIONS

Granzotto, A., Bolognin, S., Scancar, J., Milacic, R., Zatta, P. 2011. Beta-amyloid toxicity increases with hydrophobicity in the presence of metal ions. Monatsh Chem 142(4), 421-30.

Granzotto, A., Zatta, P. 2011. Resveratrol acts not through anti-aggregative pathways but mainly via its scavenging properties against Abeta and Abeta-metal complexes toxicity. PLoS One 6(6), e21565.

Granzotto, A., Suwalsky, M., Zatta, P. 2011. Physiological cholesterol concentration is a neuroprotective factor against beta-amyloid and beta-amyloid-metal complexes toxicity. J Inorg Biochem 105(8), 1066-72.

Granzotto, A., Zatta, P. 2012. Metal ions and beta amyloid: conformational modifications and biological aspects. in: Linert, W., Kozlowski, H. (Eds.). Metal Ions in Neurological Systems. Springer-Verlag, Wien, pp 77-83.

Gatta, V., Granzotto, A., Fincati, K., Drago, D., Bolognin, S., Zatta, P., Sensi, S.L. 2012. Microarray analysis of gene expression profiles in human neuroblastoma cells exposed to Aβ-Zn and Aβ-Cu complexes. Future Neurol 7(4), 483-97.

Gatta, V., Granzotto, A., D'Aurora, M., Stuppia, L., Sensi, S.L., Early and sustained expression of age-related genes in 3xTg-AD mice *(submitted)*.

Canzoniero, M. L., Granzotto, A., Turetsky, M.D., Choi, W.D., Dugan, L.L., Sensi, S.L., nNOS(+) striatal neurons possess functional NMDA receptors but fail to generate mitochondrial ROS in response to an excitotoxic challenge *(submitted).*